

Layered Compounds

2D = Two-dimensional layers

Graphite and Graphene

Clay Minerals, Mica

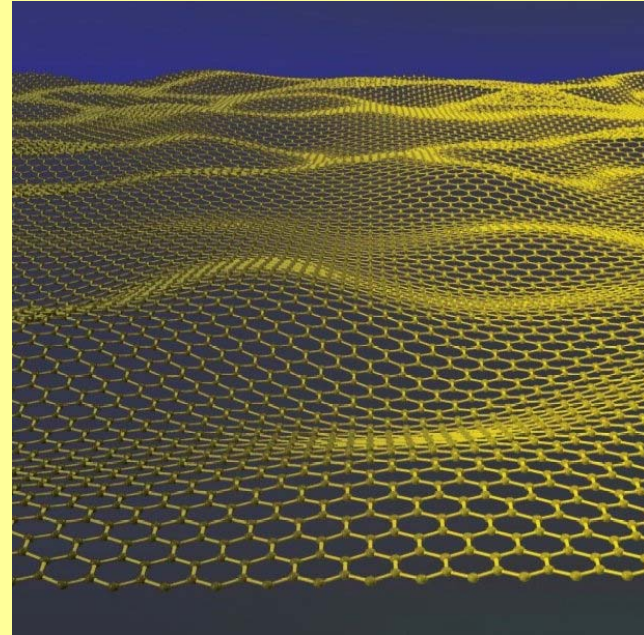
Layered Double Hydroxides (LDHs)

Layered Zirconium Phosphates and Phosphonates

Layered Metal Oxides

Layered Metal Chalcogenides - MS_2 , MPS_3 (M = Ti, V, Mo, W, Mn, Fe, Co, Ni, Zn)

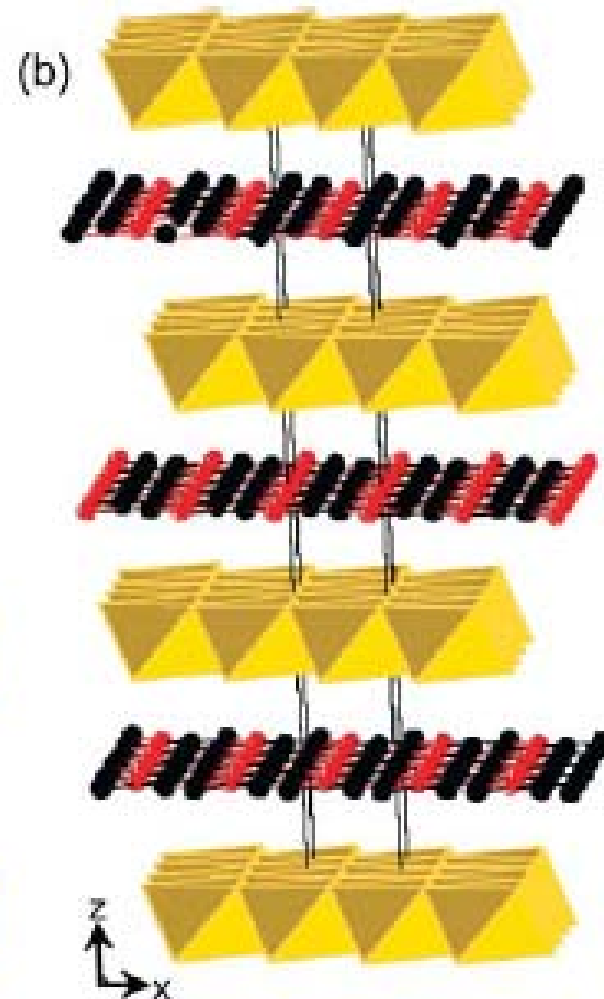
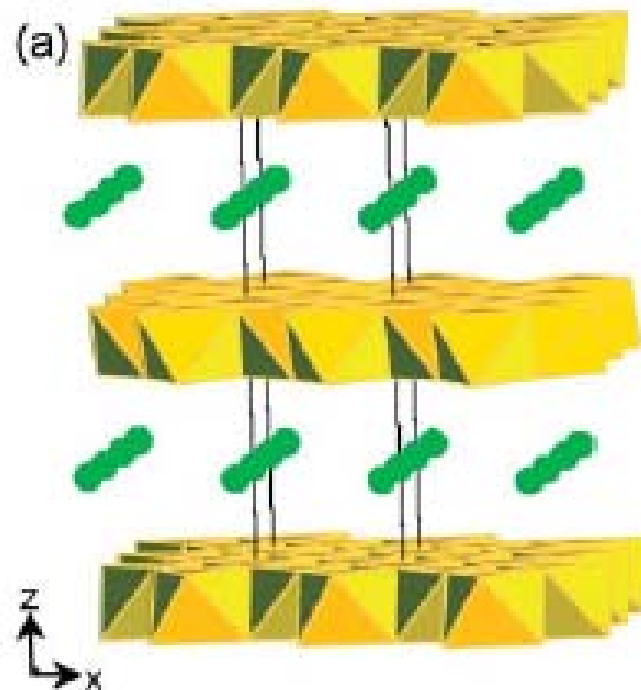
Alkali Silicates and Crystalline Silicic Acids



Layered Compounds

**Intralayer bonding - strong
(covalent, ionic)**

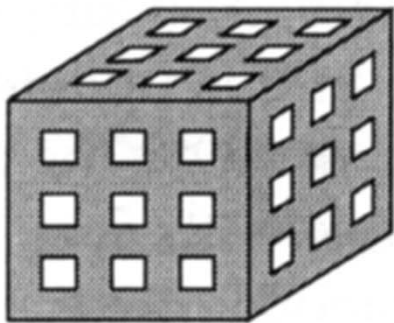
**Interlayer bonding - weak
(H-bonding, vdWaals)**



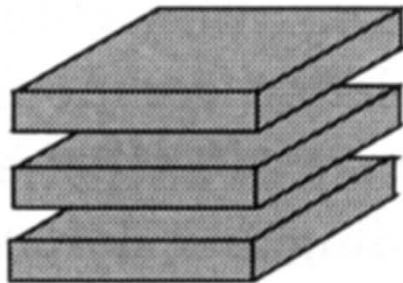
Host-Guest Structures

Host dimensionality

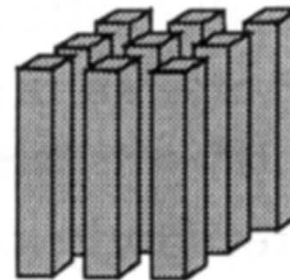
3D



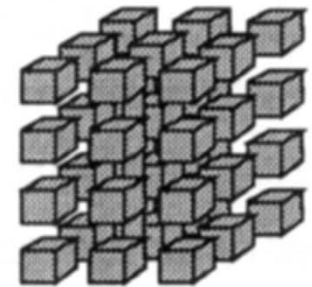
2D



1D



0D

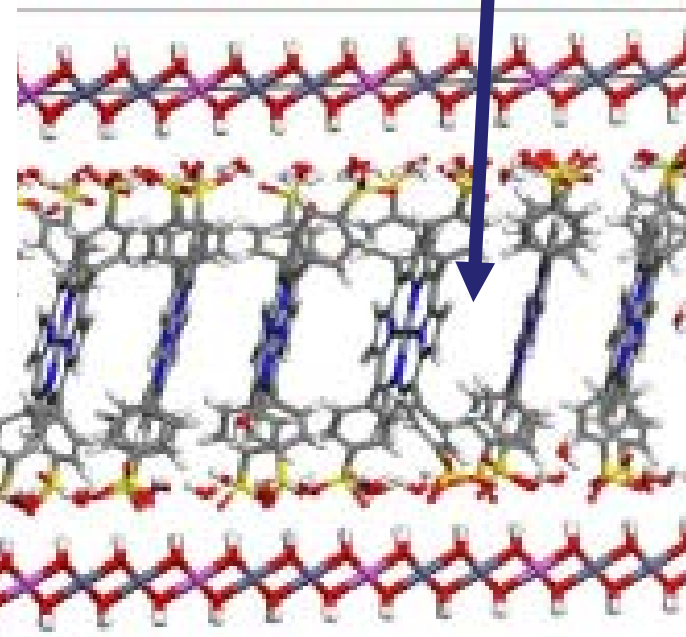
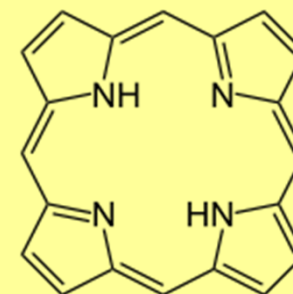
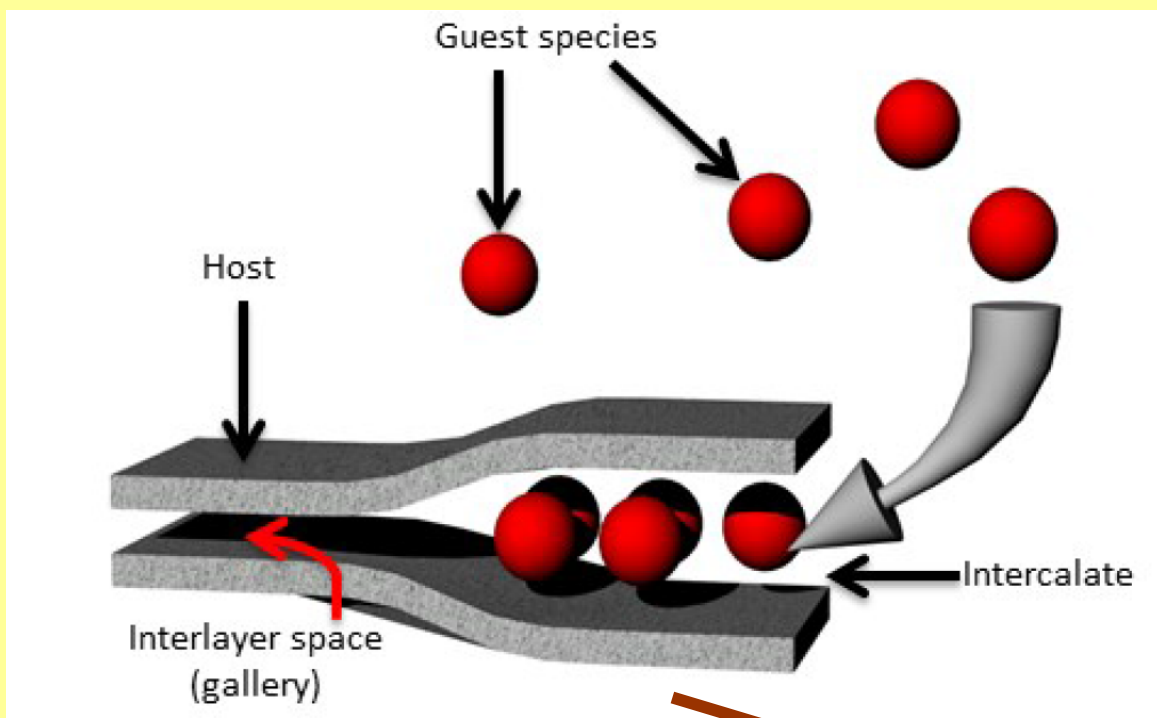


TOPOTACTIC SOLID-STATE REACTIONS = modifying existing solid state structures while maintaining the integrity of the overall structure

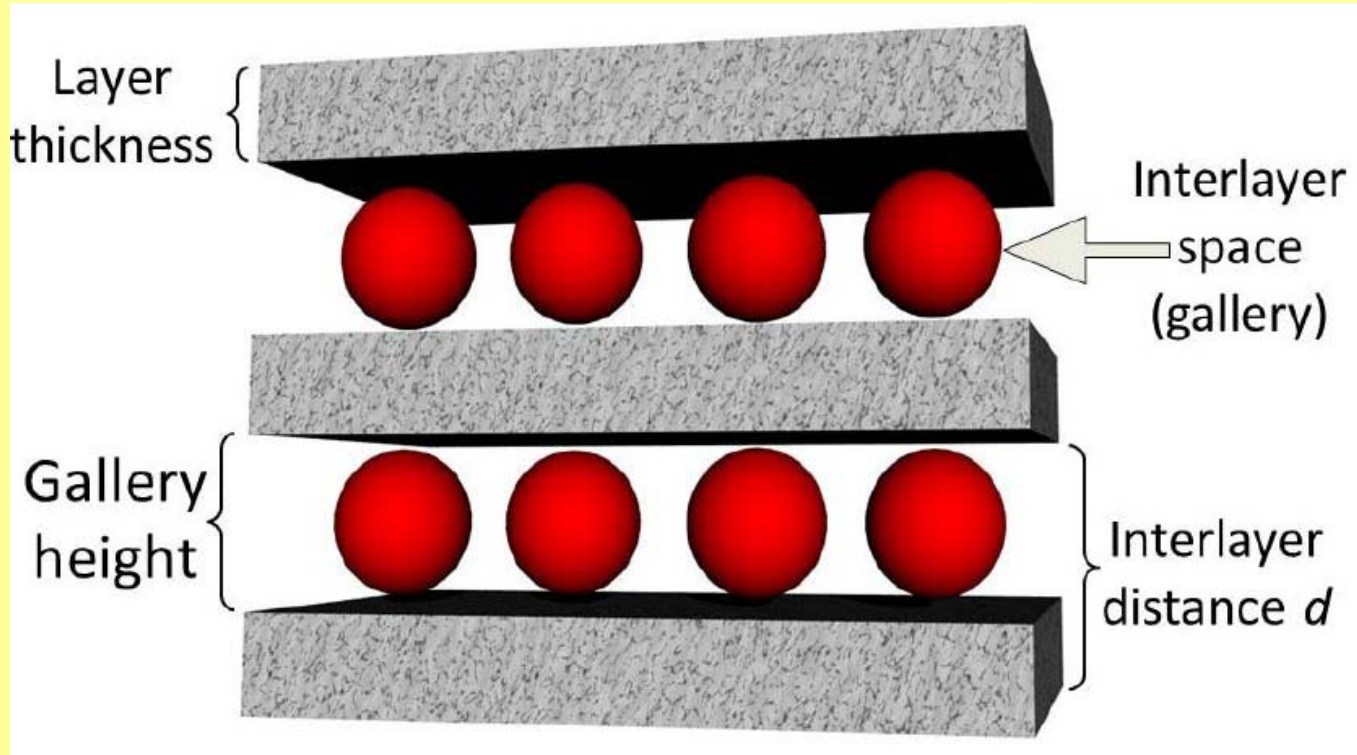
Intercalation

Intercalation

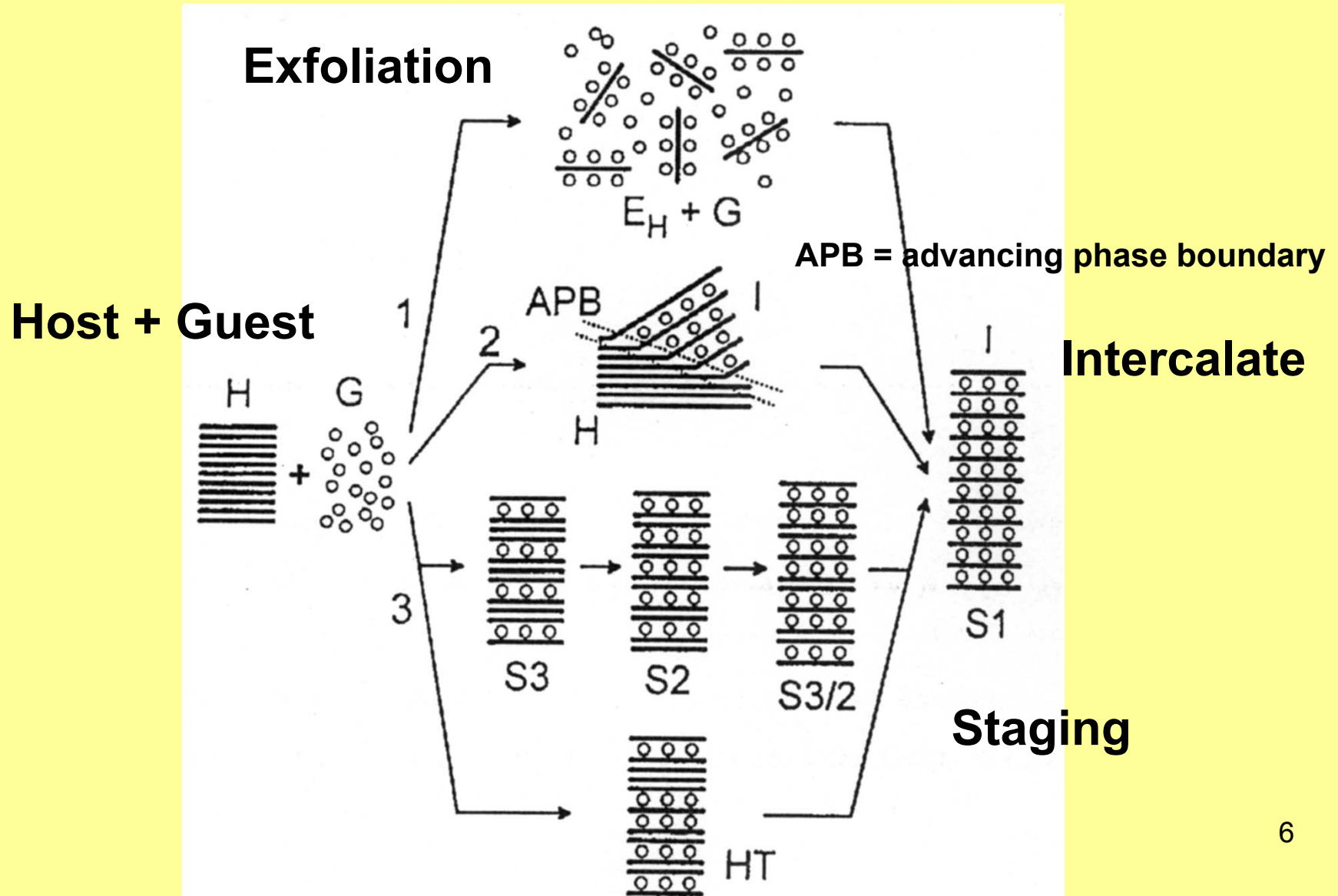
Insertion of molecules between layers



Intercalation

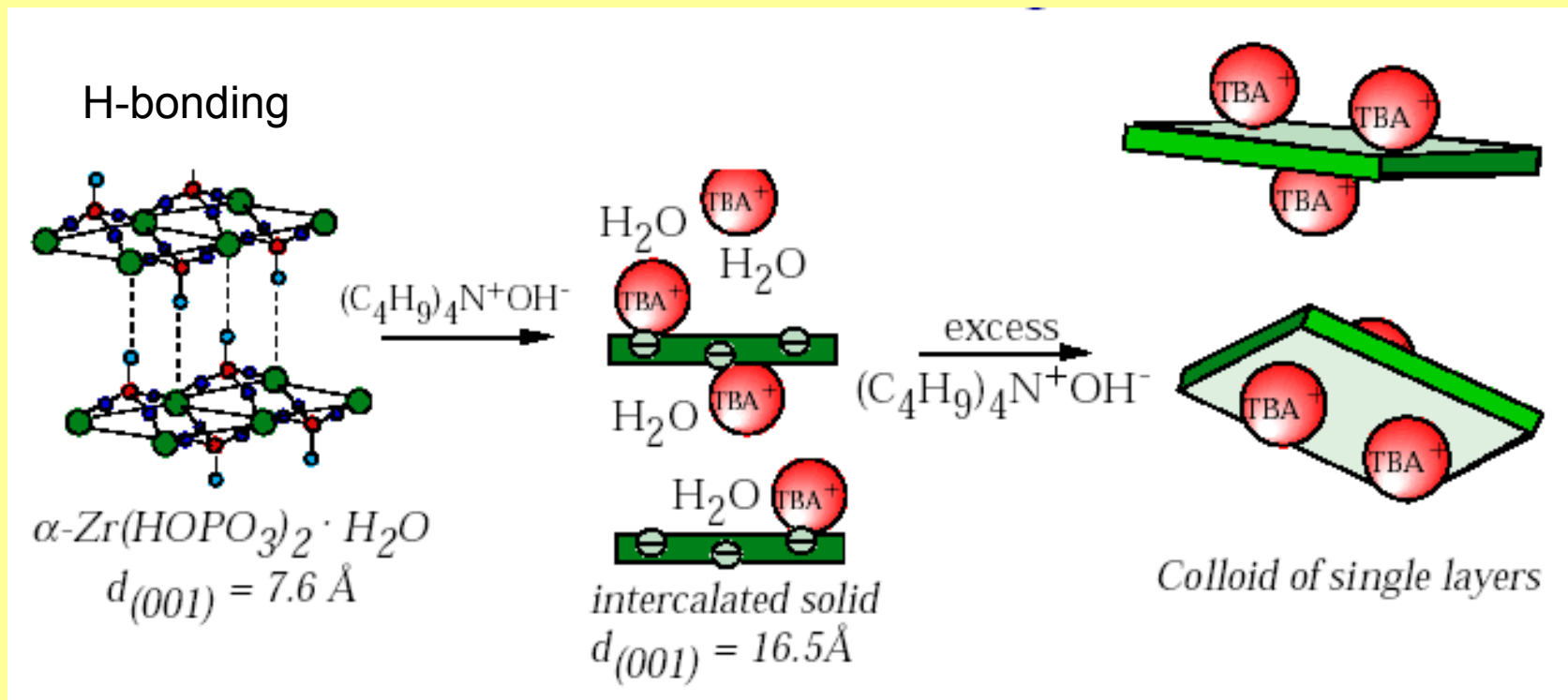


Intercalation



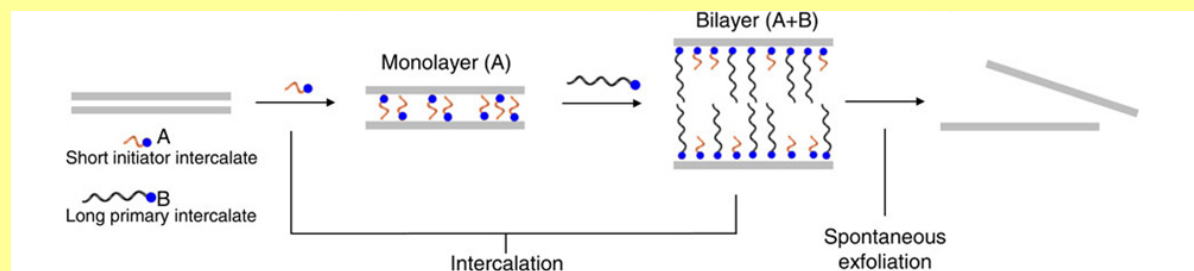
Exfoliation

Decrease attractive forces between layers
Separate layers

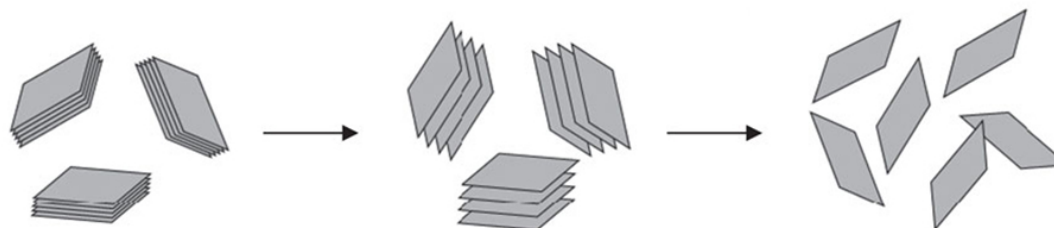


Tandem Molecular Intercalation

Lewis base short initiator first intercalates to open up the interlayer gap, and the long molecules then bring the gap to full width and overcome the interlayer attractive force resulting in spontaneous exfoliation

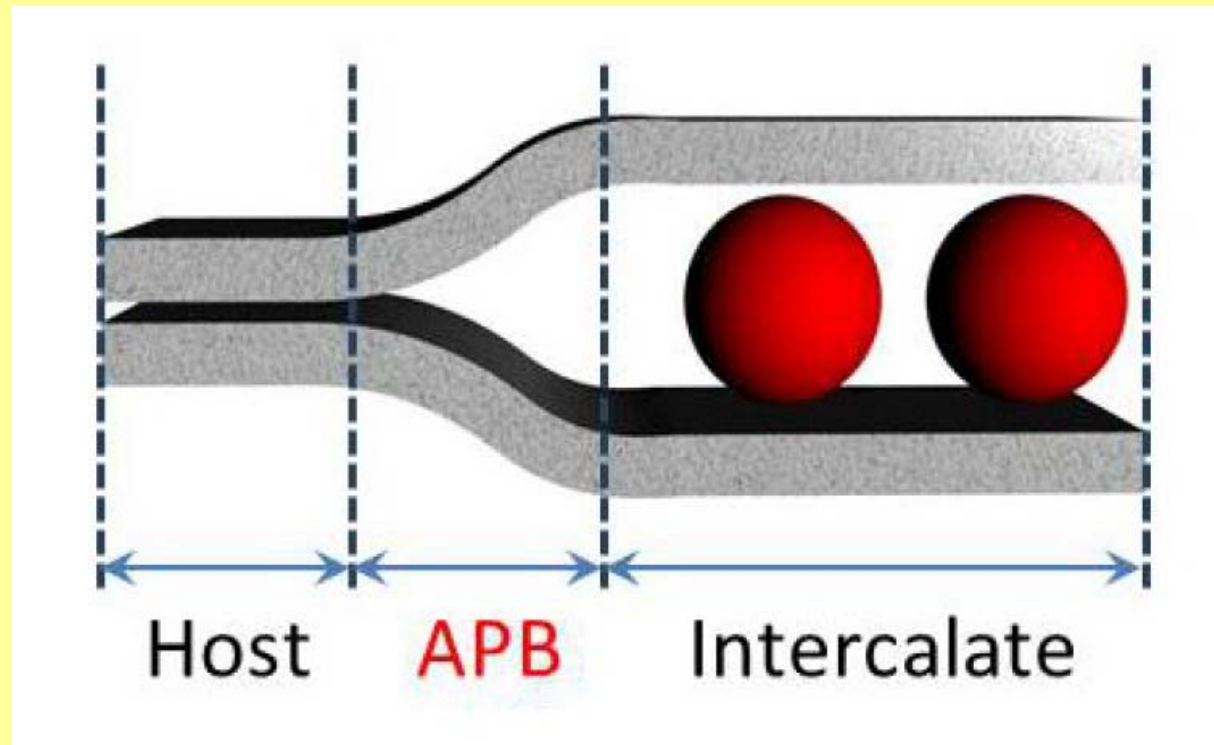


Transition-Metal Chalcogenides



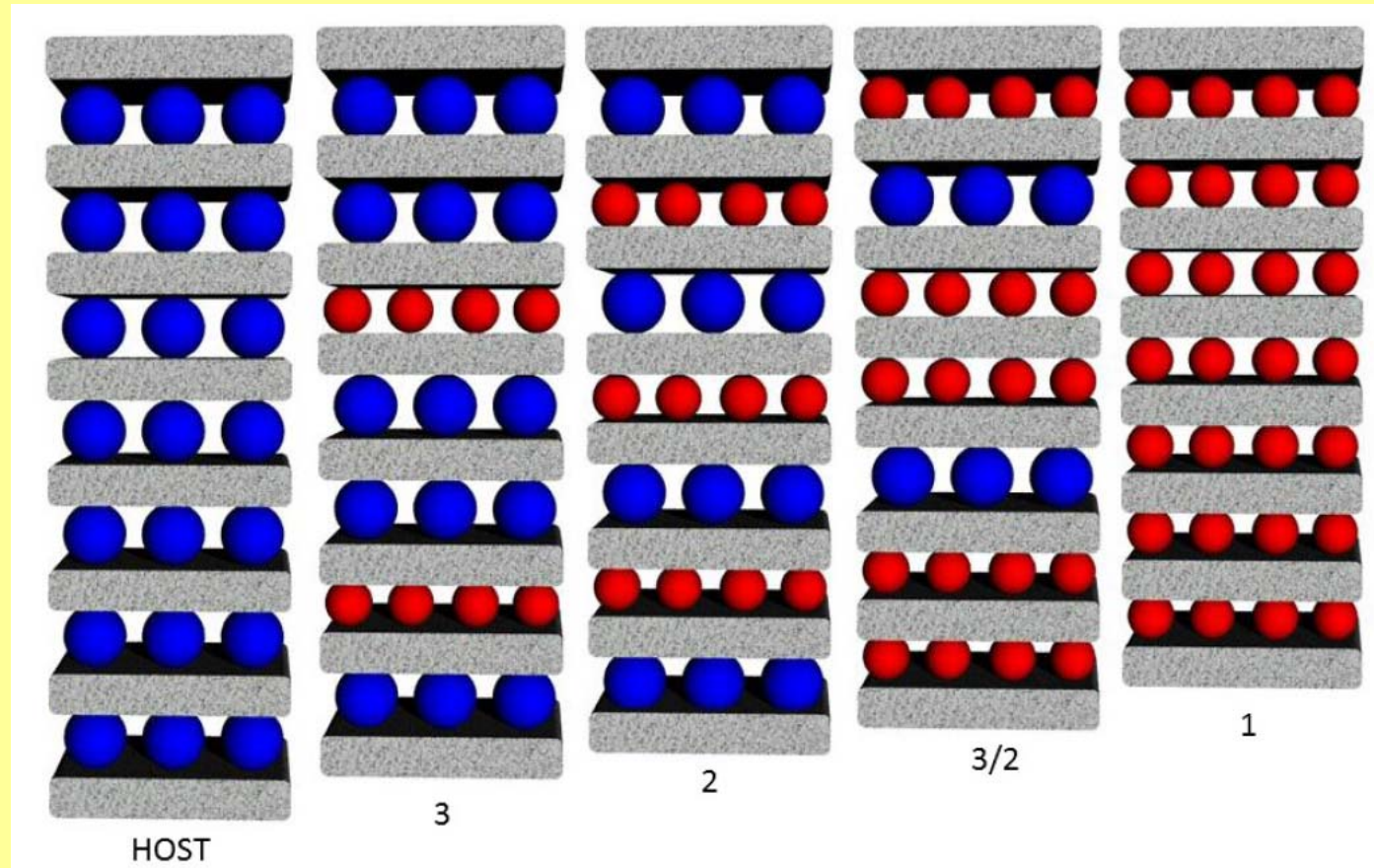
Nat. Commun. 2015,6, 5763, Jan. 9, 2015

APB = Advancing Phase Boundary

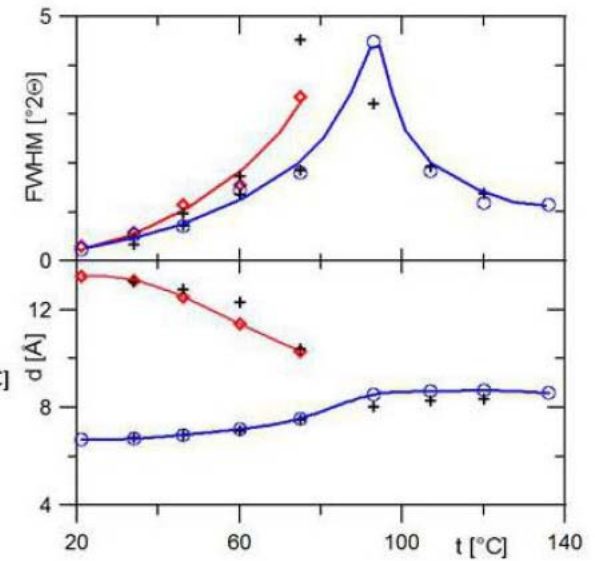
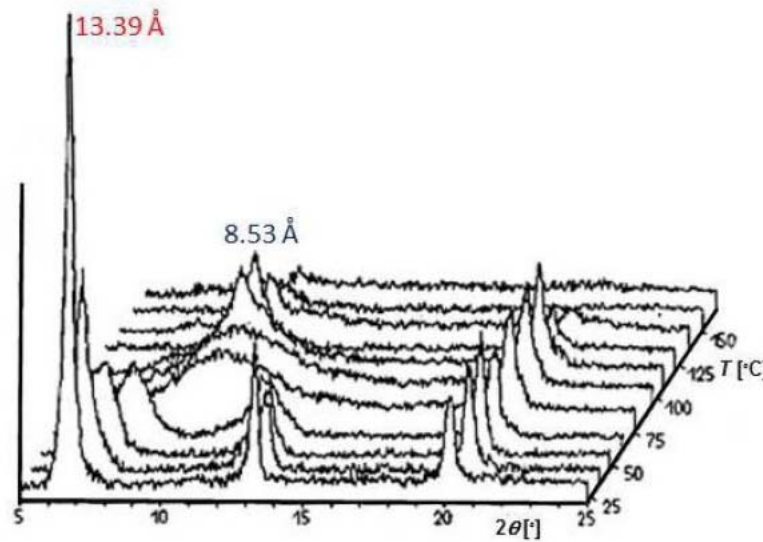
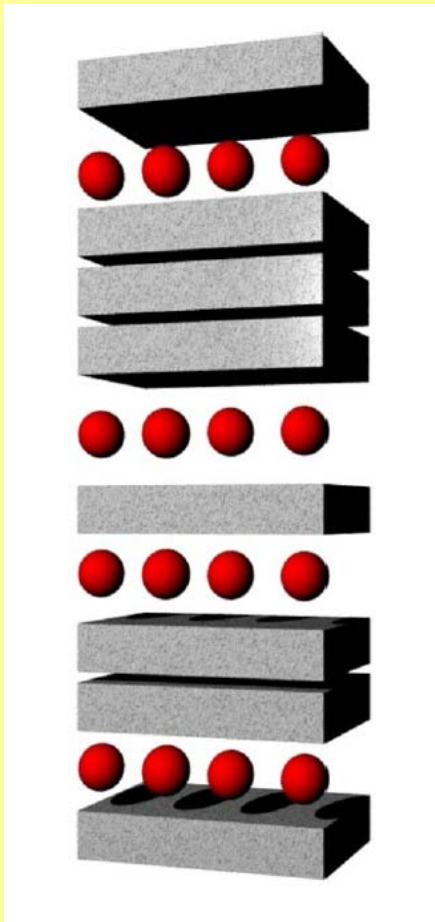


APB = advancing phase boundary

Staging

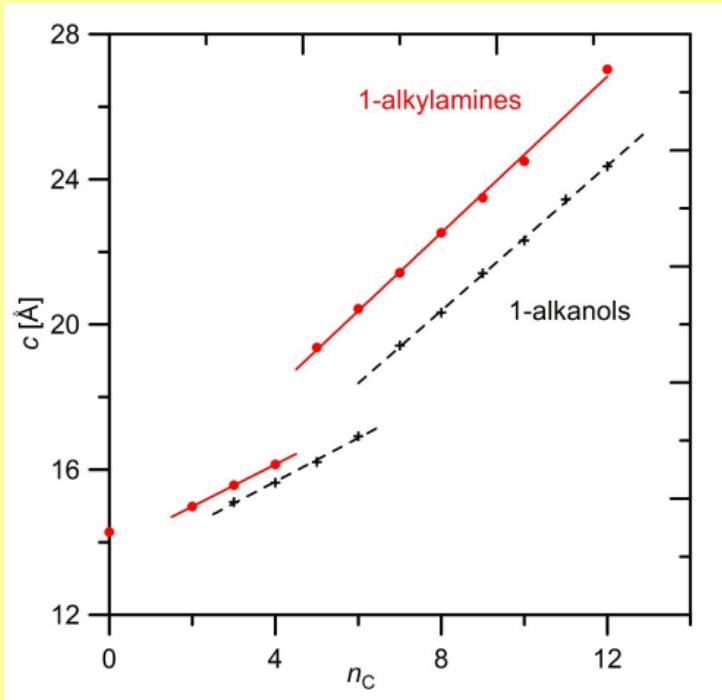


Hendricks-Teller Effect

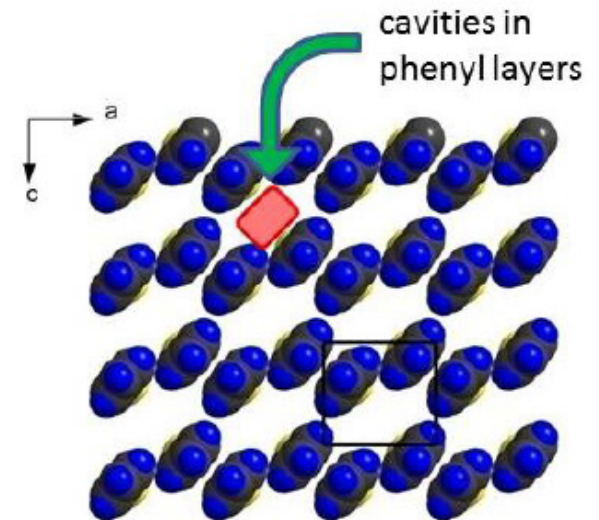
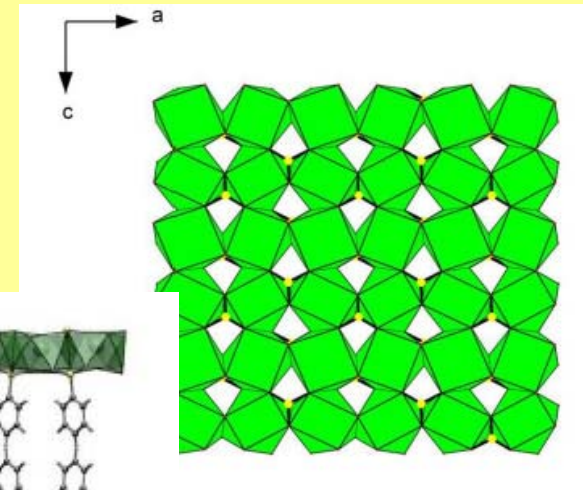
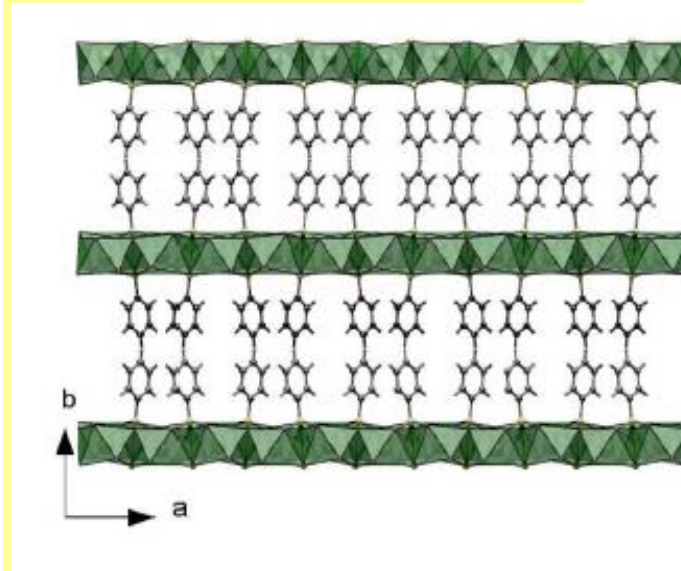


HT = galleries are filled randomly

Intercalation

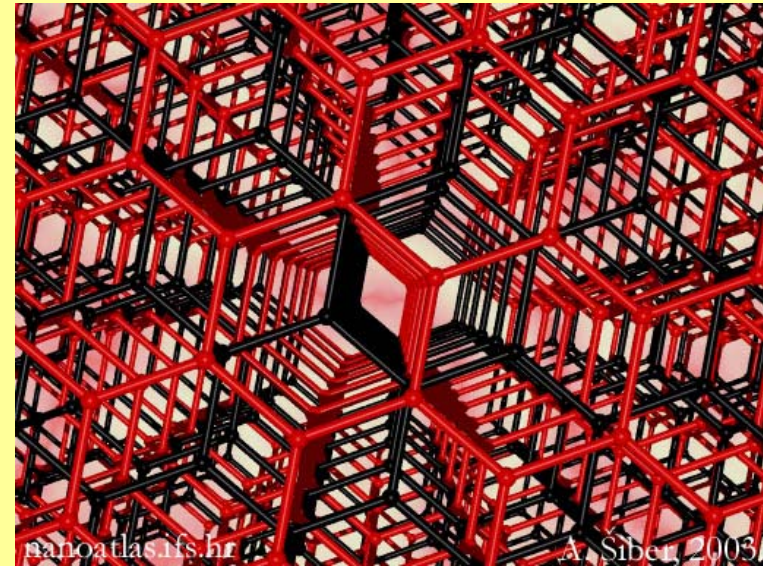
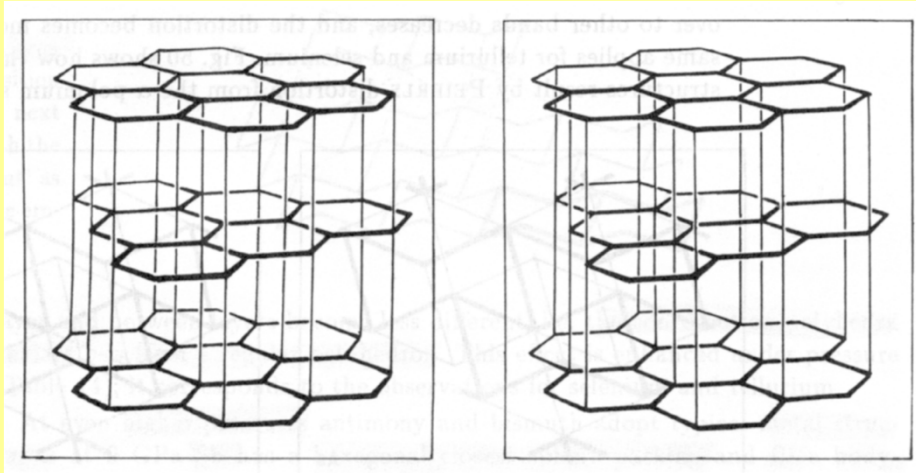


Dependence of the basal spacing of the intercalates of the alkylamines (circles) and alkanols (crosses) on the number of carbon atoms n_C in $\text{SrC}_6\text{H}_5\text{PO}_3 \cdot 2\text{H}_2\text{O}$



Graphite

ABABAB

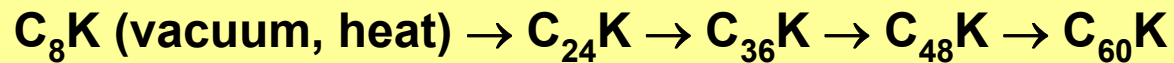


**Graphite sp^2 sigma-bonding in-plane p-p-bonding out of plane
Hexagonal graphite = two-layer ABAB stacking sequence**

**SALCAOs of the p-p-type create the valence and conduction
bands of graphite, very small band gap, metallic conductivity
properties in-plane, 10^4 times that of out-of plane conductivity**

Graphite

GRAPHITE INTERCALATION



C₈K potassium graphite ordered structure

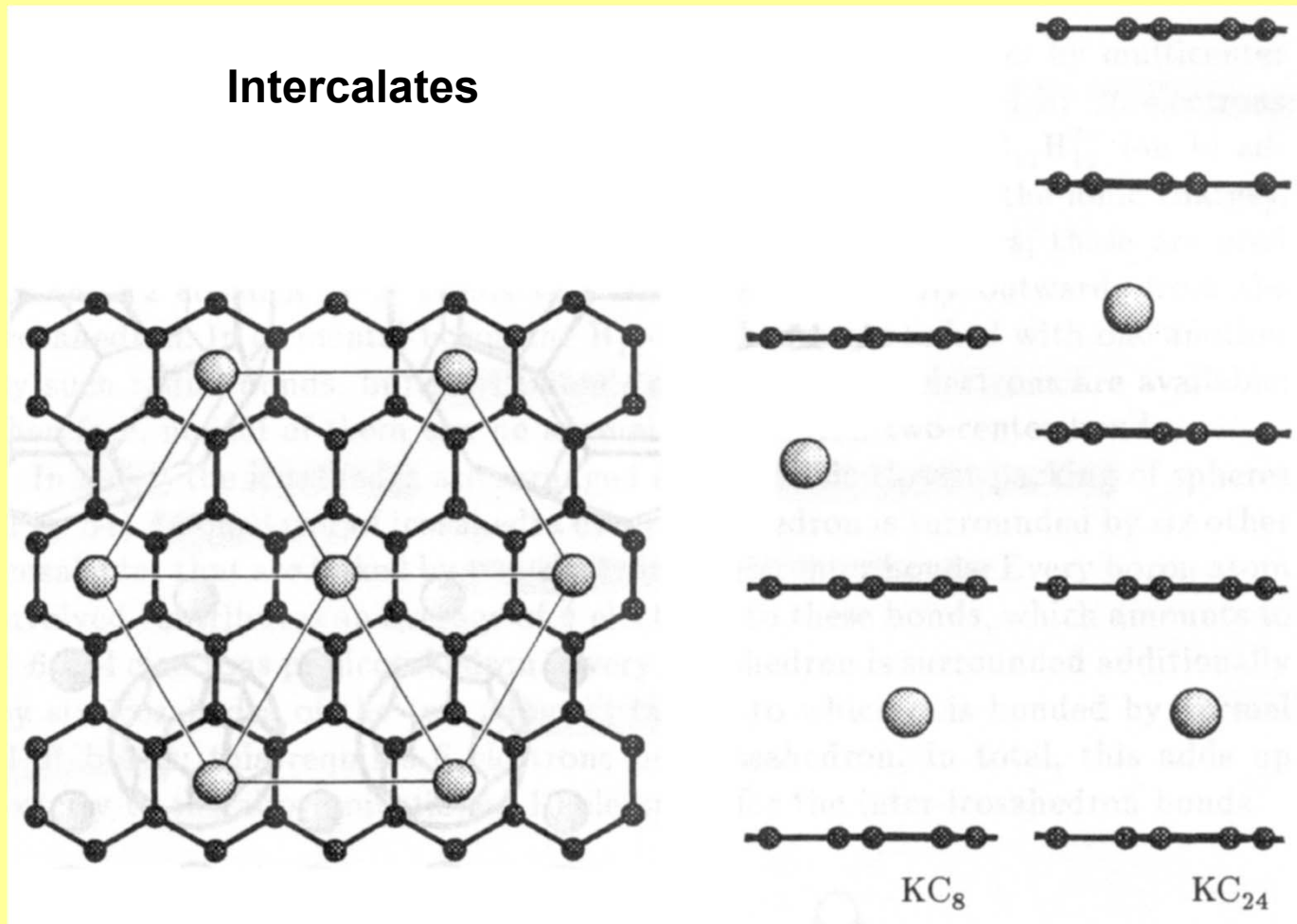
Ordered K guests between the sheets, K to G charge transfer

AAAA stacking sequence

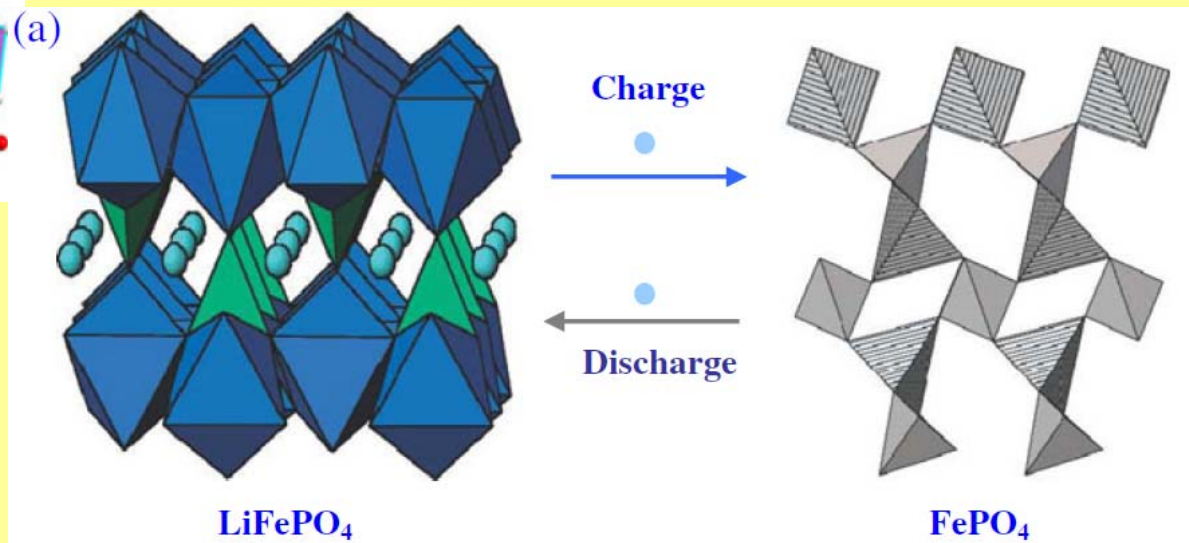
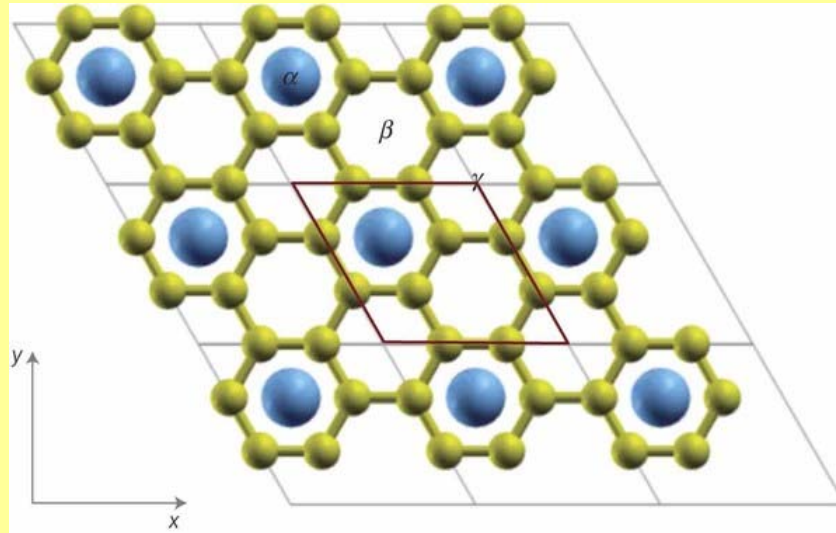
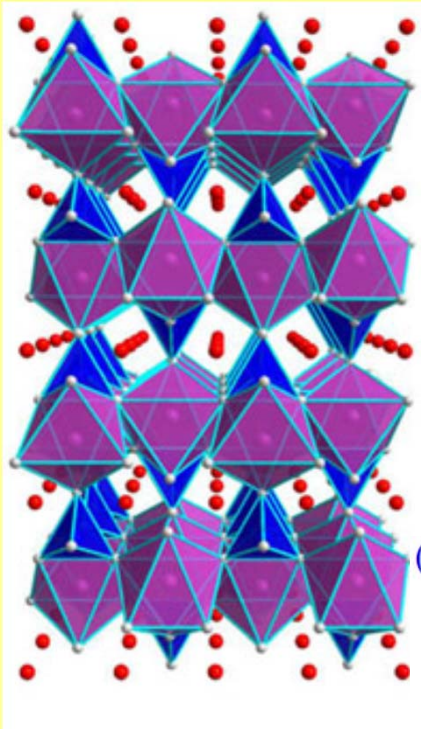
reduction of graphite sheets, electrons enter CB

K nesting between parallel eclipsed hexagonal planar carbon six-rings

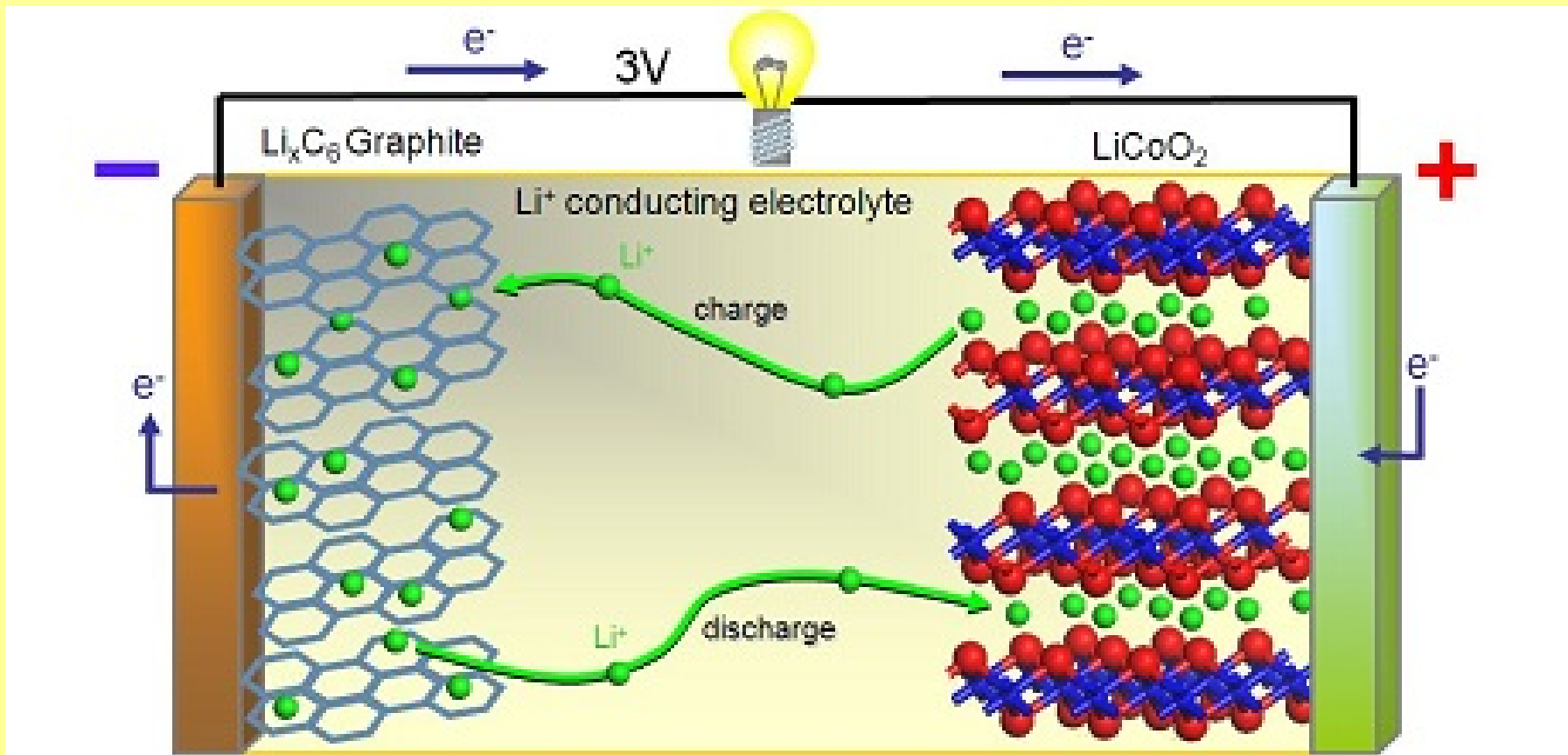
Graphite



Intercalation in Li-ion Cells



Intercalation in Li-ion Cells



Graphene

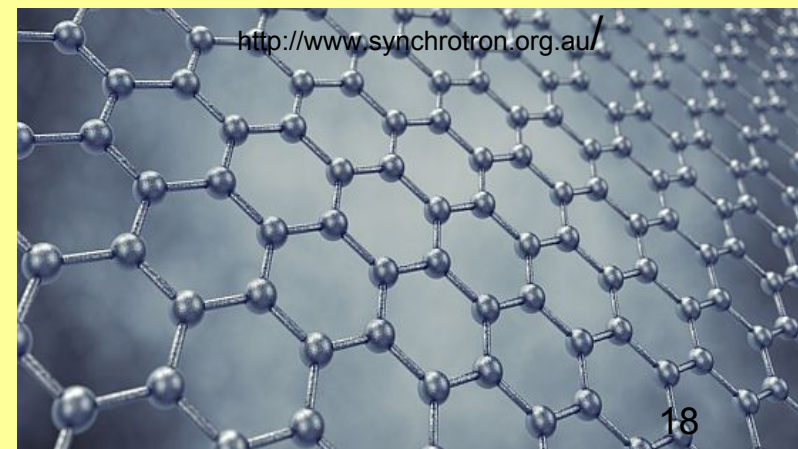
- **Discovery – 2004**
- **Exotic properties:**
 - Firm structure
 - Inert material
 - Hydrofobic character
 - Electric and thermal conductivity
 - High mobility of electrons
 - Specific surface area
(theoretically):
 $2630 \text{ m}^2\text{g}^{-1}$



K. Novoselov

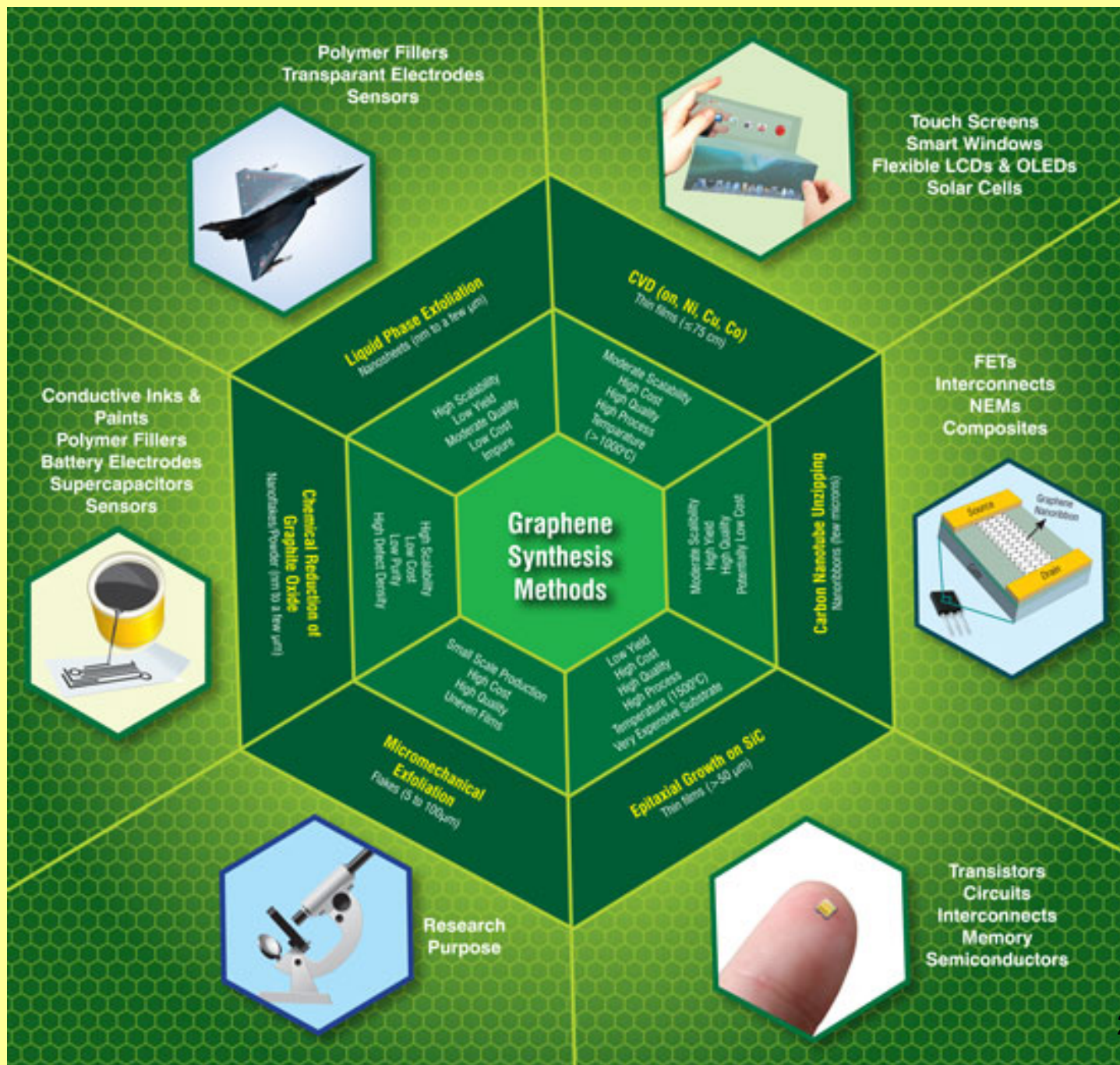


A. Geim

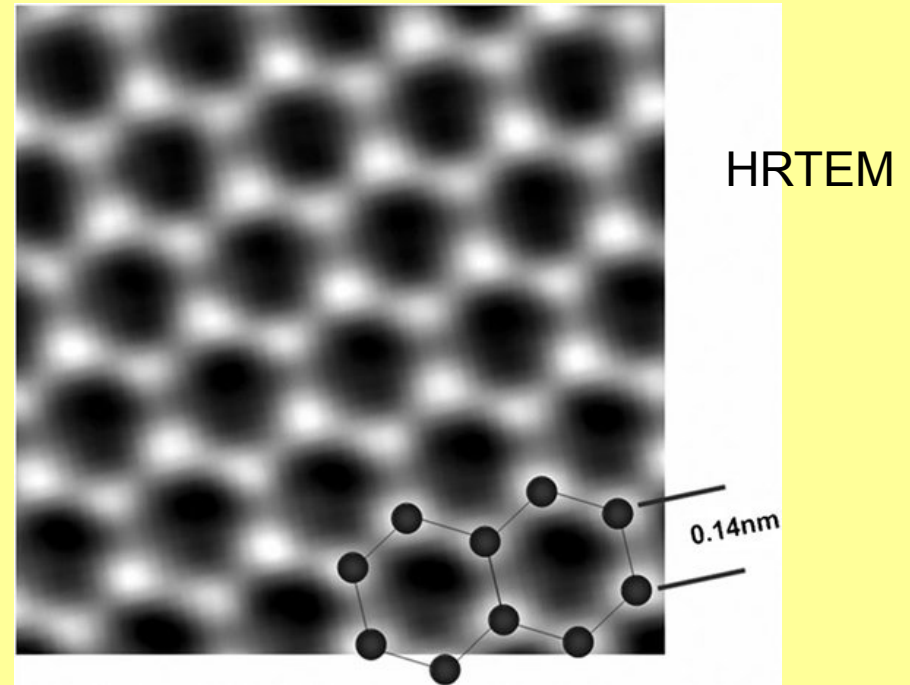
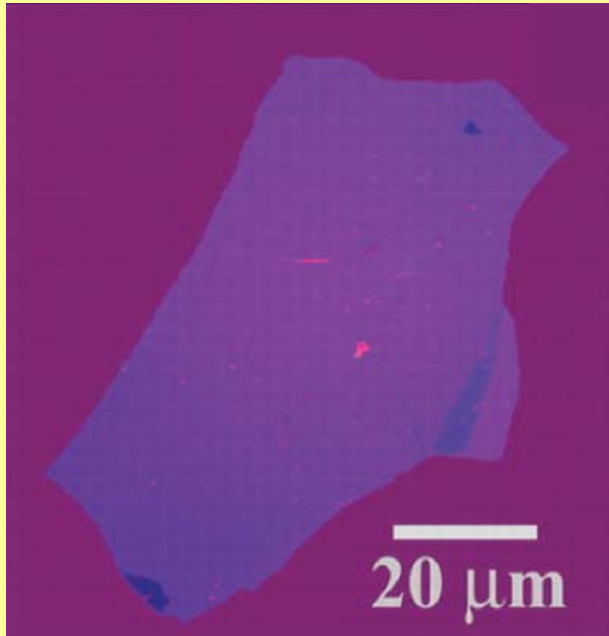


Synthesis of graphene

- **Top down**
 - Mechanical exfoliation
 - Chemical exfoliation
- **Bottom up**
 - CVD, epitaxial growth, ...
- **Defects**
- **Application: diodes, sensors, solar cell, energy storage, composites, ...**



Graphene

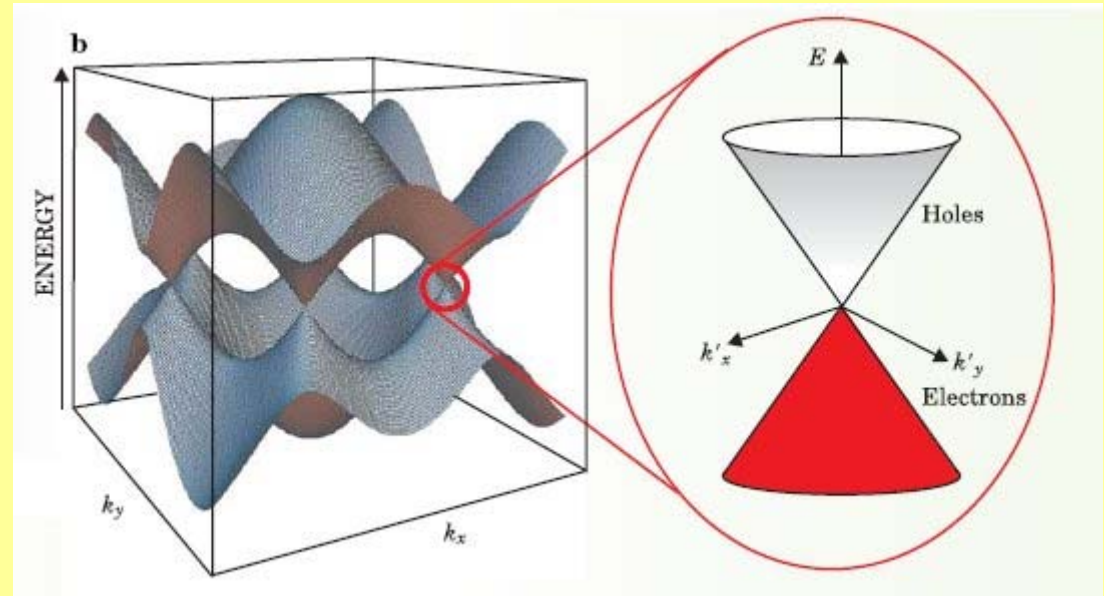
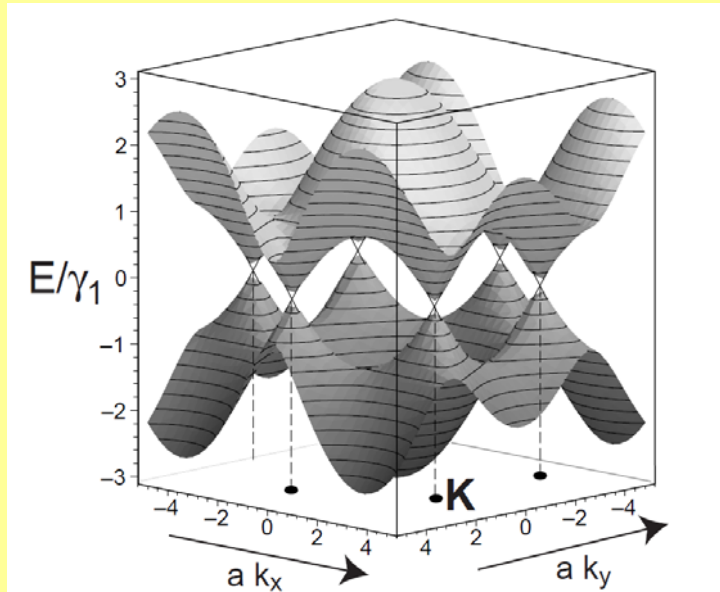


High electric conductivity (metallic)

Optically transparent – 1 layer absorbs 2.3% of photons

High mechanical strength

Graphene

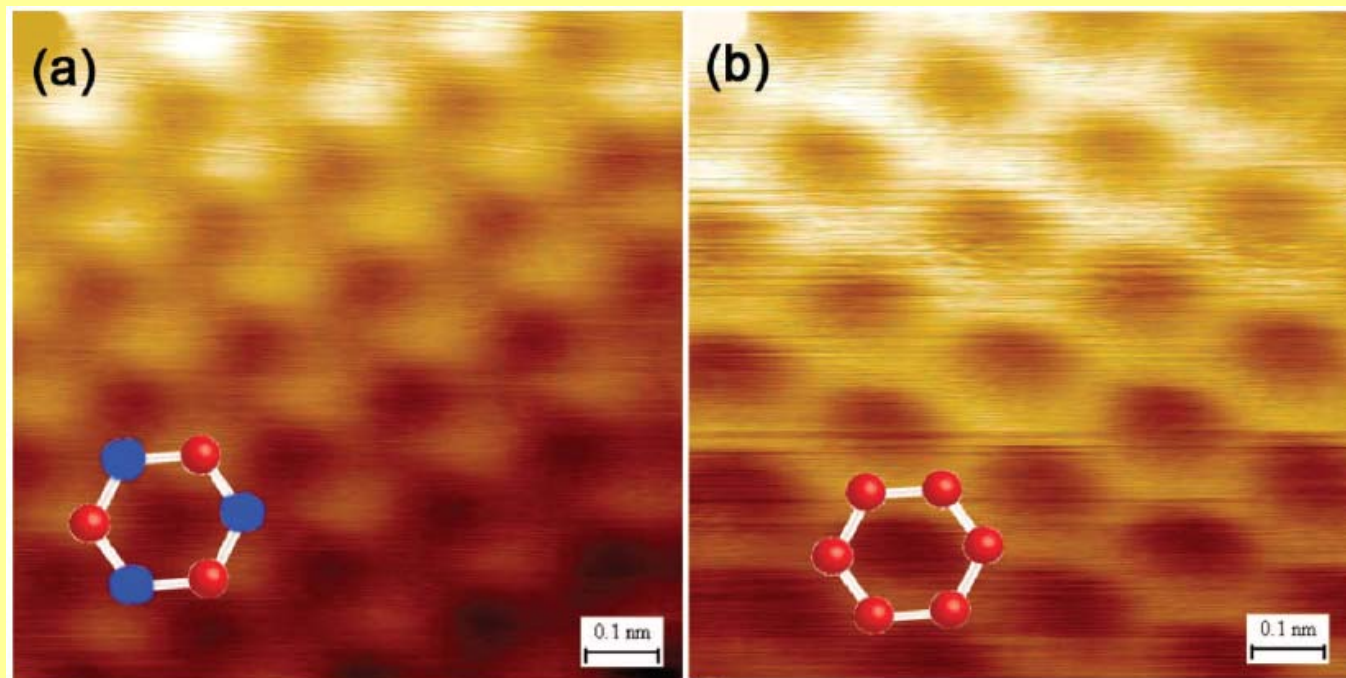


LCAO-band structure of graphene

Graphene

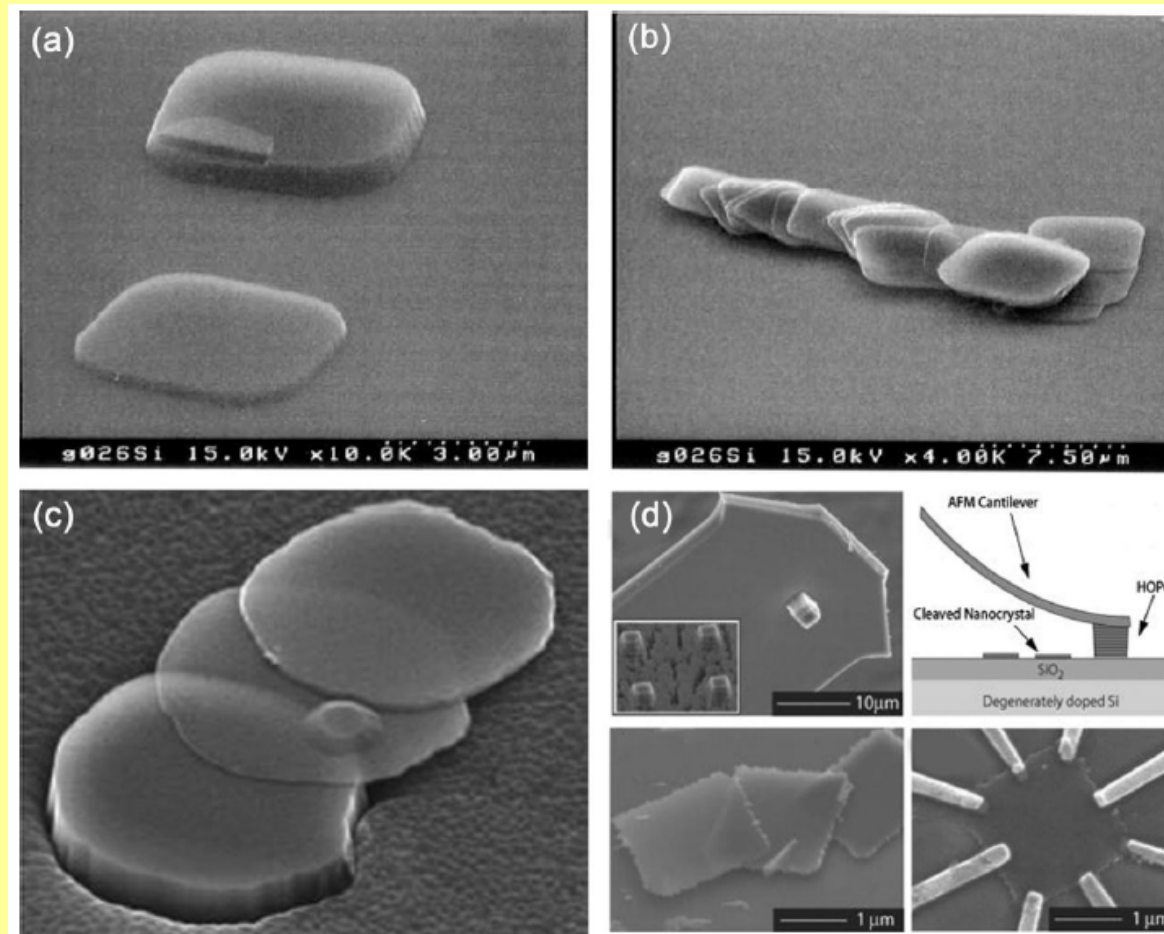
Preparation:

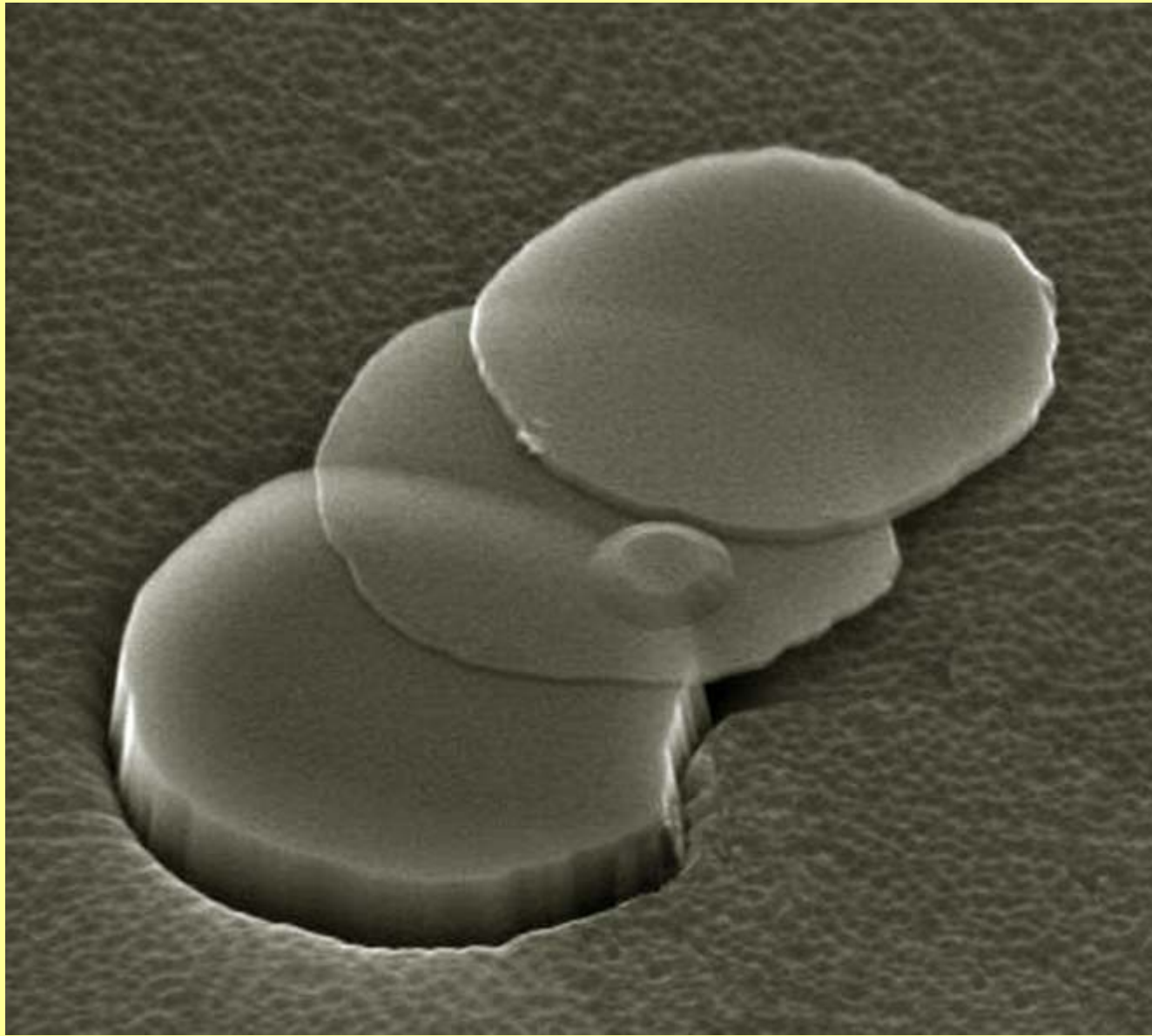
- Scotch tape – layer peeling, flaking
- SiC pyrolysis – epitaxial graphene layer on a SiC crystal
- Exfoliation of graphite (chemical, sonochemical)
- CVD from CH_4 , CH_2CH_2 , or CH_3CH_3 on Ni (111), Cu, Pt surfaces



Scotch tape – Layer peeling

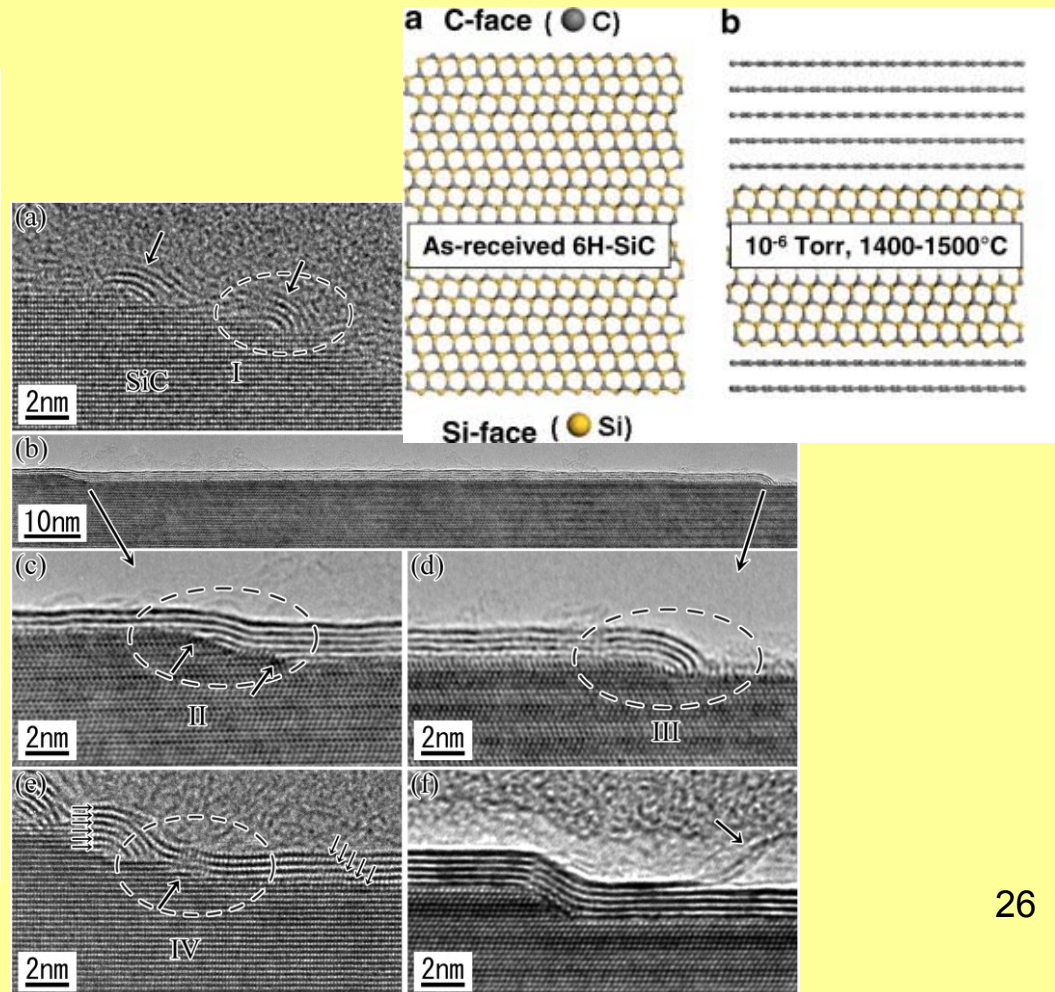
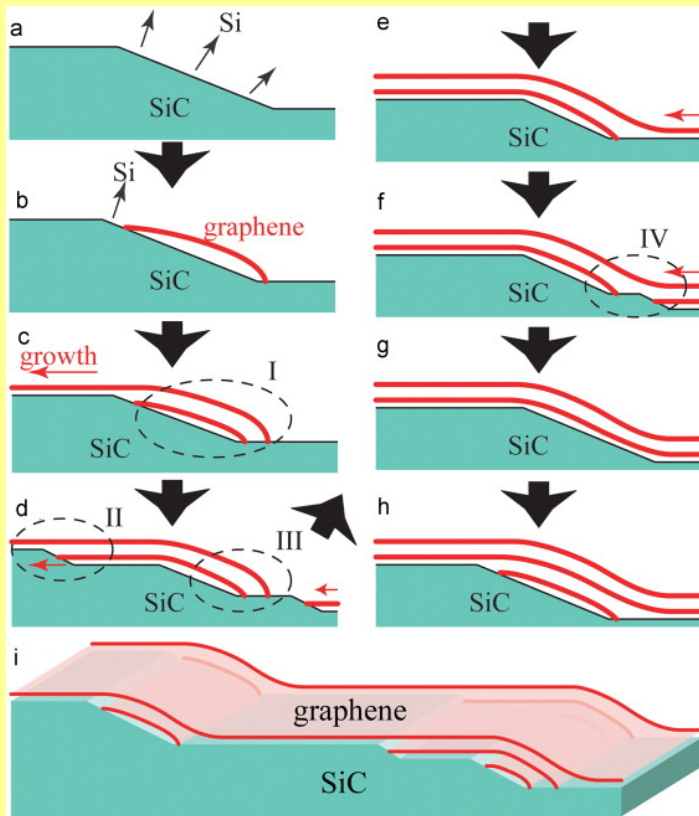
Mechanical exfoliation

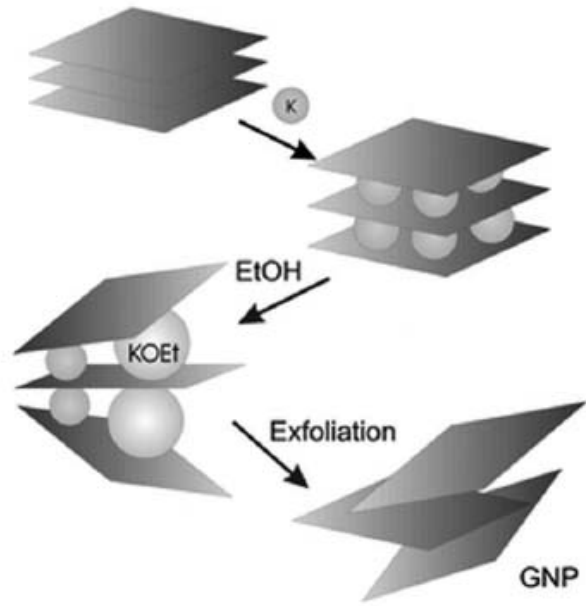




SiC pyrolysis

- Annealing of the SiC crystal in a vacuum furnace (UHV 10^{-10} Torr)
- Sublimation of Si from the surface at 1250 - 1450 °C
- The formation of graphene layers by the remaining carbon atoms

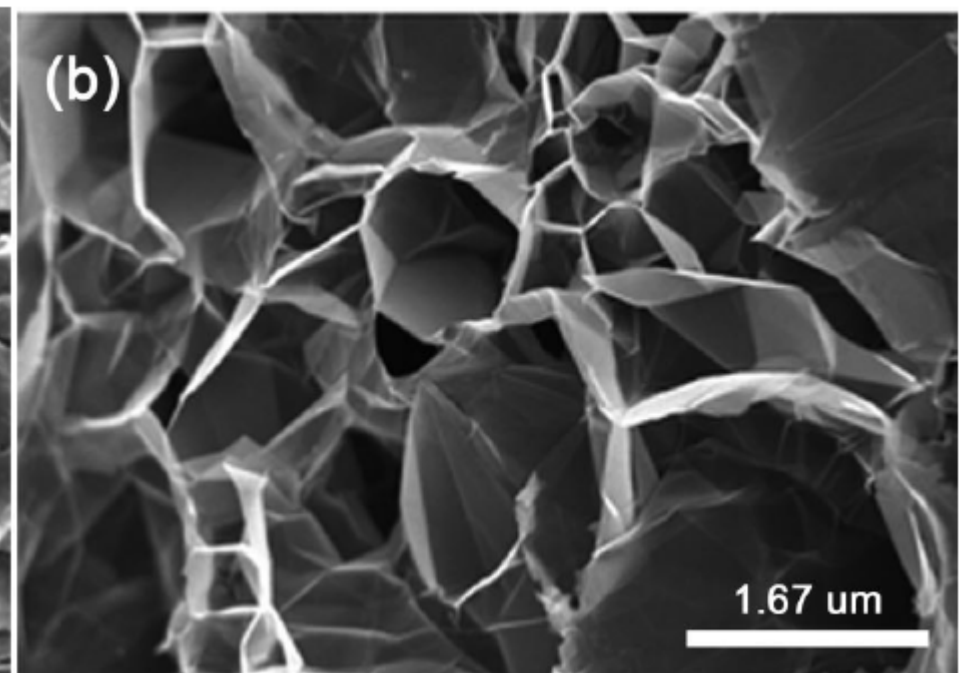
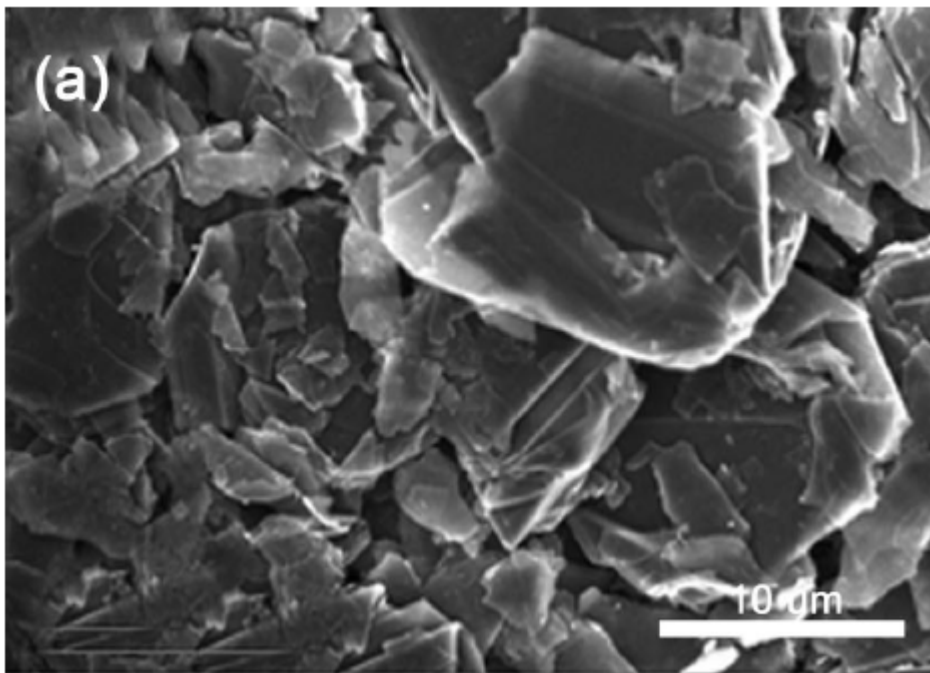




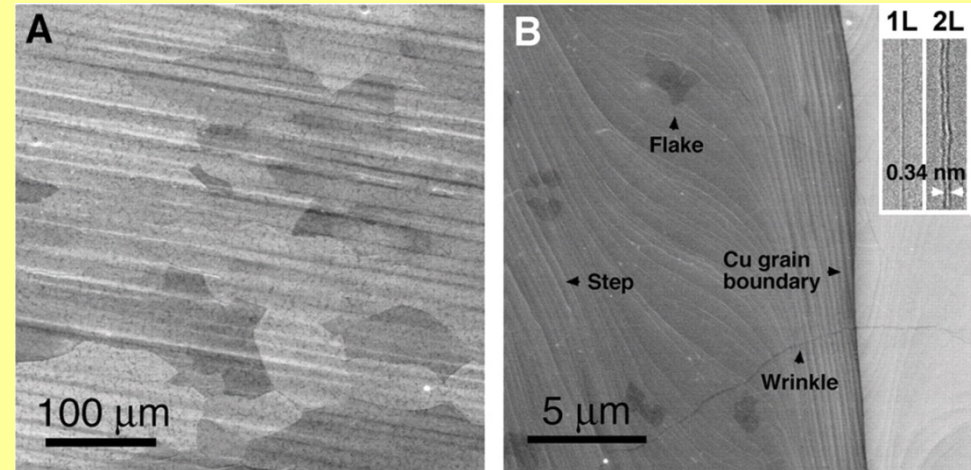
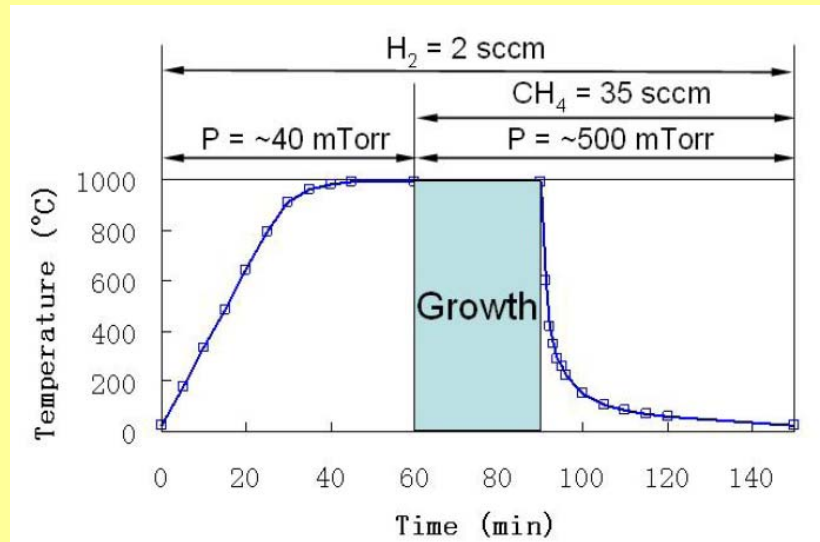
Exfoliation

Chemical exfoliation (surfactant)

Sonochemical exfoliation

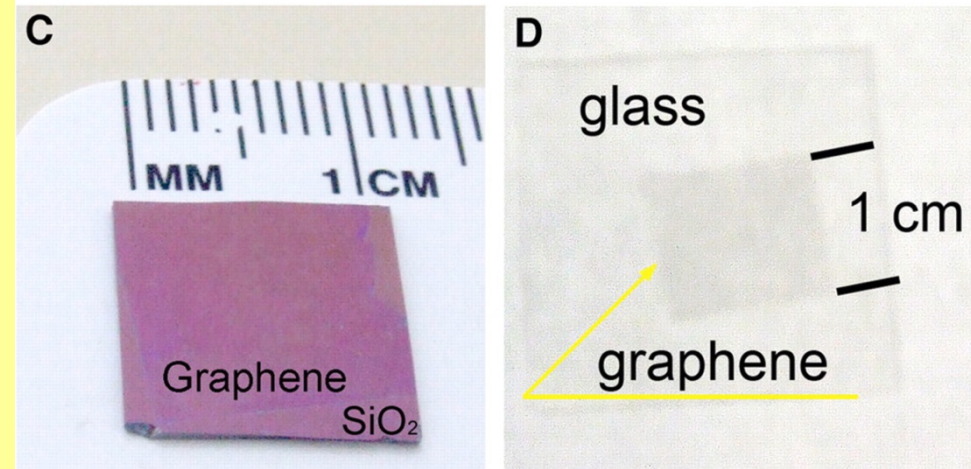


CVD from CH₄ / H₂ on Metal Surfaces



(A) SEM - graphene on a copper foil

(B) High-resolution SEM - Cu grain boundary and steps, two- and three-layer graphene flakes, and graphene wrinkles. Inset (B) TEM images of folded graphene edges. 1L, one layer; 2L, two layers.



Graphene transferred onto
(C) a SiO₂/Si substrate
(D) a glass plate

Graphene on SiO₂



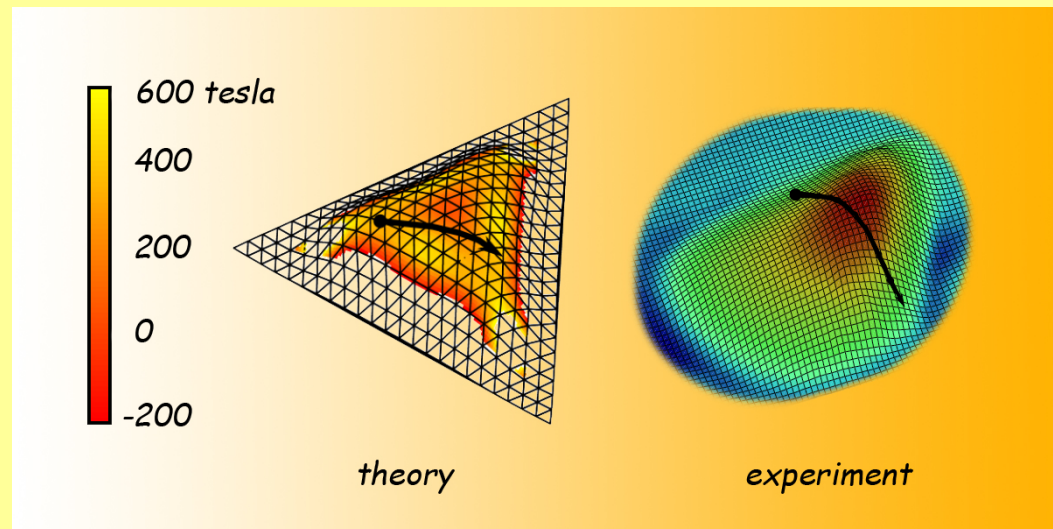
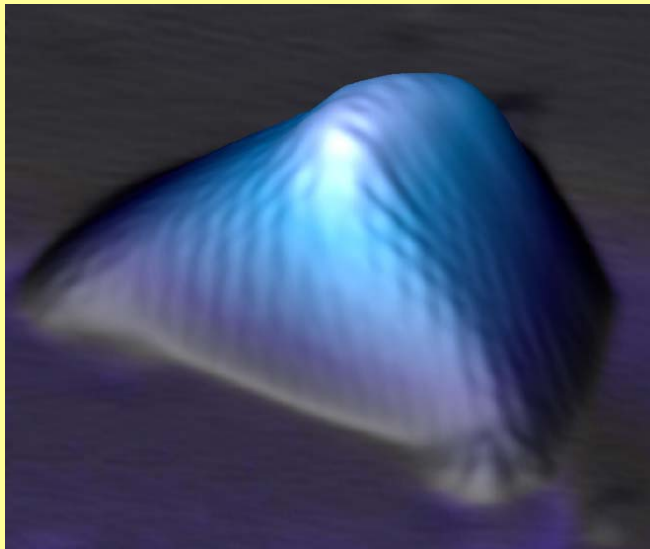
Pseudo-magnetism

Graphene on platinum grown from ethylene at high temperatures. Cooled to low temperature to measure STM to a few degrees above absolute zero.

Both the graphene and the platinum contracted – but Pt shrank more, excess graphene pushed up into bubbles, size 4-10 nm x 2-3 nm

The stress causes electrons to behave as if they were subject to huge magnetic fields around 300 T

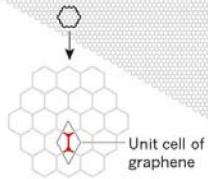
(record high in a lab, max 85 T for a few ms)



Twisted Bilayer Graphene

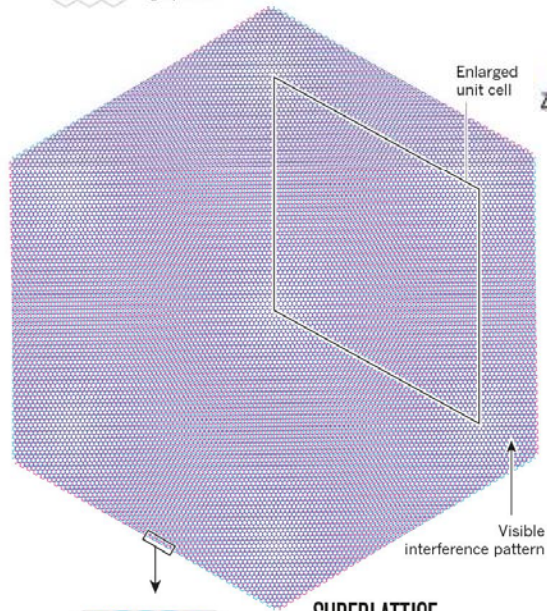
MAGIC ANGLE

Stacking one sheet of graphene on top of another can have a range of effects. If the sheets are rotated with respect to one another at just the right angle, the interaction of electrons in the two layers can give rise to new electronic properties.



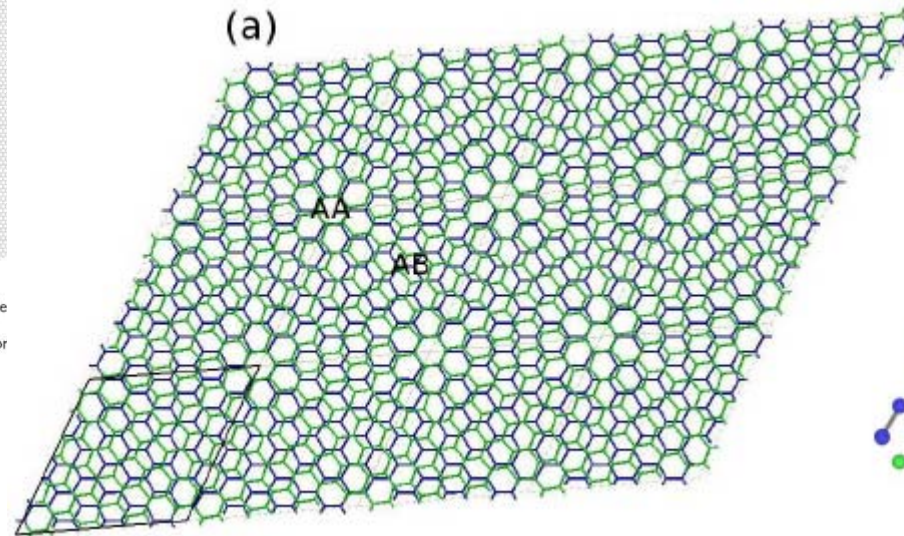
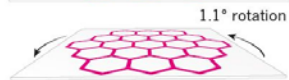
SIMPLE STRUCTURE

The crystal structure of a single layer of graphene can be described as a simple repetition of two atoms — its 'unit cell'.

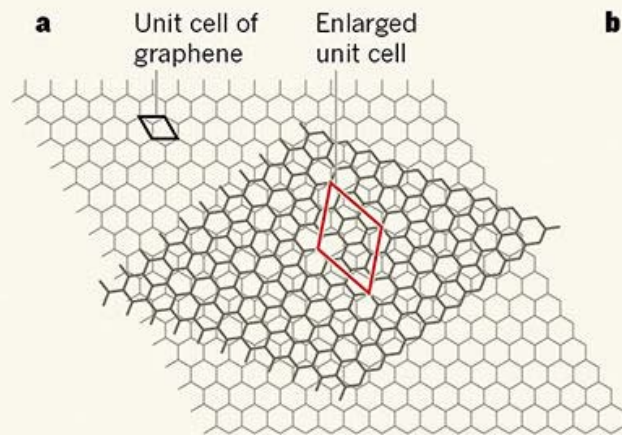
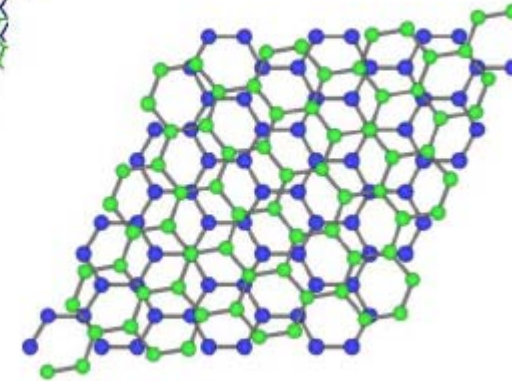


SUPERLATTICE

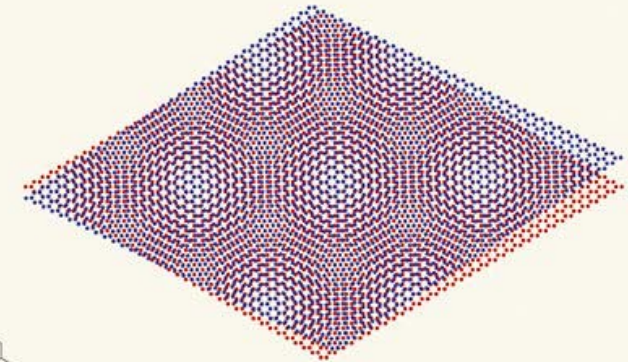
With some rotations, a two-layer stack forms a more complex repeating structure called a superlattice, with a larger unit cell. Electrons can move between the two layers.



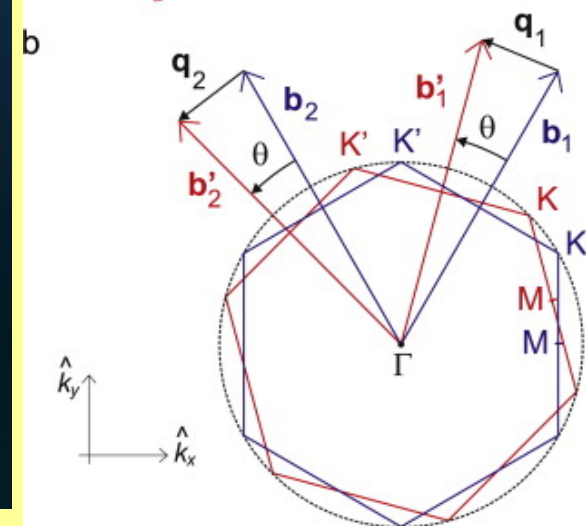
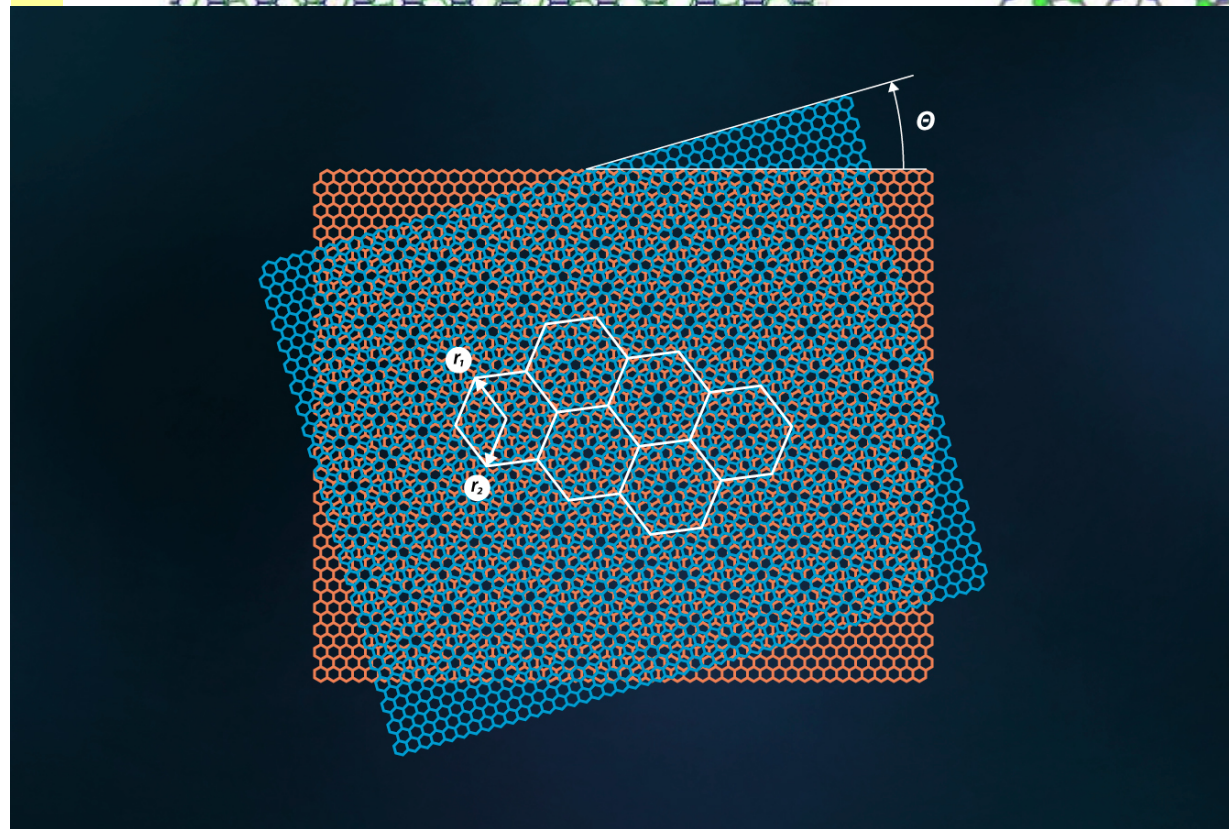
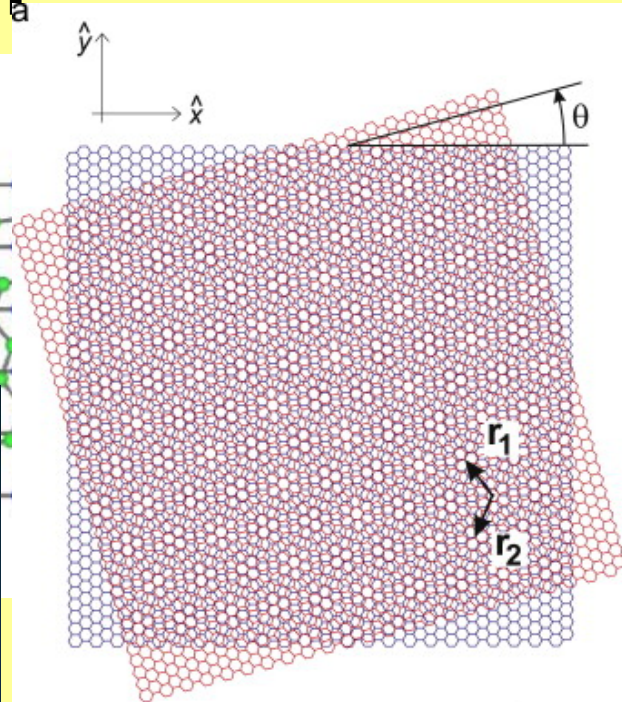
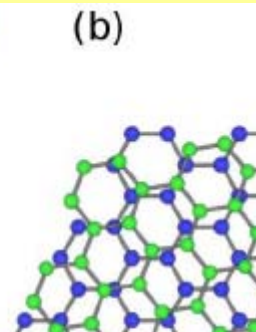
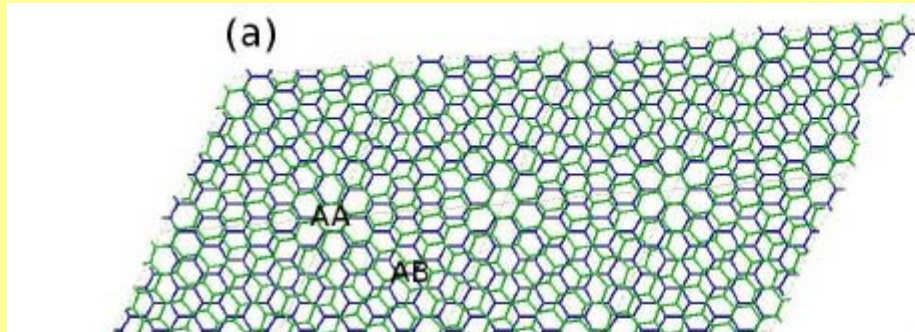
(b)



b



Twisted Bilayer Graphene



Graphene Family

Graphene

h-BN

BCN

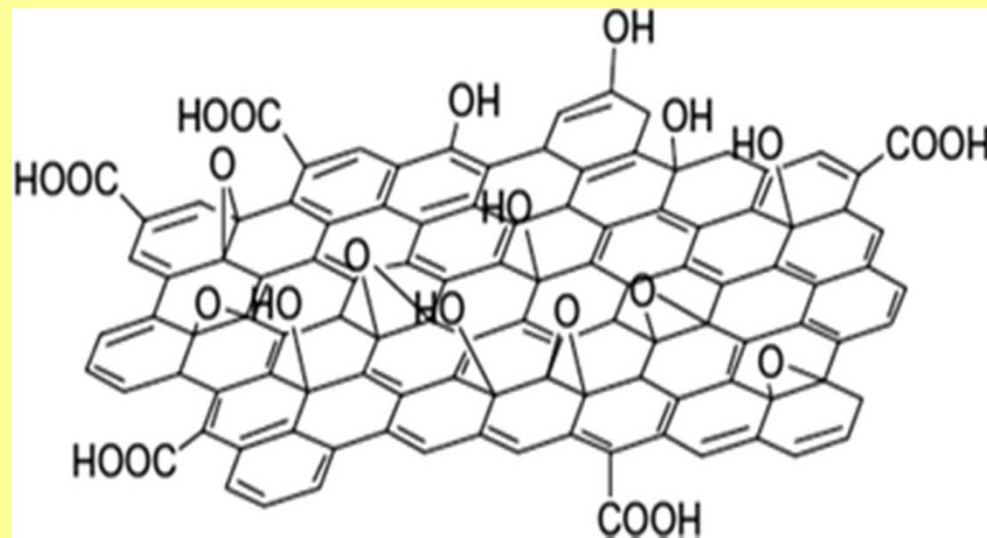
Fluorographene

Graphene oxide

C_3N_4

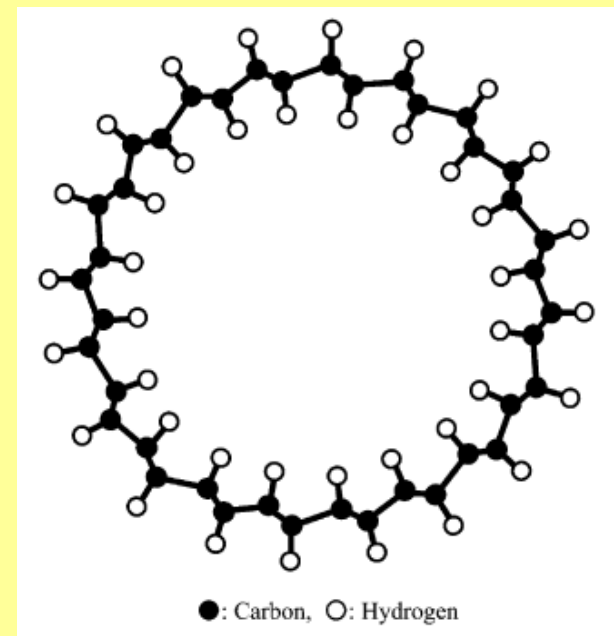
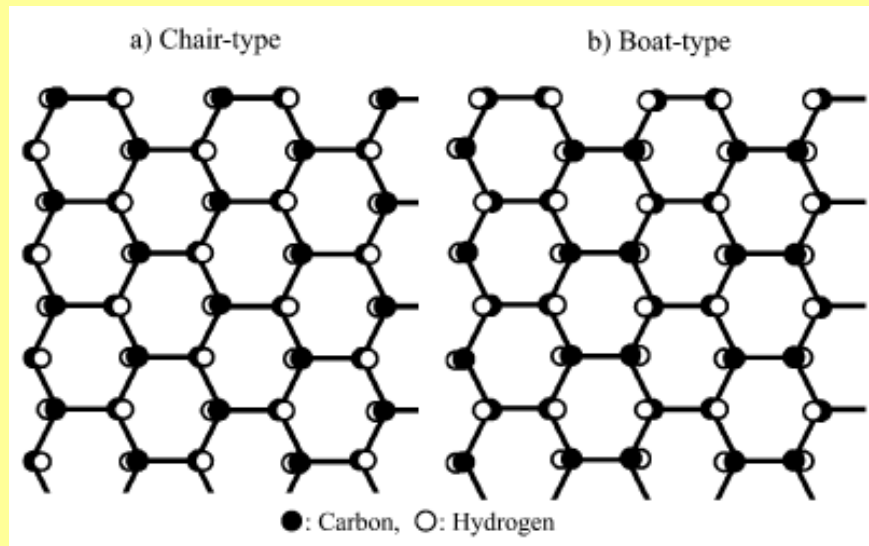
Graphene Oxide

- More reactive than graphene
- Presence of oxygen groups: -OH, -COOH, =O, -O-
hydrophilic character
- Electric insulator
- Specific SA (theoretically): 1700-1800 m²g⁻¹
- Hummers method

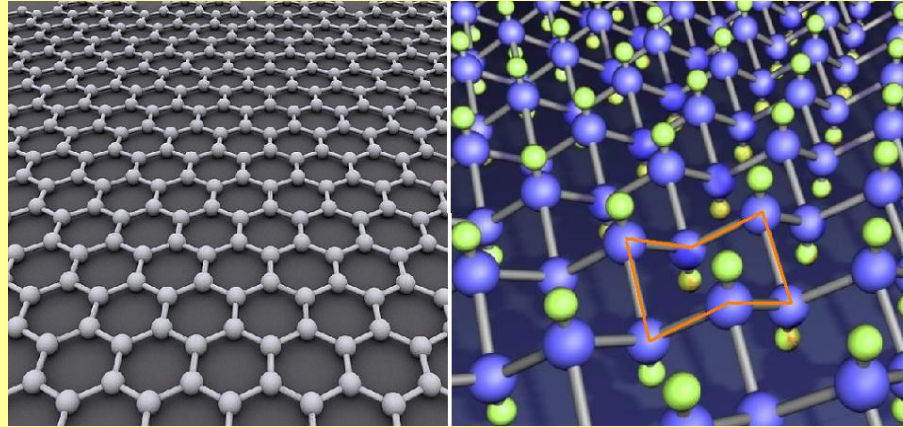


Graphane – Hydrogenated Graphene

- 2009 (graphene + cold hydrogen plasma)
- Two conformations: chair x boat
- Calculated binding energy = most stable compound with stoichiometric formula CH
- Chair type graphane insulating nanotubes

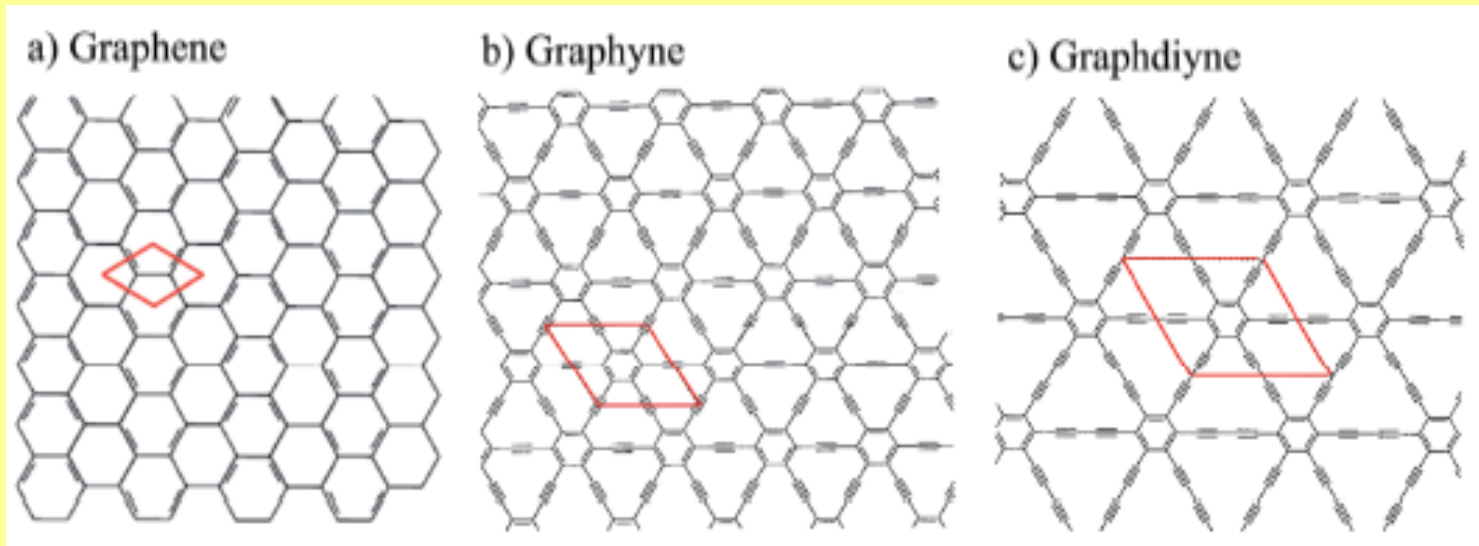


Fluorographene



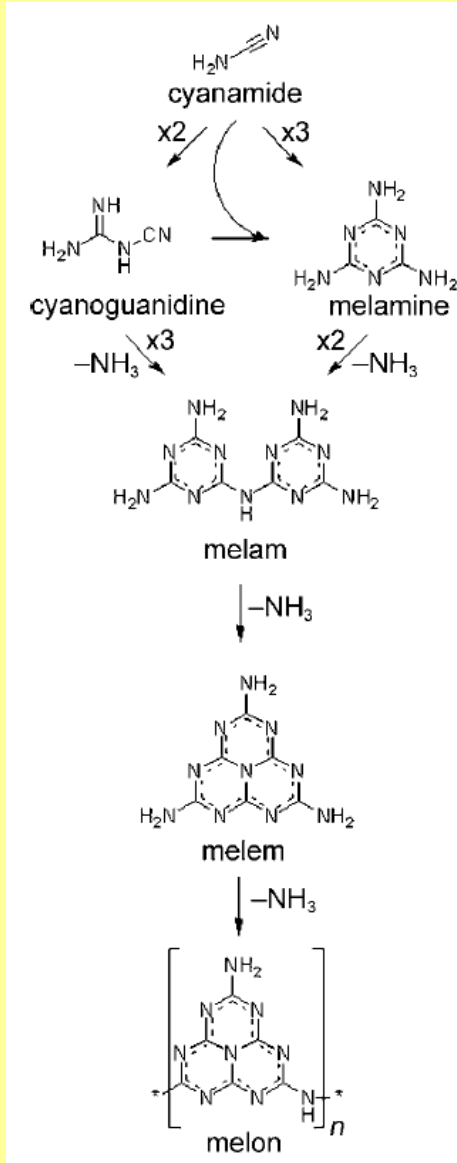
- **Monolayer of graphite fluoride**
- **Chair type x boat type-strong repulsion**
- **Synthesis:**
 - Graphene + XeF_2/CF_4 (room temperature)
 - Mechanical or chemical exfoliation of graphite fluoride
 - By heating graphene in XeF_2 gas at $250\text{ }^\circ\text{C}$
- **Graphene + XeF_2 at $70\text{ }^\circ\text{C}$ – high-quality insulator, stable up to $400\text{ }^\circ\text{C}$ (resemblance with teflon)**

Graphyn, Graphydiyn



- **Predicted**
- **“Non-derivatives“ of graphene**
- **Semiconductors**
- **Movement of electrons as in graphene but only in one direction**

Graphitic Carbon Nitride

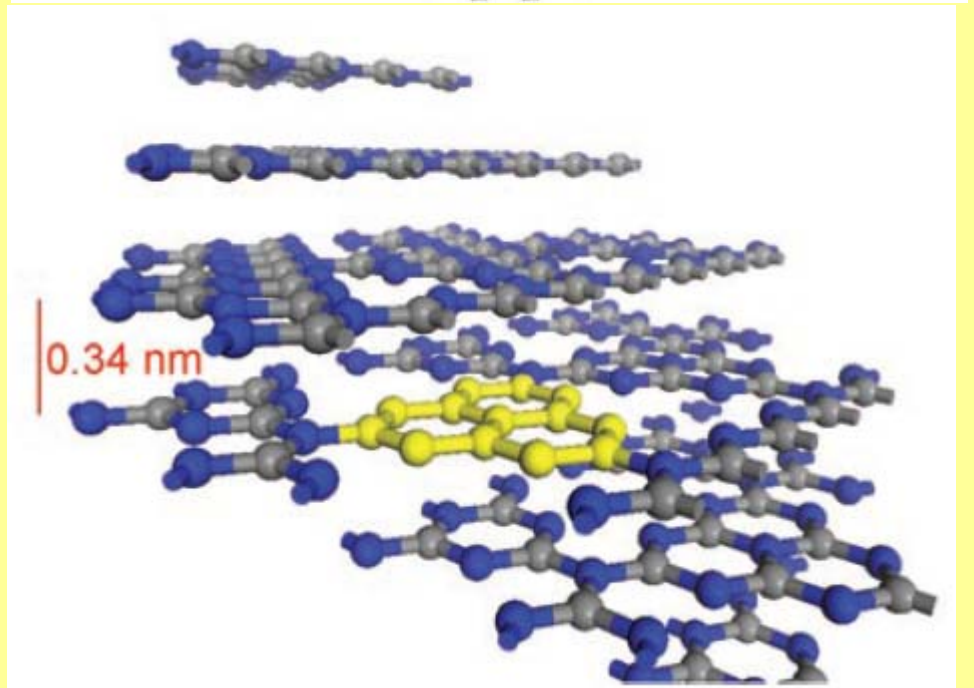
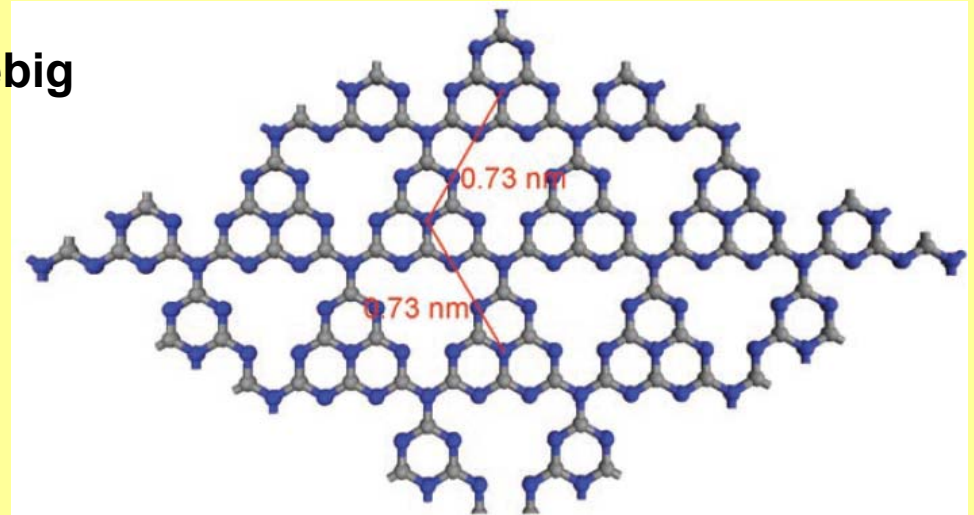


1834 Berzelius, Liebig

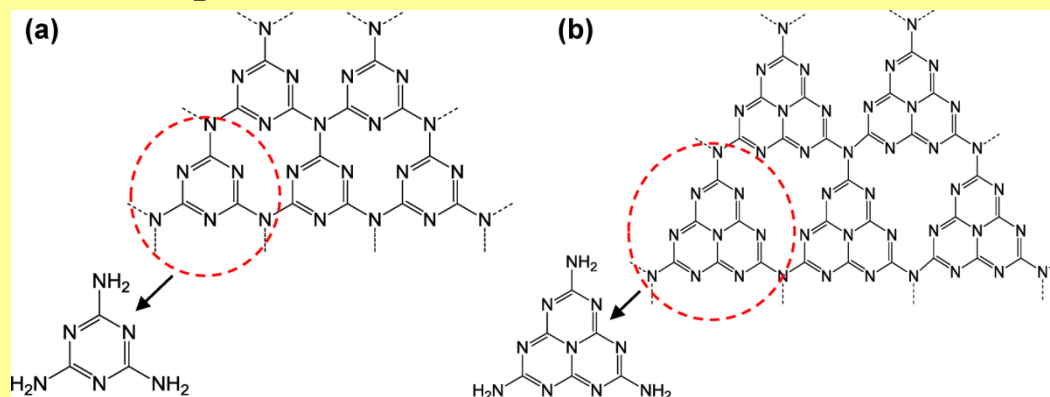
Temperature-induced condensation

dicyandiamide
 $\text{NH}_2\text{C}(\text{=NH})\text{NHCN}$

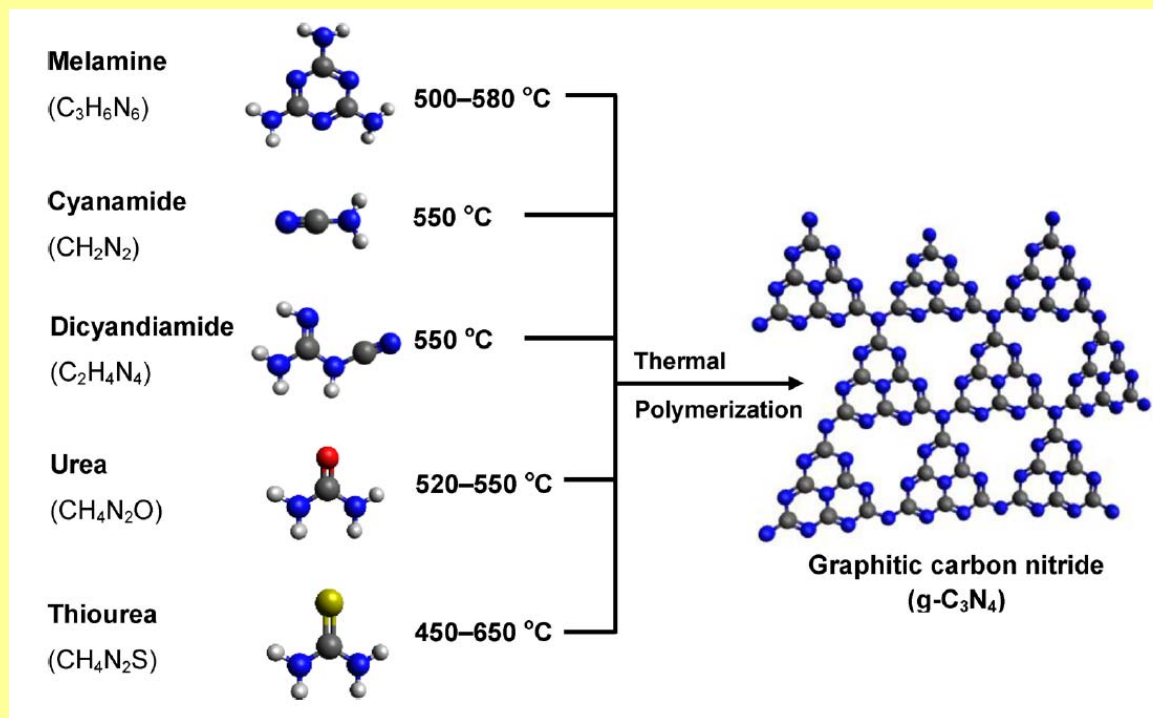
In a LiCl/KCl melt



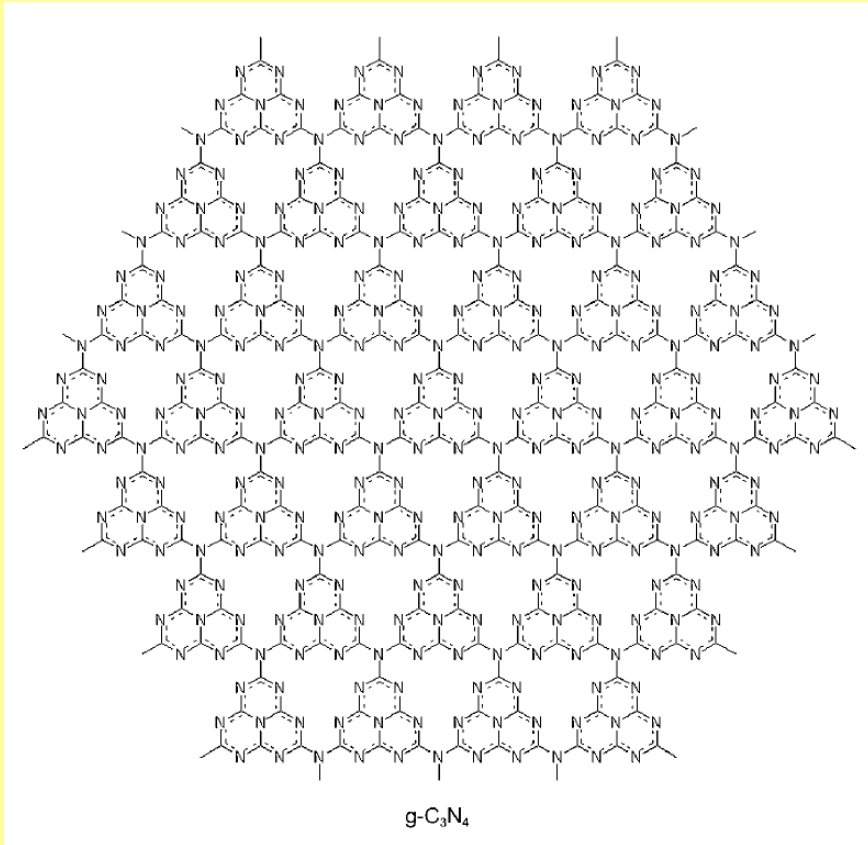
Graphitic Carbon Nitride



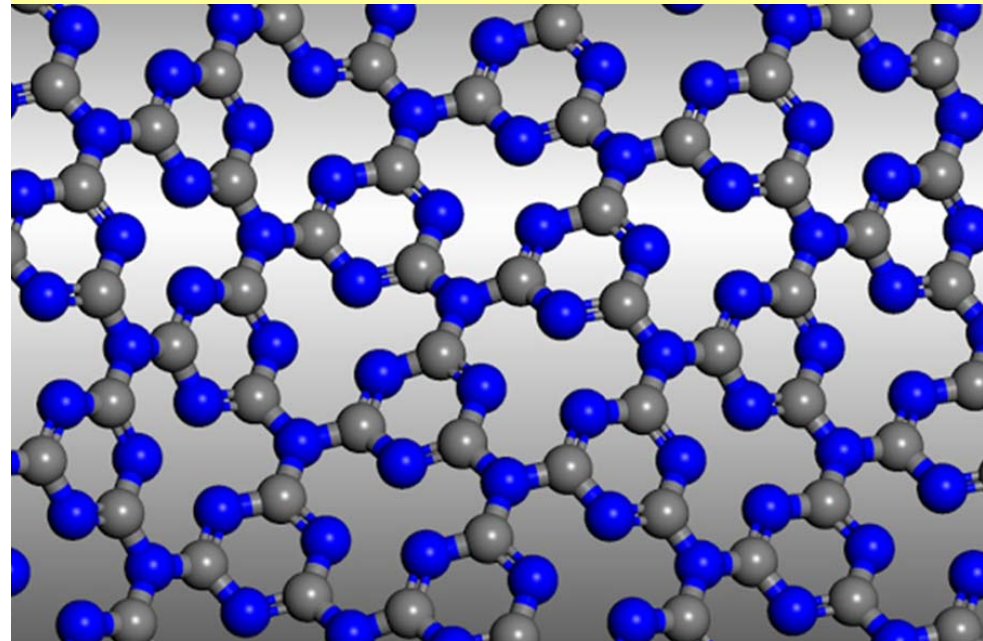
(a) triazine and (b) tri-s-triazine (heptazine)



Graphitic Carbon Nitride

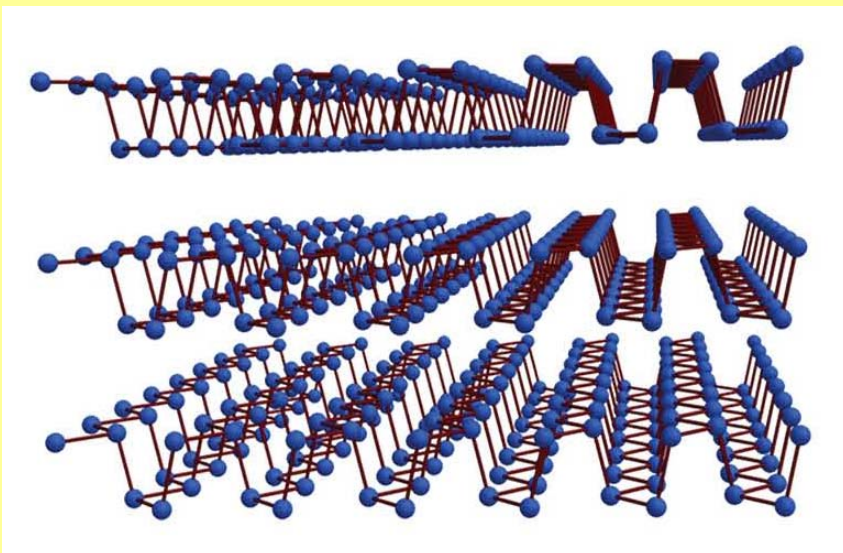


(“g-C₃N₄”)



band gap 1.6 - 2.0 eV
small band gap semiconductors
Si (1.11 eV), GaAs (1.43 eV), and GaP (2.26 eV)

Phosphorene



Black phosphorus

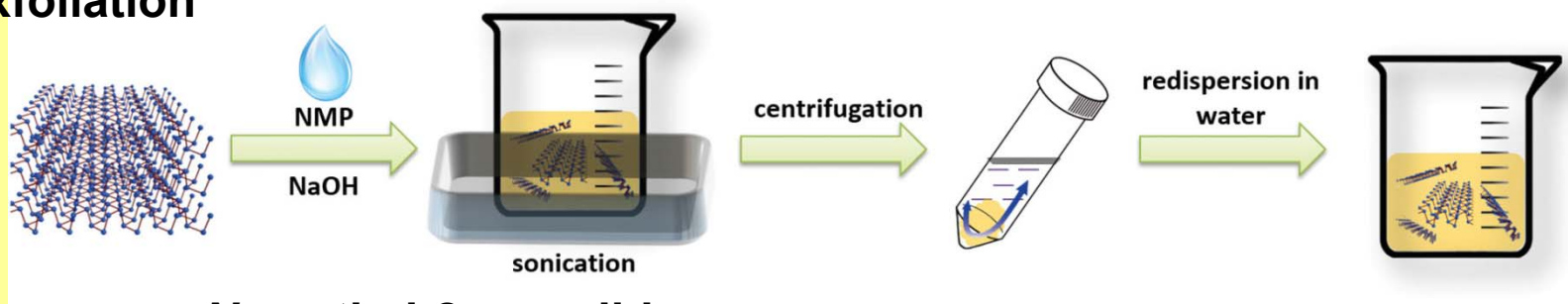
Orthorhombic

$a = 3.31 \text{ \AA}$, $b = 4.38 \text{ \AA}$, $c = 10.50 \text{ \AA}$

$\alpha = \beta = \gamma = 90^\circ$

Space group *Bmab*

Exfoliation



N-methyl-2-pyrrolidone

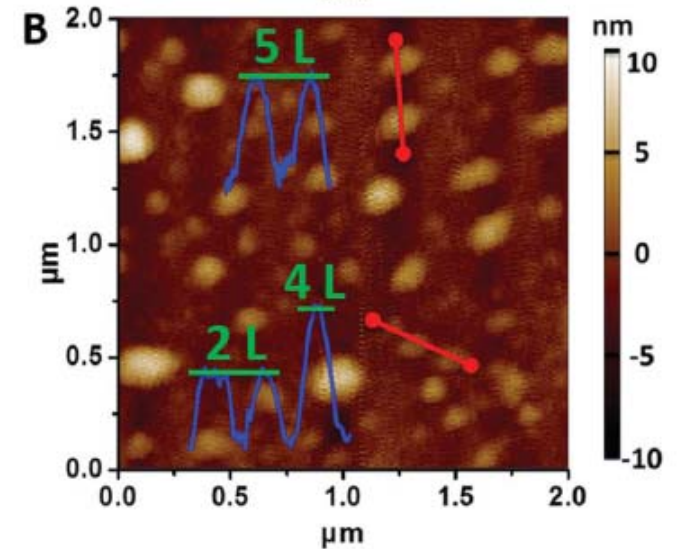
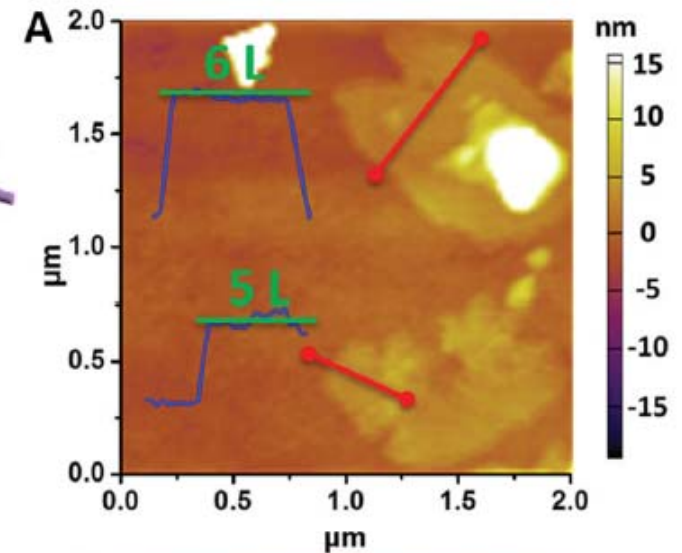
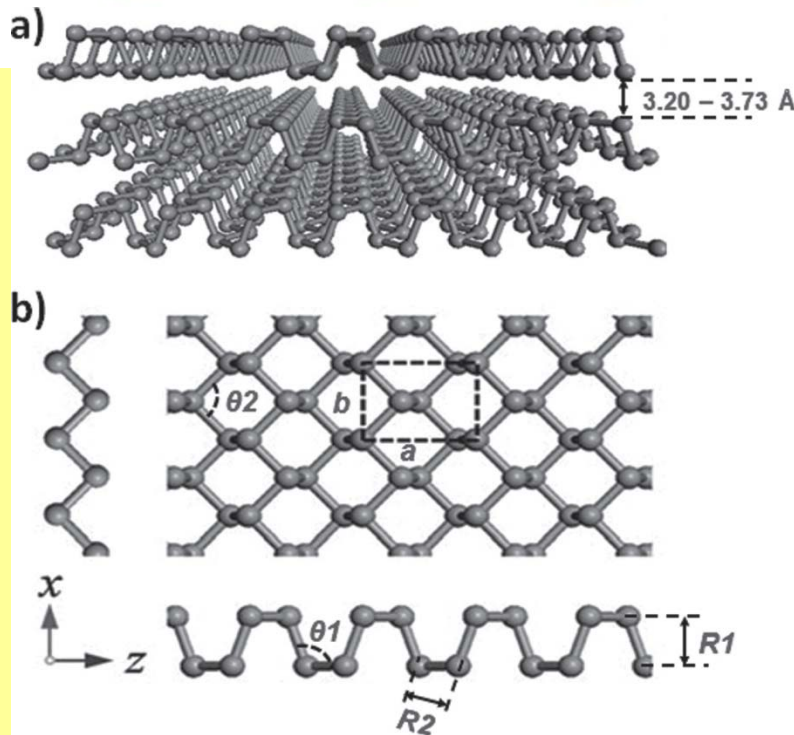
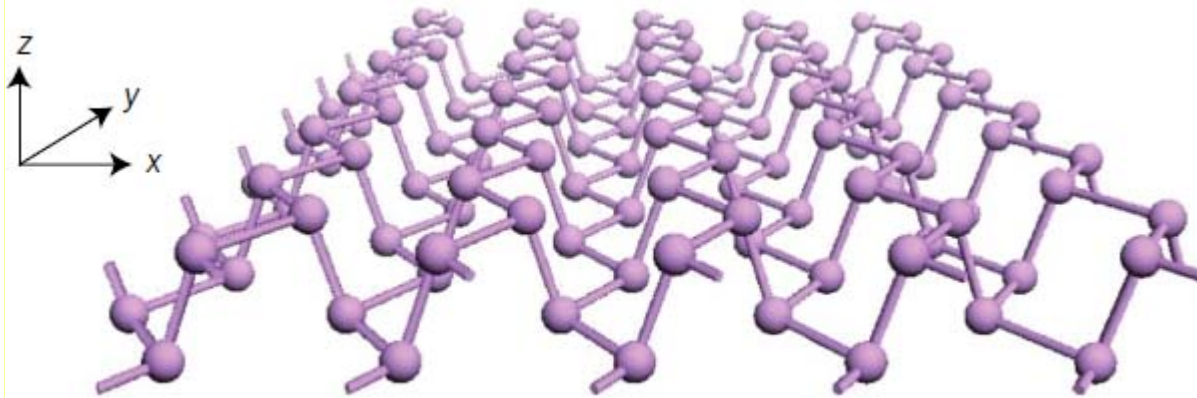
Semiconductor - direct band gap

bulk BP 0.3 eV

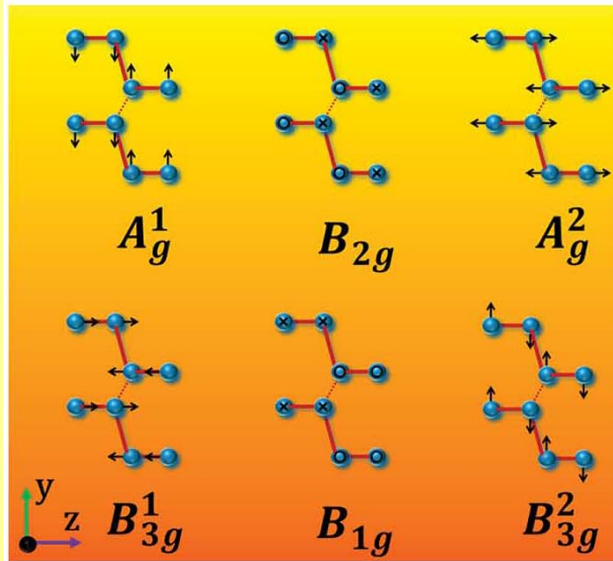
monolayer phosphorene 1.5 eV

Phosphorene

Height-mode AFM images
single-layer phosphorene
ca. 0.9 nm



Phosphorene



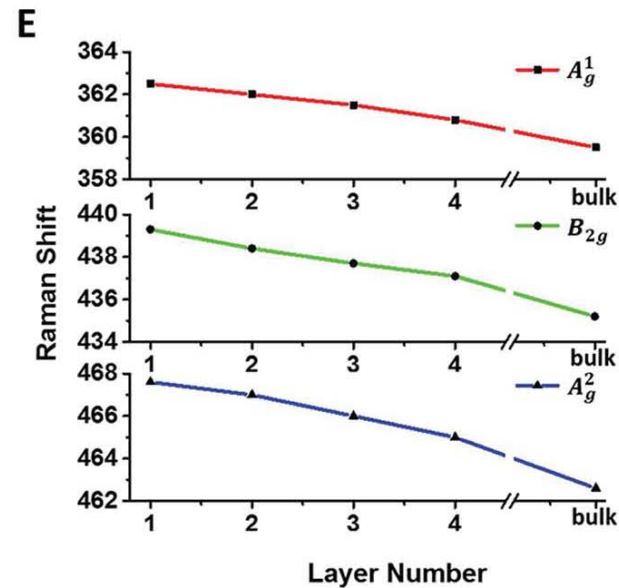
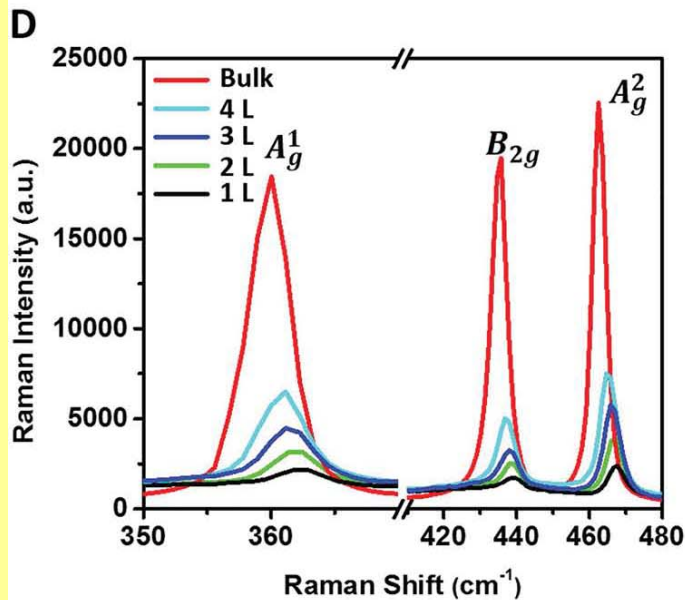
Black phosphorus

12 lattice vibrational modes

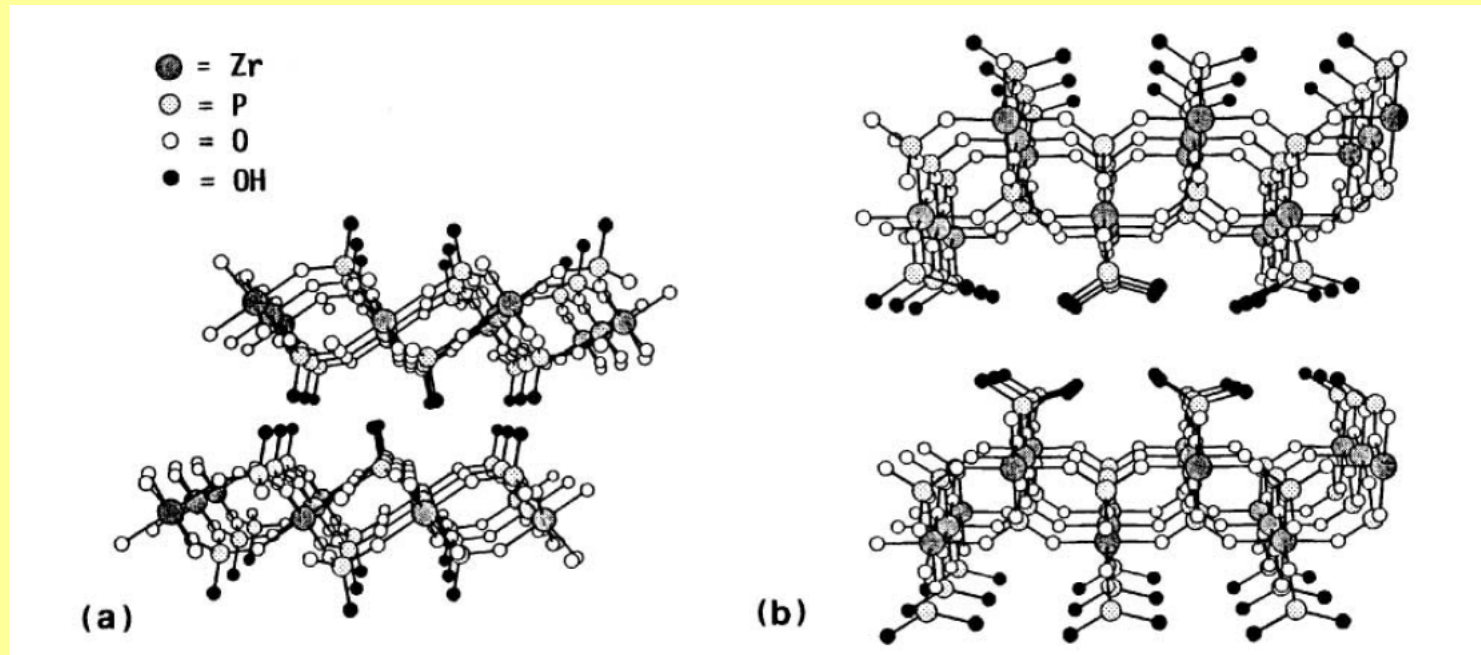
6 Raman active modes

3 vibrational modes A_{1g}^1 , B_{2g} , and A_{2g}^2 can be detected when the incident laser is perpendicular to the layered phosphorene plane: 361 cm^{-1} , 438 cm^{-1} , 465 cm^{-1}

As the number of phosphorene layers increases, the three Raman peaks red-shift



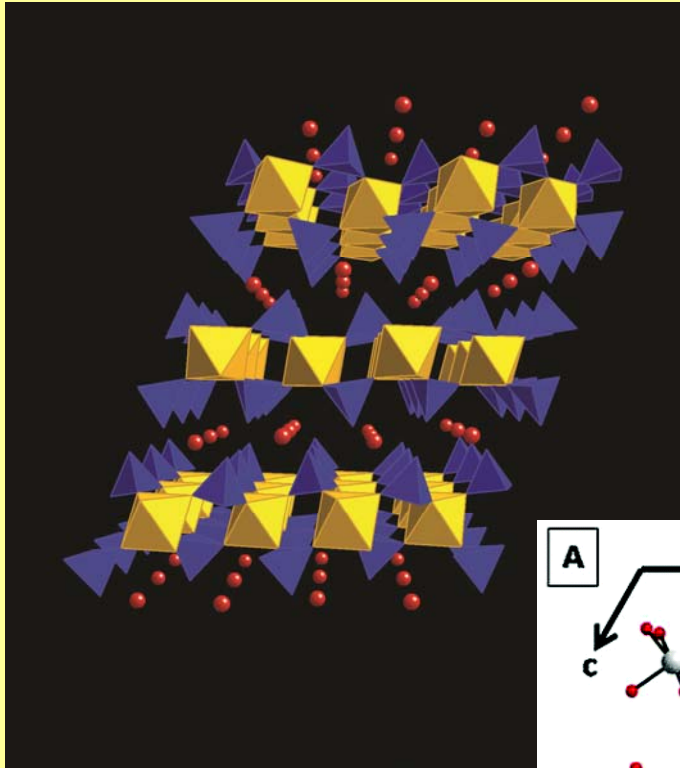
Zirconium Phosphates



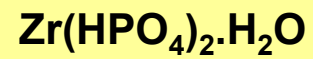
(a) α -zirconium phosphate = $\text{Zr}(\text{HPO}_4)_2 \cdot \text{H}_2\text{O}$
interlayer spacing 7.6 Å

(b) γ -zirconium phosphate = $\text{Zr}(\text{PO}_4)(\text{H}_2\text{PO}_4)_2 \cdot 2\text{H}_2\text{O}$
interlayer spacing 12.2 Å

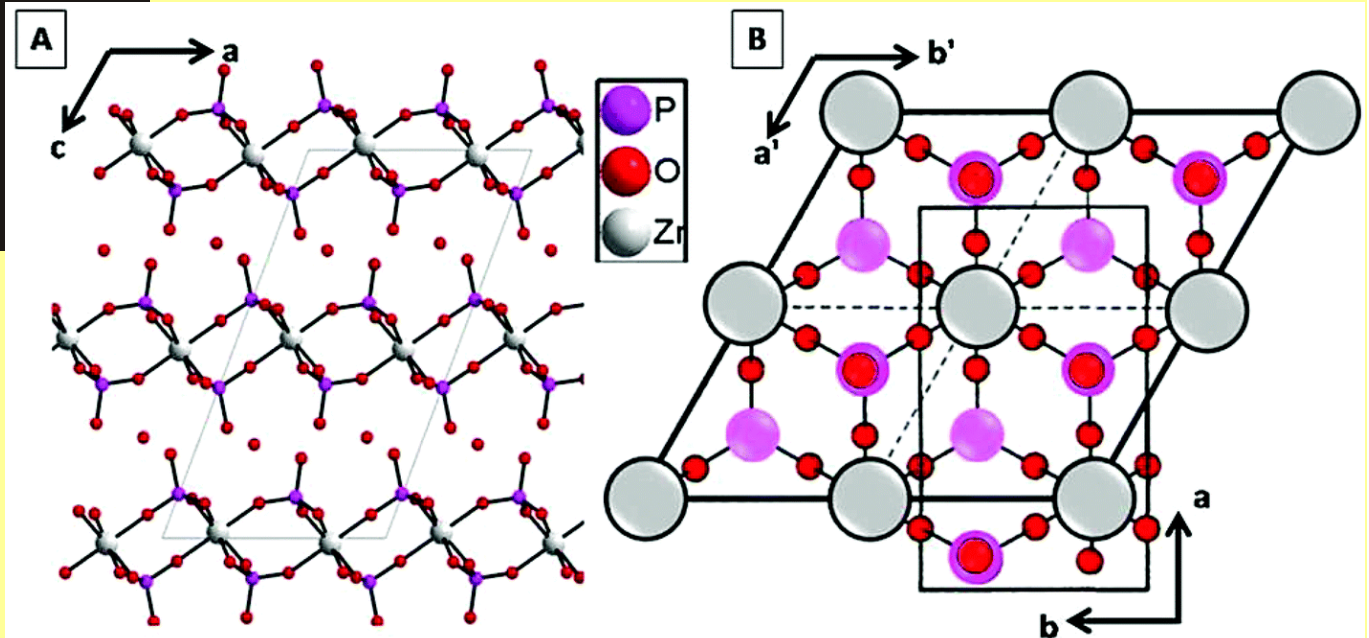
Zirconium Phosphates



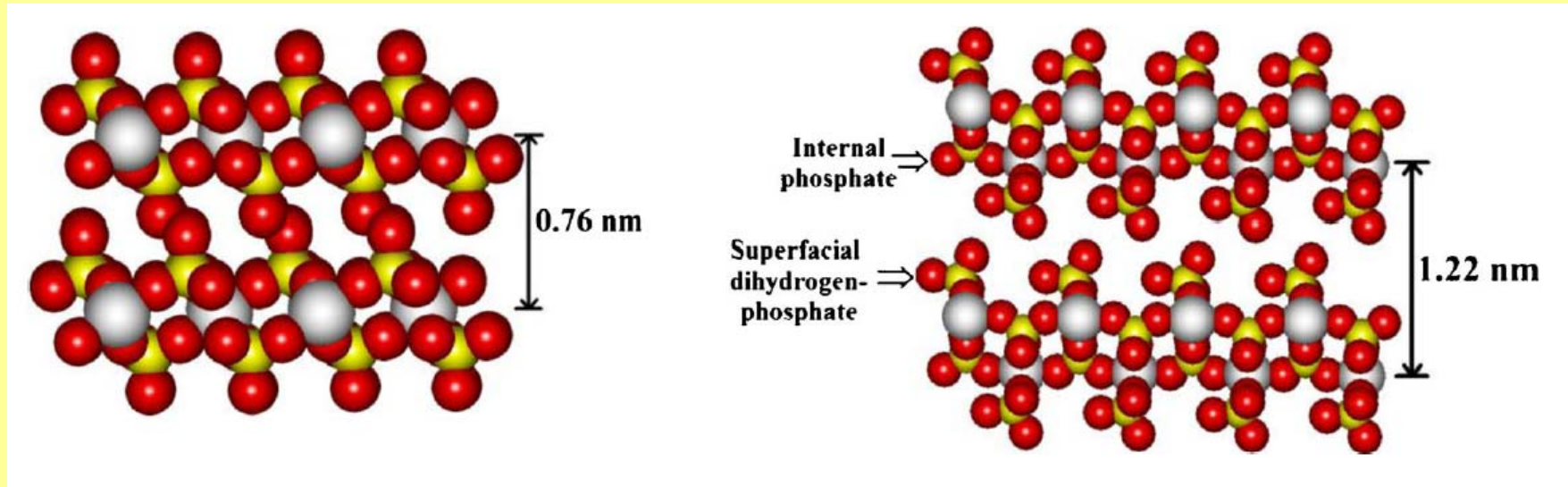
α -zirconium phosphate



interlayer spacing 7.6 Å



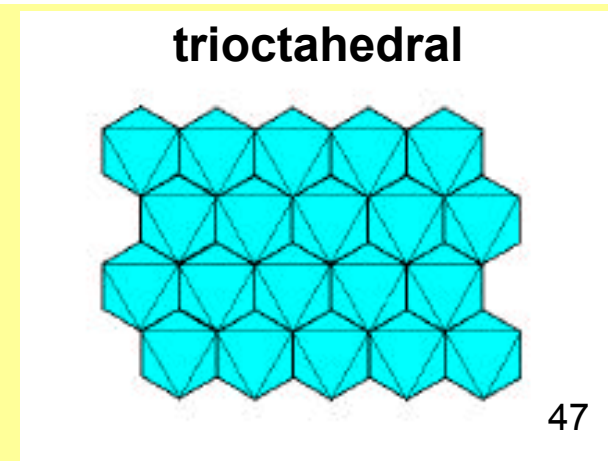
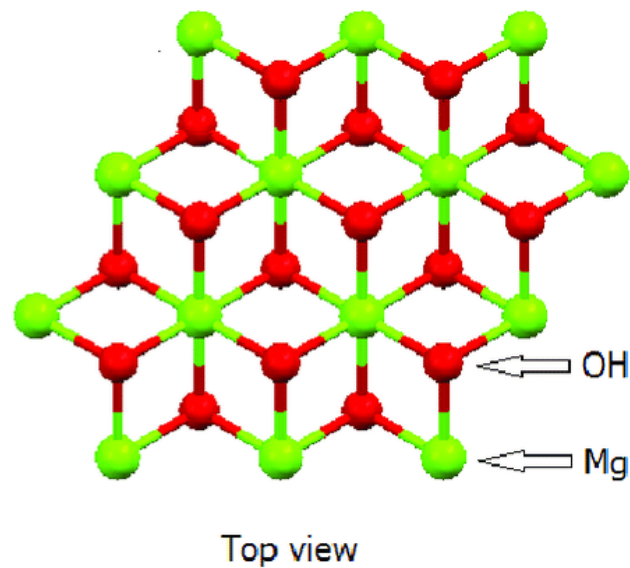
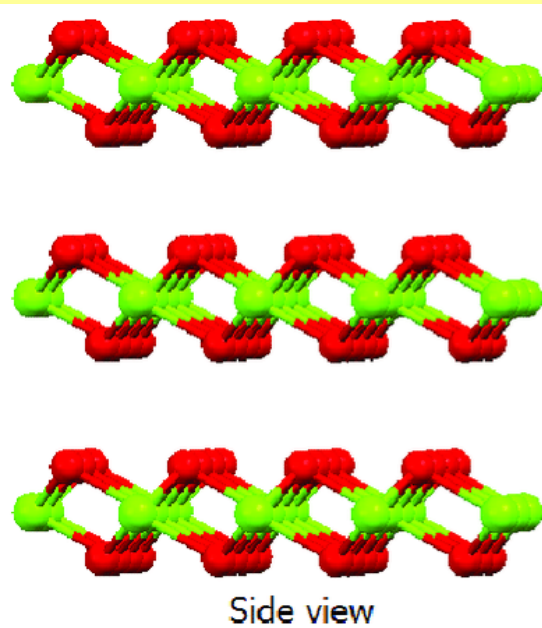
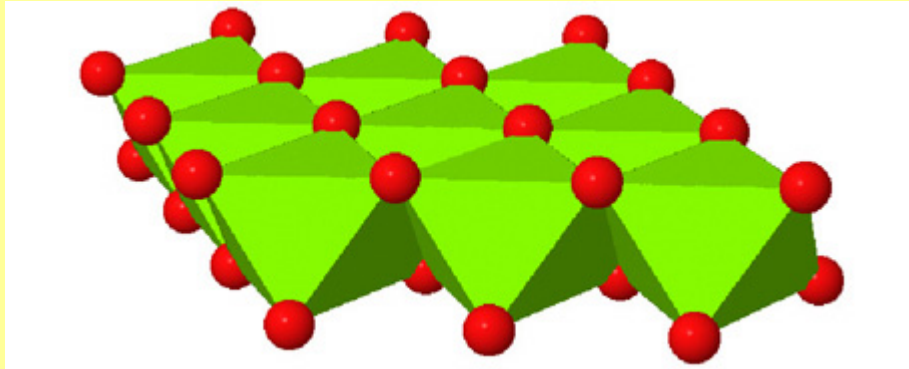
Zirconium Phosphates



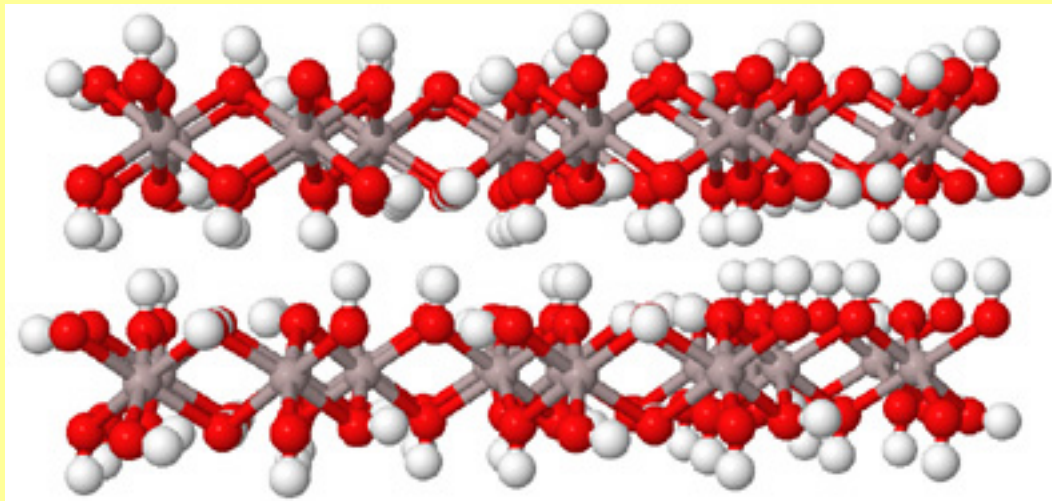
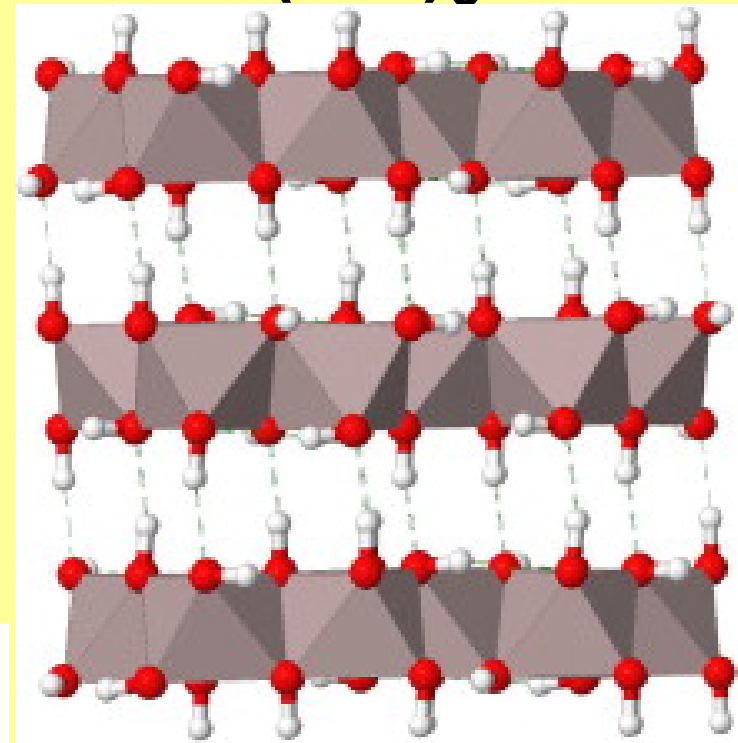
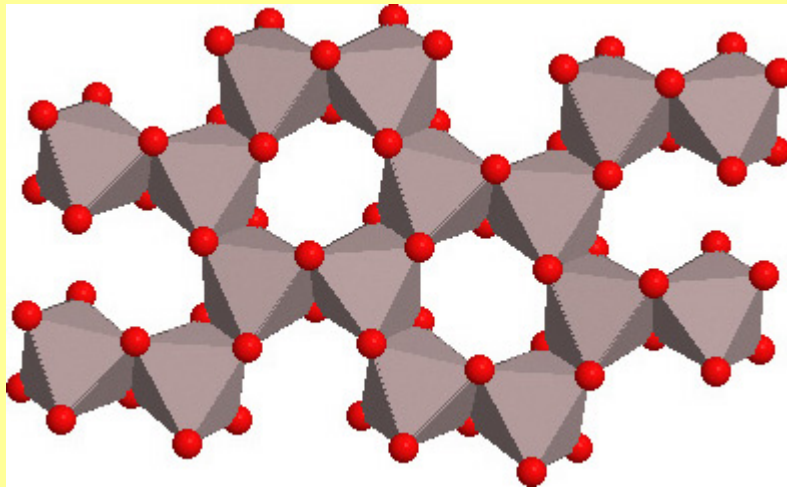
(a) α -zirconium phosphate = $\text{Zr}(\text{HPO}_4)_2 \cdot \text{H}_2\text{O}$
interlayer spacing 7.6 Å

(b) γ -zirconium phosphate = $\text{Zr}(\text{PO}_4)(\text{H}_2\text{PO}_4)2\text{H}_2\text{O}$
interlayer spacing 12.2 Å

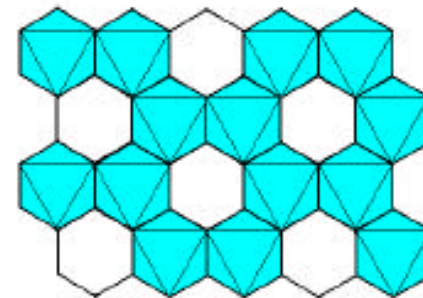
Brucite - $Mg(OH)_2$



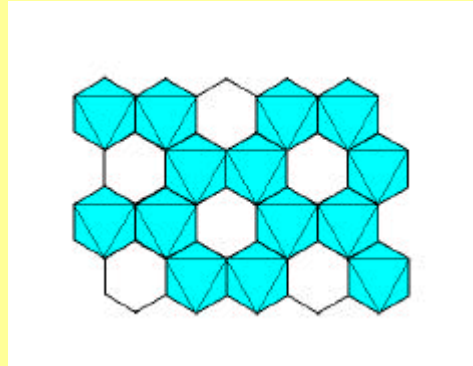
Bayerite and Gibbsite - $\text{Al}(\text{OH})_3$



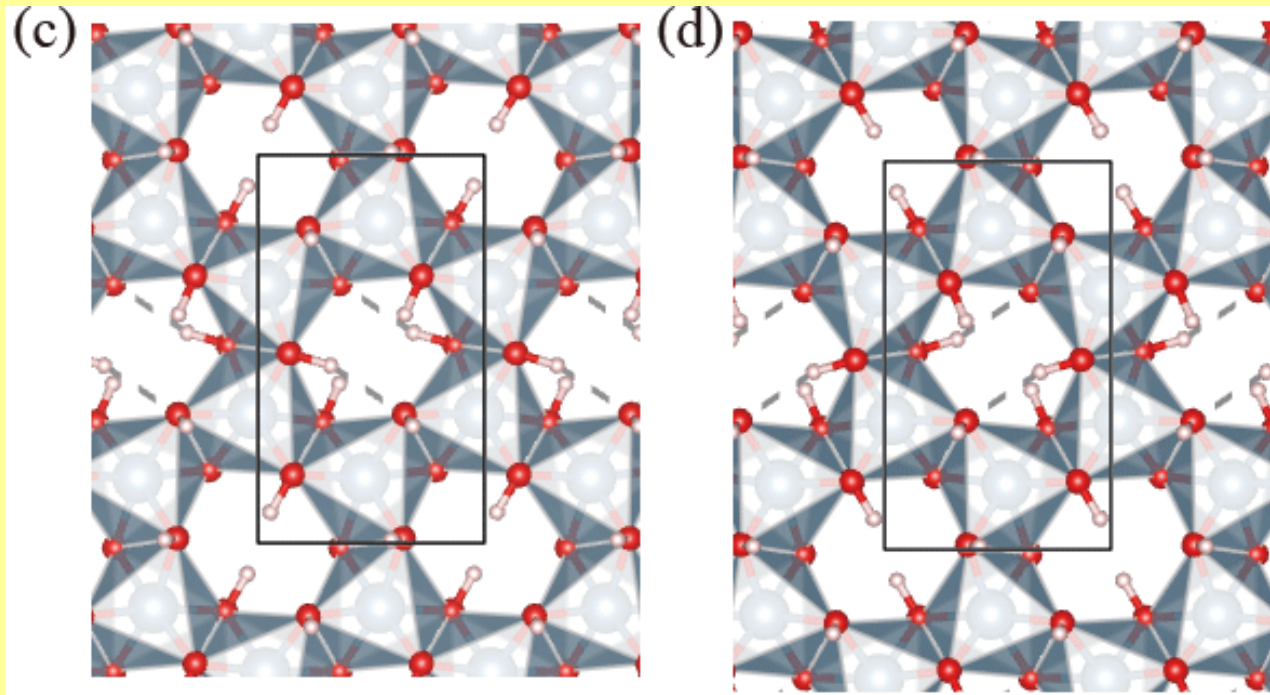
dioctahedral



Bayerite and Gibbsite - $\text{Al}(\text{OH})_3$



Opposite faces of a single layer $\text{Al}(\text{OH})_3$ (A and B sides, respectively)

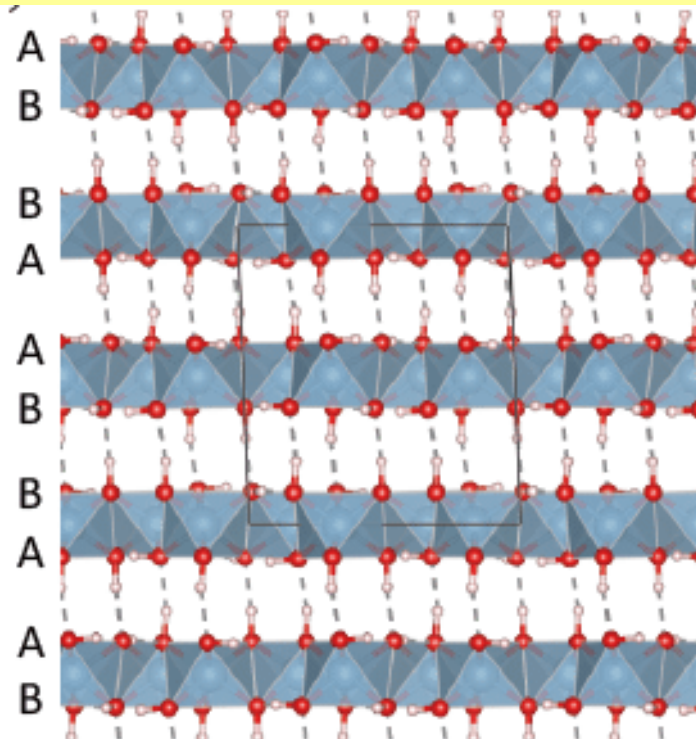
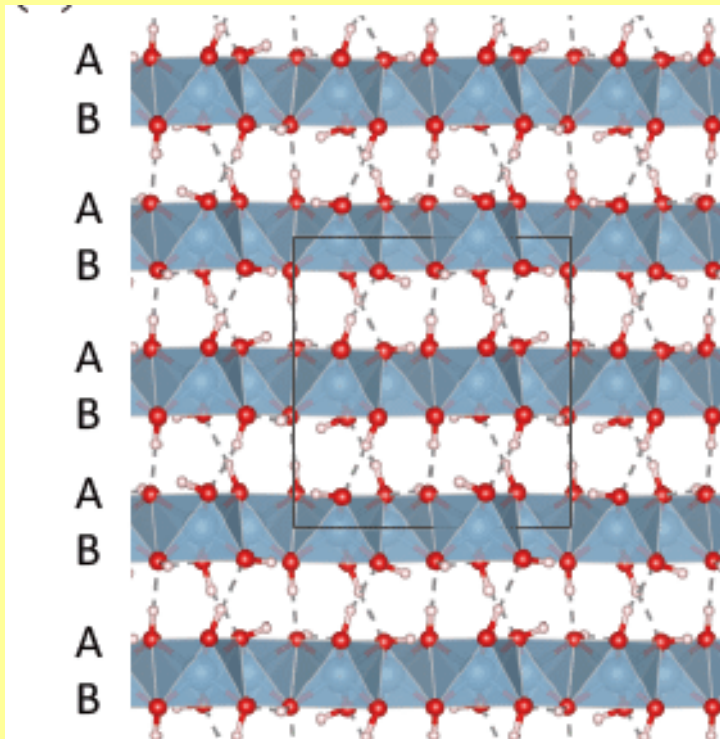


Bayerite and Gibbsite - $\text{Al}(\text{OH})_3$

Bayerite and Gibbsite phases have an identical single layer as the building block

Bayerite is stacked
by AB-AB sequence
HCP of oxides

Gibbsite is stacked
by AB-BA sequence
CCP of oxides

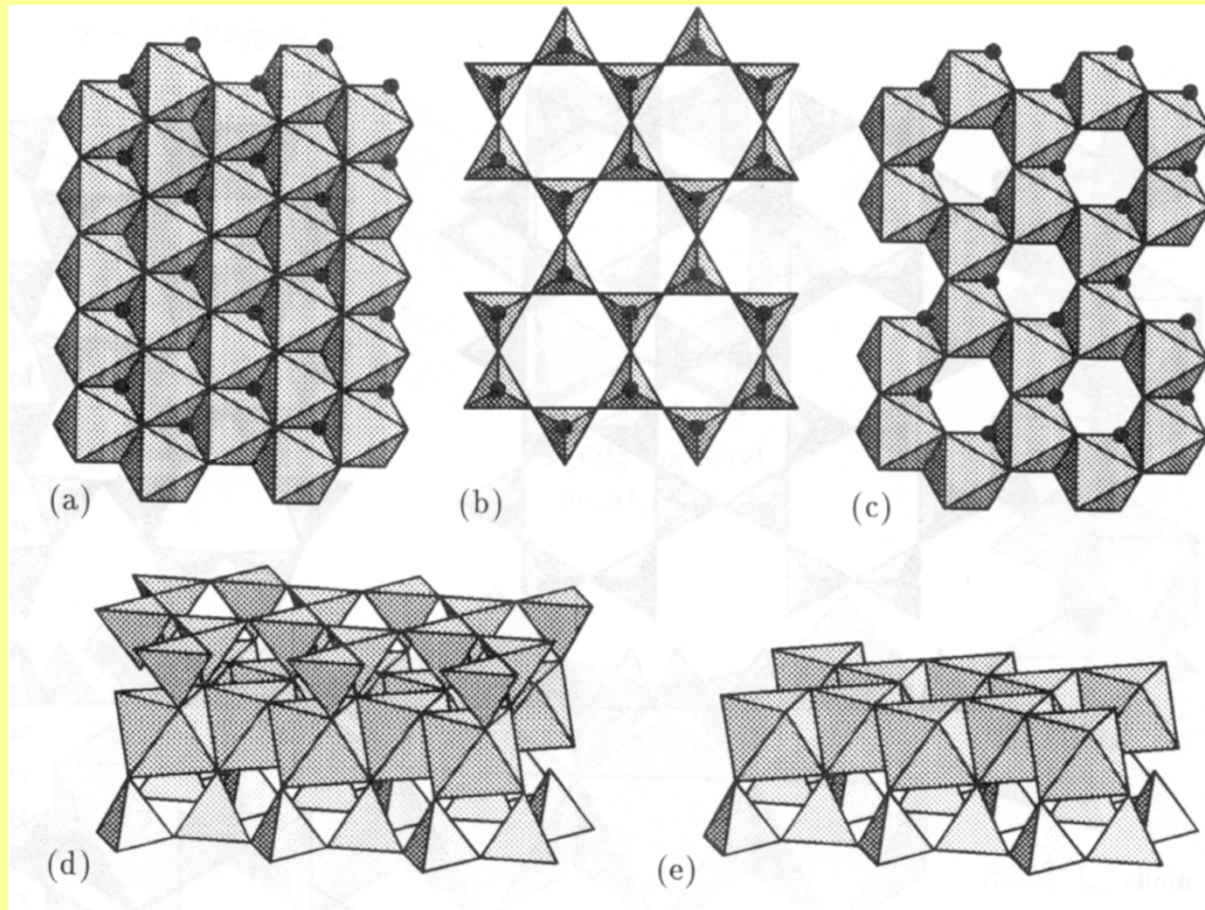


Clay Minerals

$[\text{Si}_4\text{O}_{10}]^{4-}$ tetrahedral sheet

$[\text{Mg}_6\text{O}_{12}]^{12-}$
trioctahedral
sheet of
octahedral
units

$[\text{Al}_4\text{O}_{12}]^{12-}$
dioctahedral
sheet



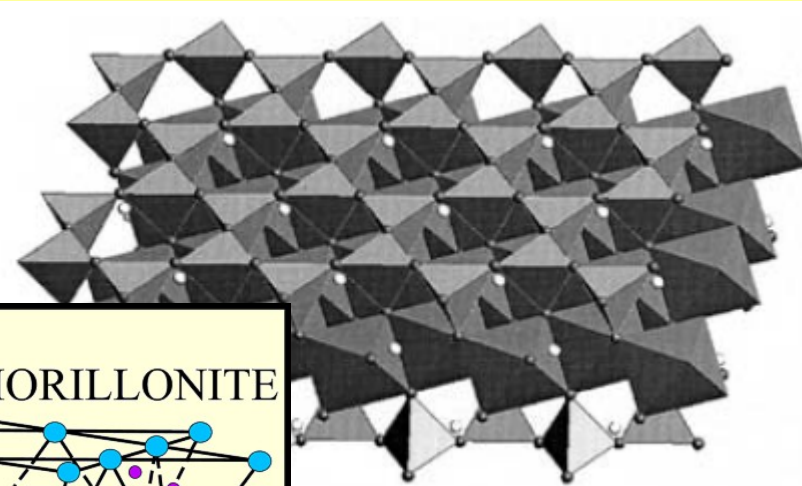
2:1

montmorillonite

1:1

kaolinite

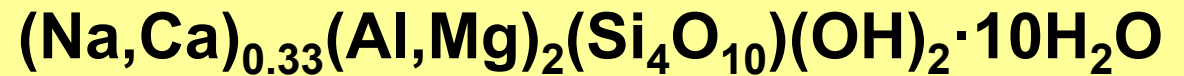
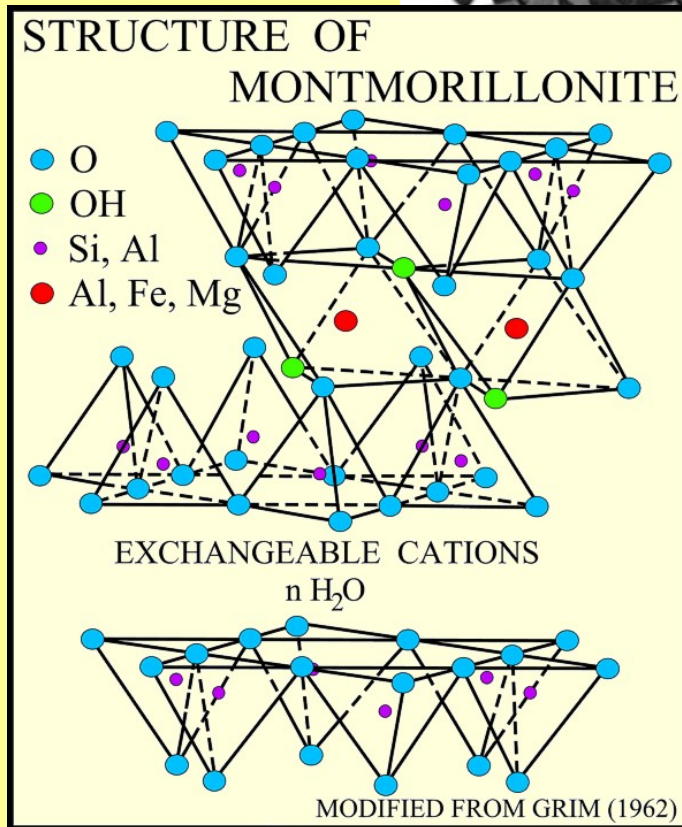
Montmorillonite



- Dioctahedral clay mineral
- $T_d-O_h-T_d$ sandwich
- Isomorphous substitution

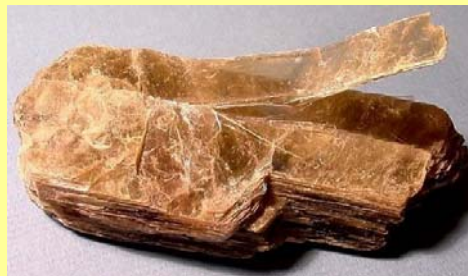
O_h : Al^{3+} by Mg^{2+}
 T_d : Si^{4+} by Al^{3+}

→ Net negative charge
 → Interlayer cations



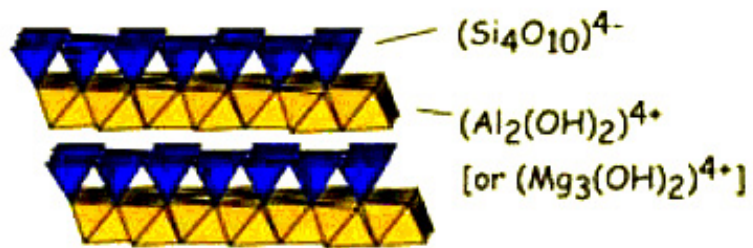
Phyllosilicate Minerals

Structure	Interlayer Charge	Trioctahedral (Y ²⁺)	Diocahedral (Y ³⁺)
O	~0	Brucite	Gibbsite
TO	~0	Serpentine	Kaolinite
TOT	~0	Talc	Pyrophyllite
TOT O TOT	~0	Chlorite	
TOT (X ⁺ , X ²⁺ , H ₂ O) TOT expandable clay	~0.2-0.6	Saponite (smectite)	Montmorillonite (smectite)
	~0.6-0.9	Vermiculite	
TOT (X ⁺ , X ²⁺) TOT non-expandable clay	~0.5-0.75	-	Illite
TOT X ⁺ TOT true mica	1	Phlogopite, Biotite	Muscovite, Paragonite
TOT X ²⁺ TOT brittle mica	2	Clintonite	Margarite

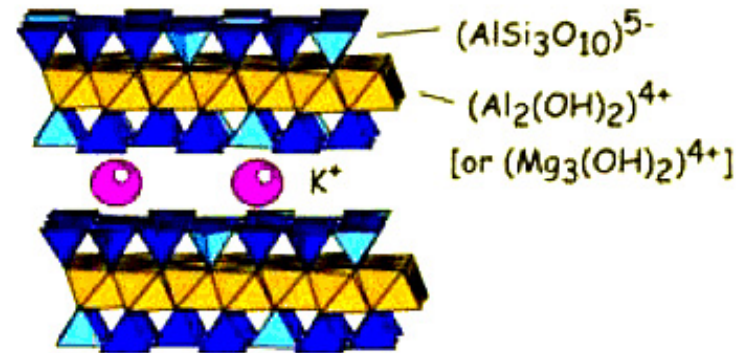


Phyllosilicate Minerals

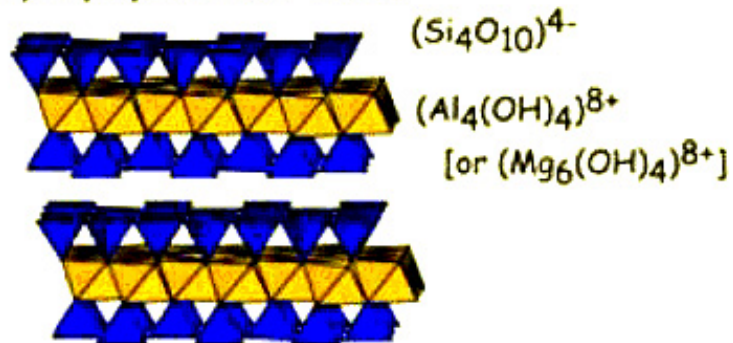
Kaolinite (or Antigorite)



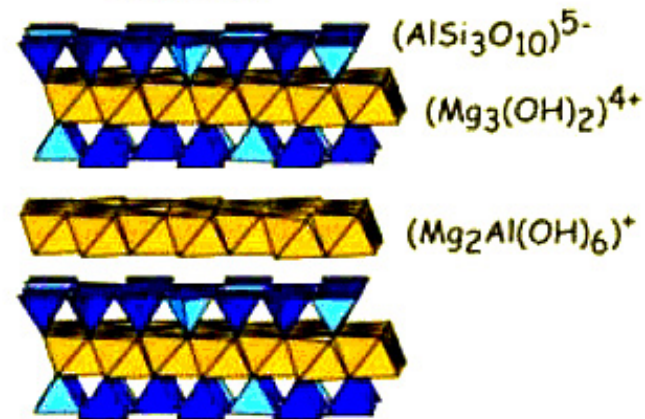
Muscovite (or Phlogopite)



Pyrophyllite (or Talc)



Chlorite



Clay Minerals

N₂ sorption isotherms

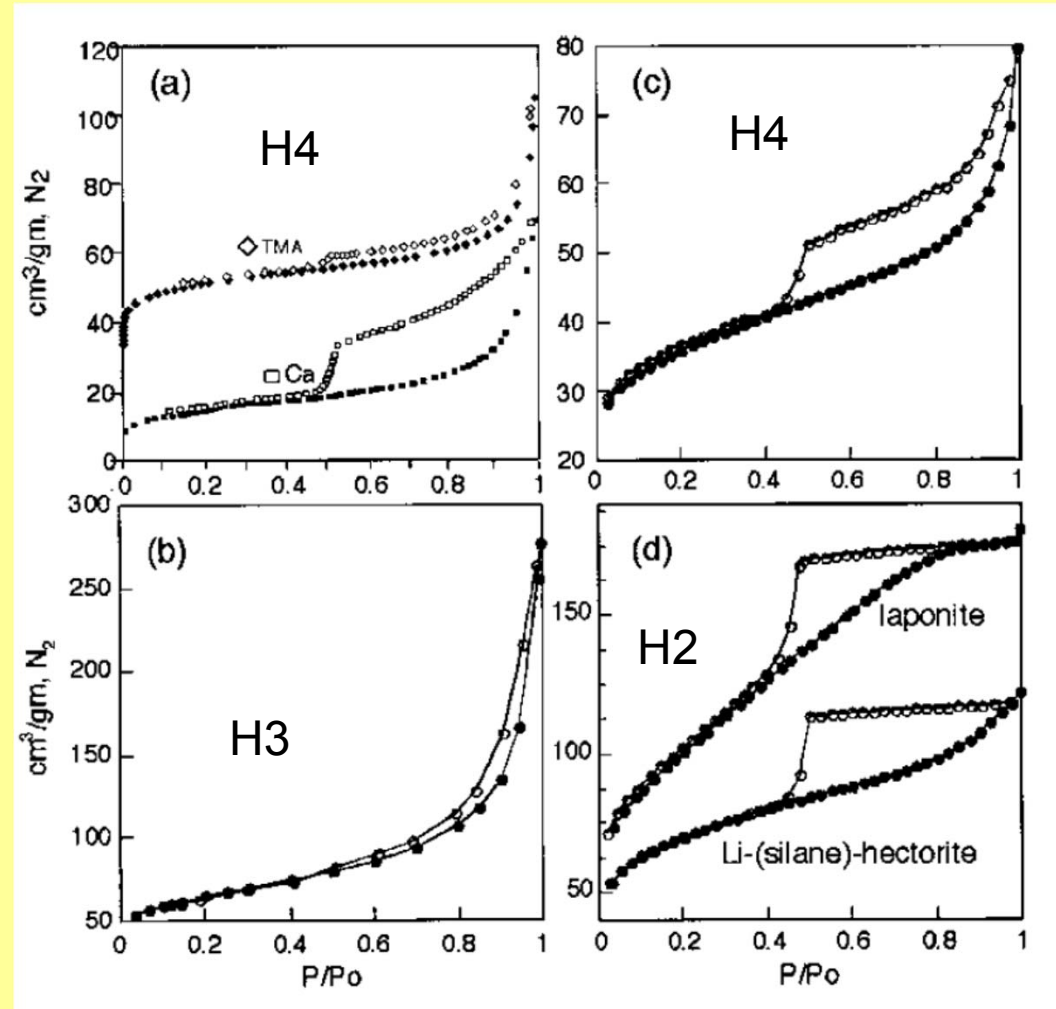
(a) TMA- and Ca-montmorillonite

(b) An Italian sepiolite

(c) Natural SHCa-1 Na-hectorite

(d) synthetic laponite and Li-(silane)-hectorites

Closed symbols = adsorption
Open symbols = desorption



Surface Area

the most important parameters of clays with respect to catalytic applications

TABLE 3 N₂ BET Surface Areas of Various Clay Minerals

Clay	Outgassing conditions	S. A., m ² /g
Kaolinite ^{a,b}	200 °C, overnight, <10 ⁻² torr	8.75
Na,Ca-montmorillonite ^{a,c}	same	31.0
Ca-montmorillonite ^{a,d}	same	80.2
Ca-montmorillonite ^{a,e}	same	93.9
Na-hectorite ^{a,f}	same	64.3
Laponite ^g	105 °C, overnight, 10 ⁻³ torr	360
Sepiolite ^h	96 °C, 3 h	378
Palygorskite ^h	95 °C, <70 h	192

nonpolar guest molecules N₂ do not penetrate the interlayer regions

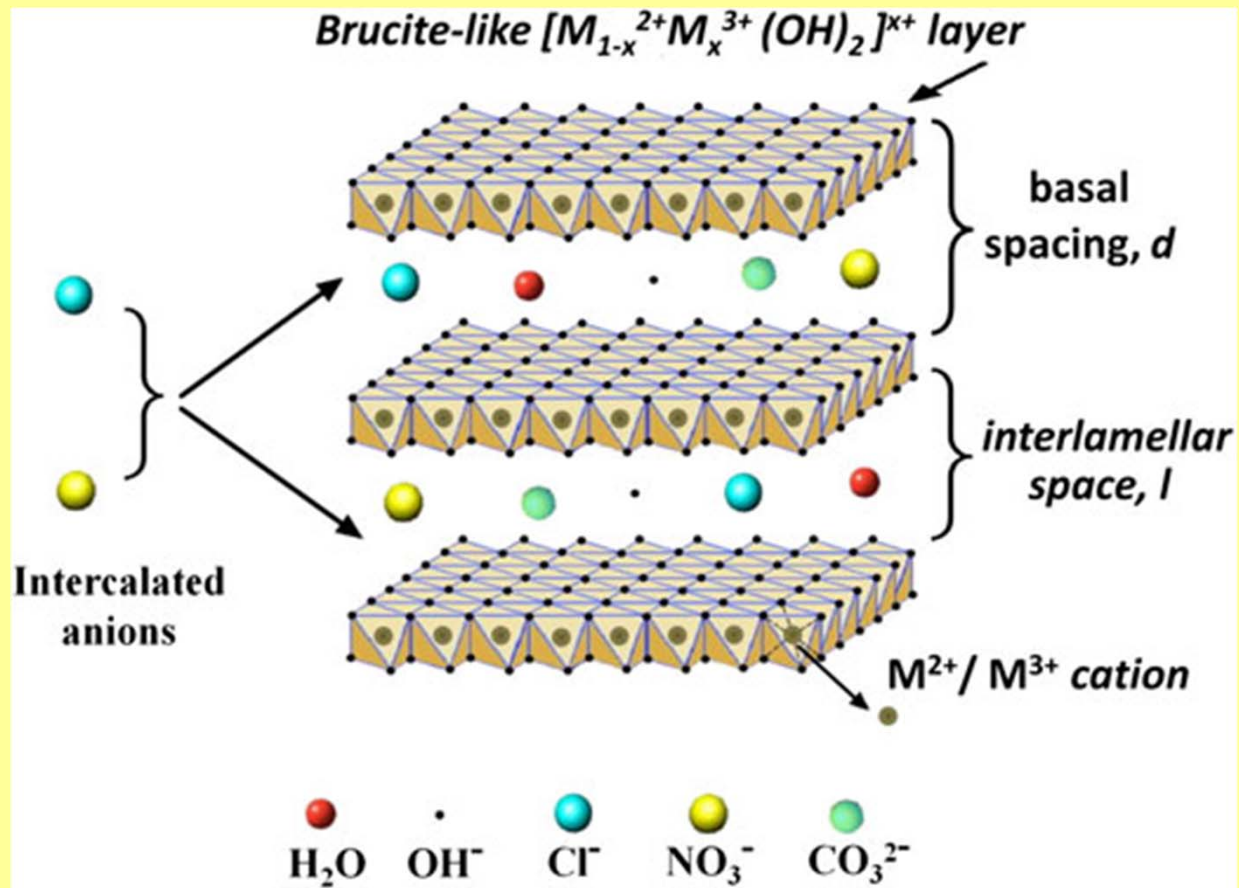
Na⁺ forms of smectites and vermiculites – no penetration

larger ions (Cs⁺ and NH₄⁺ keep the basal planes far enough) - limited penetration

Layered Double Hydroxides

LDH = layered double hydroxides

HT = hydrotalcites



Layered Double Hydroxides

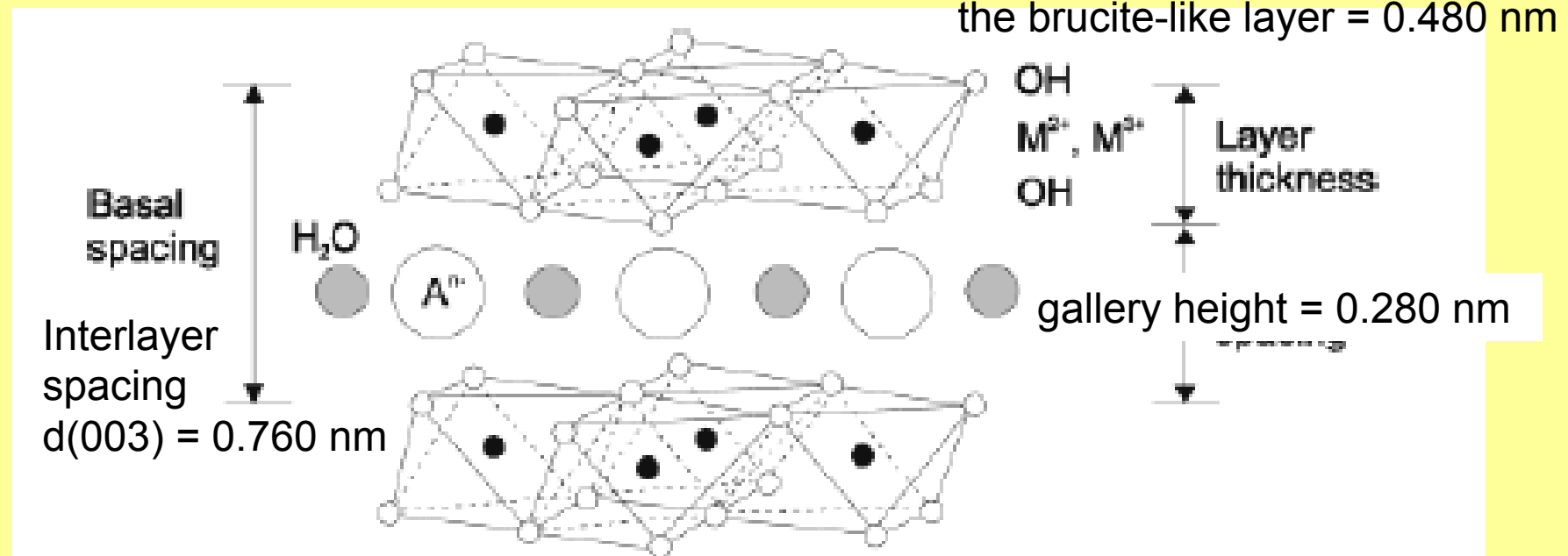
LDH = layered double hydroxides

HT = hydrotalcites

Natural mineral hydrotalcite $\text{Mg}_6\text{Al}_2(\text{OH})_{16}\text{CO}_3 \cdot 4\text{H}_2\text{O}$

Brucite layers, Mg^{2+} substituted partially by Al^{3+}

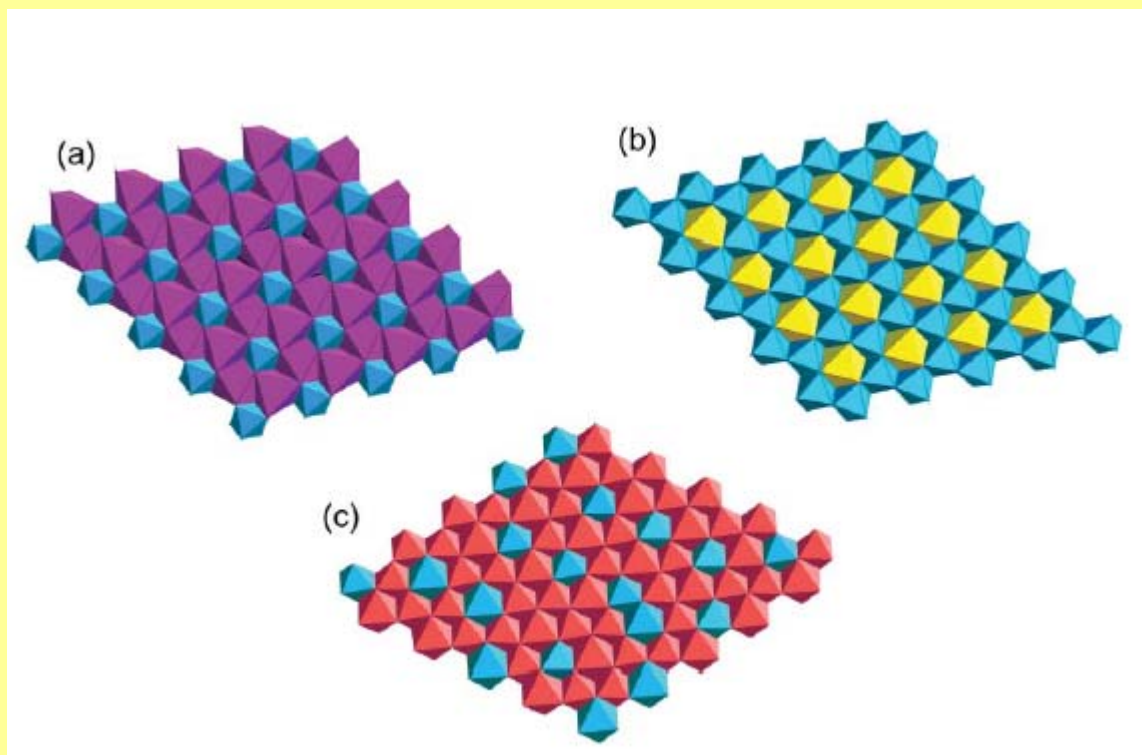
Layers have positive charge



Hydrotalcite $\text{Mg}_6\text{Al}_2(\text{OH})_{16}\text{CO}_3 \cdot 4\text{H}_2\text{O}$

Hydrotalcites

Brucite layers, Mg^{2+} substituted partially by Al^{3+}
Layers have positive charge



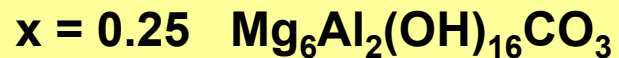
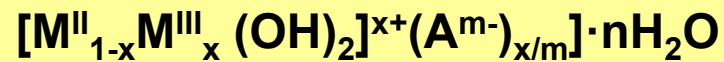
(a) $[\text{Ca}_2\text{Al}(\text{OH})_6]_2\text{SO}_4 \cdot 6\text{H}_2\text{O}$ (b) $[\text{LiAl}_2(\text{OH})_6]\text{Cl}$ (c) $[\text{Mg}_{2.25}\text{Al}_{0.75}(\text{OH})_6]\text{OH}$

Hydrotalcite

The layered structure of LDH is closely related to brucite $\text{Mg}(\text{OH})_2$

a brucite layer, Mg^{2+} ions octahedrally surrounded by six OH^-
the octahedra share edges and form an infinite two-dimensional layer
the brucite-like layers stack on top of one another
either rhombohedral (3R) or hexagonal (2H) sequence

Hydrotalcite $\text{Mg}_6\text{Al}_2(\text{OH})_{16}\text{CO}_3 \cdot 4\text{H}_2\text{O}$ - 3R stacking



Hydrotalcite

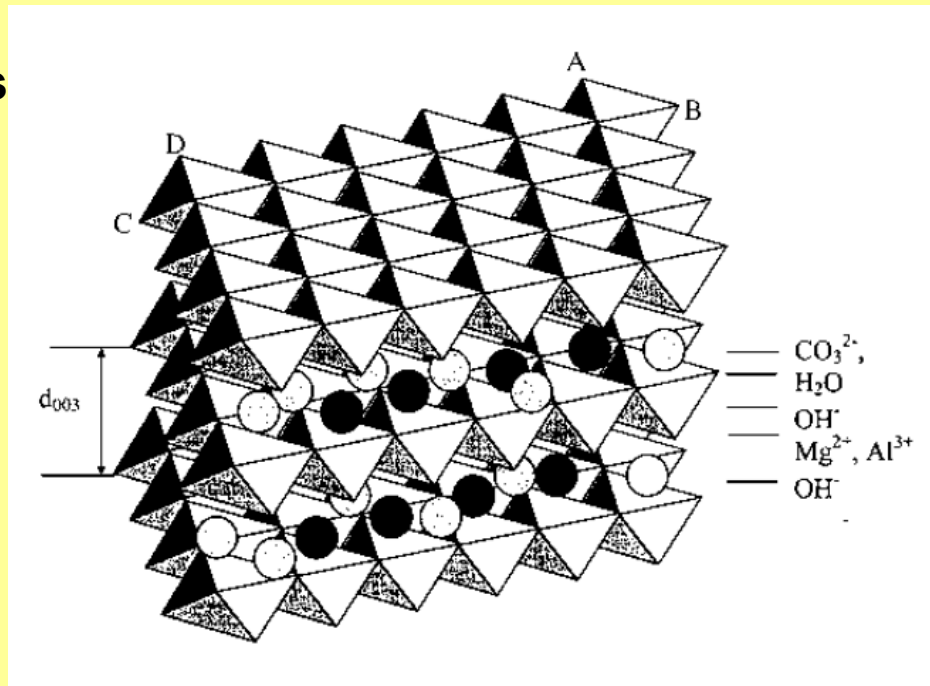
The interlayer spacing c' is equal to d_{003} , $2d_{006}$, $3d_{009}$, etc.;

$$c' = (d_{003} + 2d_{006} + \dots + nd_{00(3n)}) / n$$

The cell parameter c is a multiple of the interlayer spacing c'

$$c = 3c' \text{ for rhombohedral (3R)}$$

$$c = 2c' \text{ for hexagonal (2H) sequences}$$



Hydrotalcite

Hydrotalcite $\text{Mg}_6\text{Al}_2(\text{OH})_{16}\text{CO}_3 \cdot 4\text{H}_2\text{O}$ - 3R stacking

unit cell parameters

$$a = 0.305 \text{ nm} \quad c = 3d(003) = 2.281 \text{ nm}$$

the interlayer spacing: $d(003) = 0.760 \text{ nm}$

the spacing occupied by the anion (gallery height) = 0.280 nm

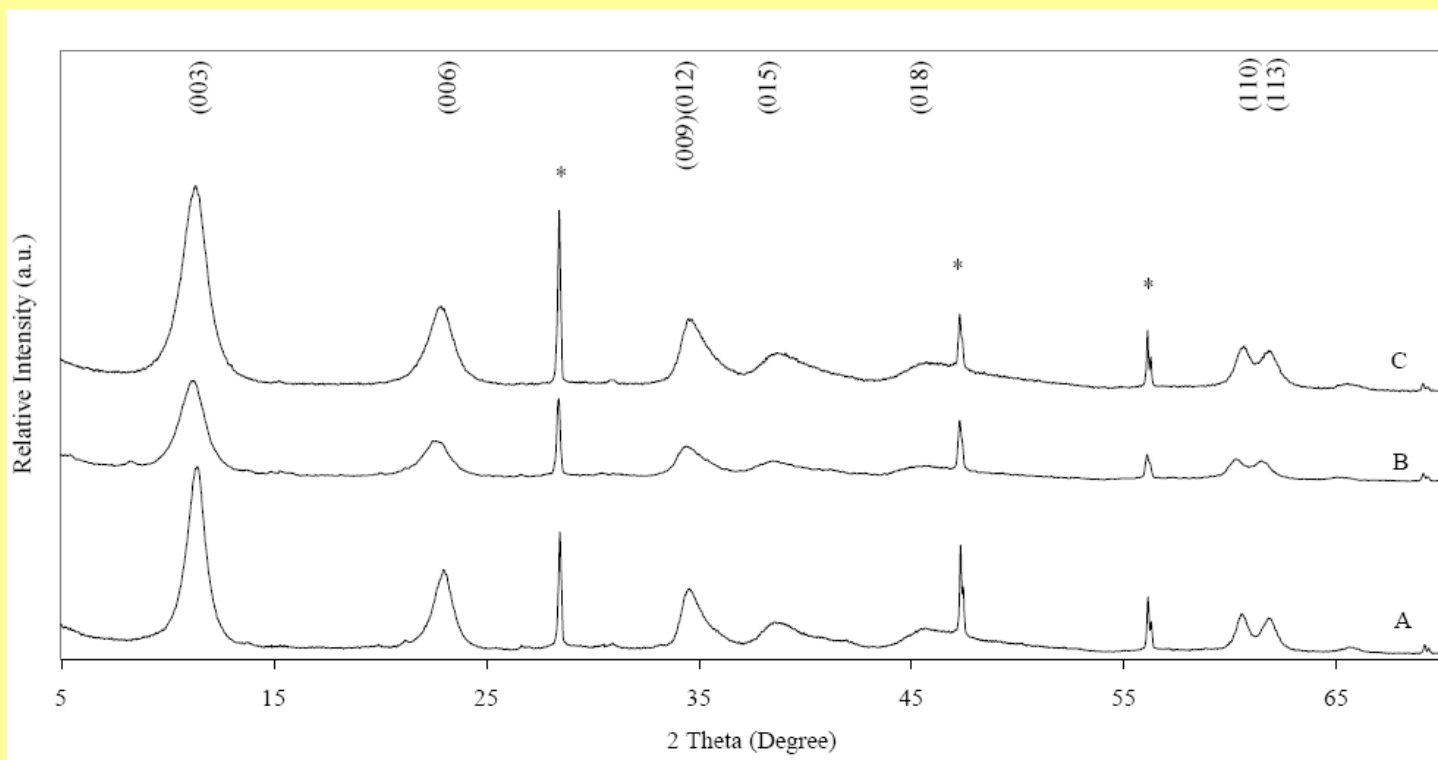
a thickness of the brucite-like layer = 0.480 nm

the average M—O bond = 0.203 nm

the distance between two nearest OH^- ions in the two opposite side layers = 0.267 nm shorter than a (0.305 nm) and indicative of some contraction

along the c -axis.

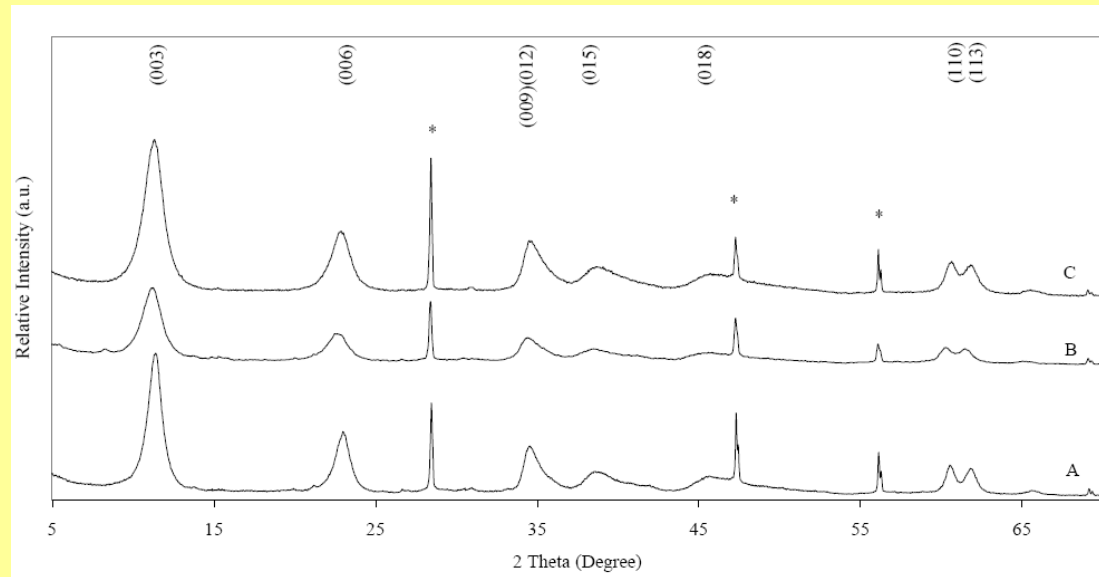
XRD Patterns of LDH



**XRD patterns of layered double hydroxides synthesized by coprecipitation method with various cations composition:
A – Mg/Al; B- Mg/Co/Al; C- Mg/Ni/Al**

*** = Reflections from Si crystal used as a reference**

XRD Patterns of LDH



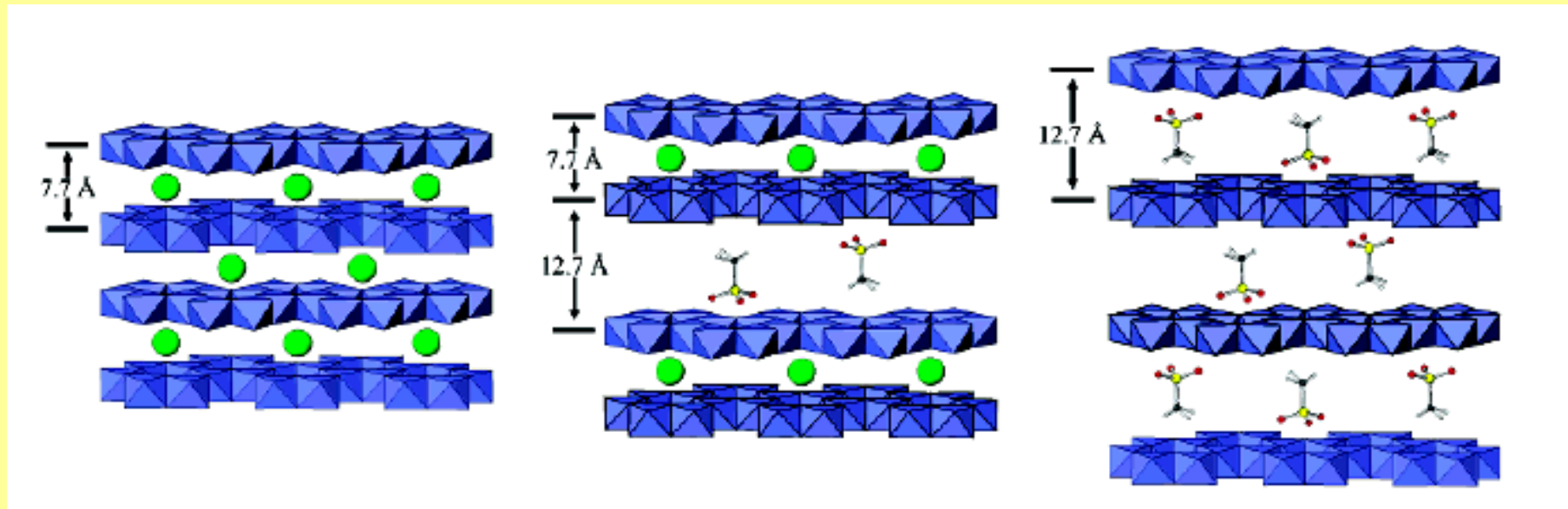
rhombohedral structure
the cell parameters c and a

The lattice parameter $a = 2d(110)$ corresponds to an average cation-cation distance

The c parameter corresponds to three times the thickness of $d003$

$$c = 3/2 [d003 + 2d006]$$

Intercalation to LDH



the intercalation of methylphosphonic acid into Li/Al LDH

(a) $[\text{LiAl}_2(\text{OH})_6]\text{Cl}\cdot\text{H}_2\text{O}$

(b) second-stage intermediate, alternate layers occupied by Cl and MPA anions

(c) first-stage product with all interlayer regions occupied by MPA.

Intercalation to LDH

LDH = layered double hydroxides

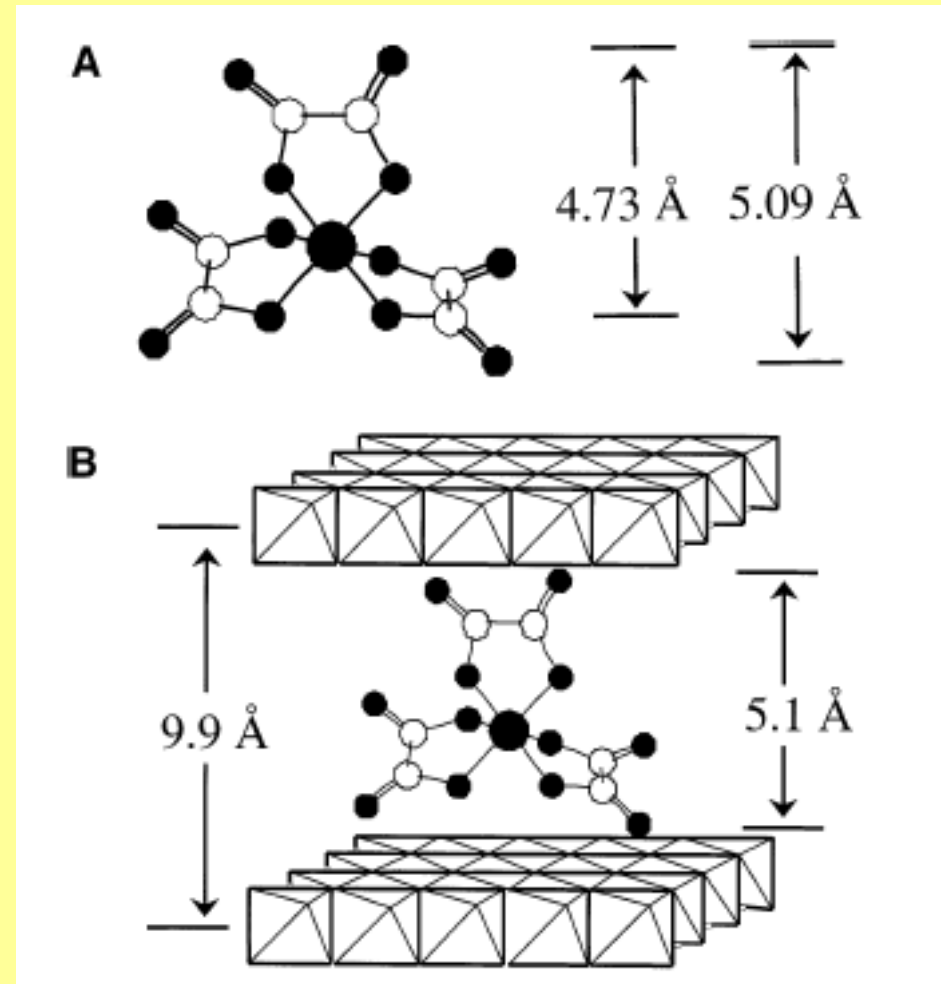
hydrotalcites

mineral $\text{Mg}_6\text{Al}_2(\text{OH})_{16}\text{CO}_3 \cdot 4\text{H}_2\text{O}$

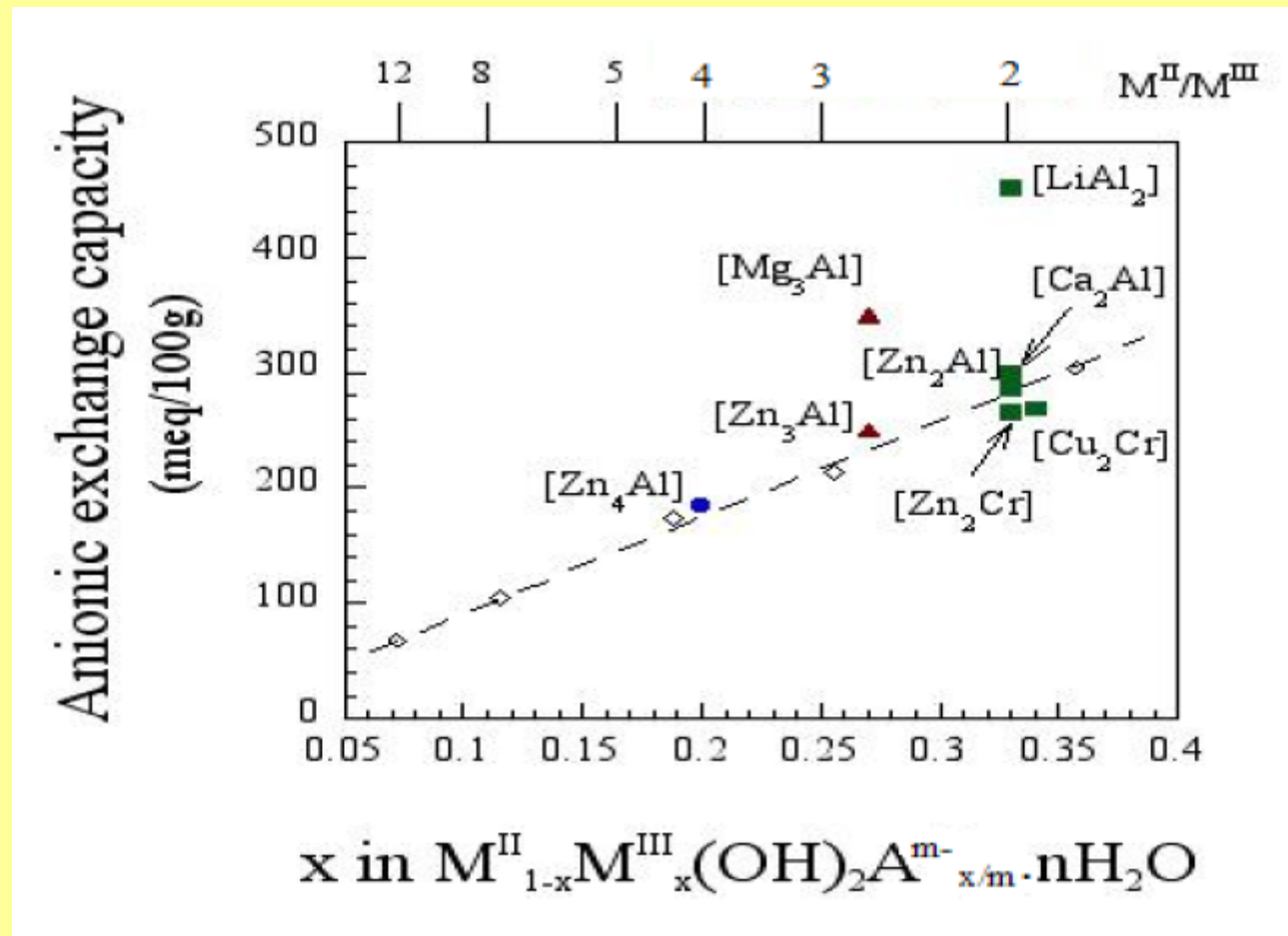
Brucite layers, Mg^{2+} substituted partially by Al^{3+}

Layers have positive charge

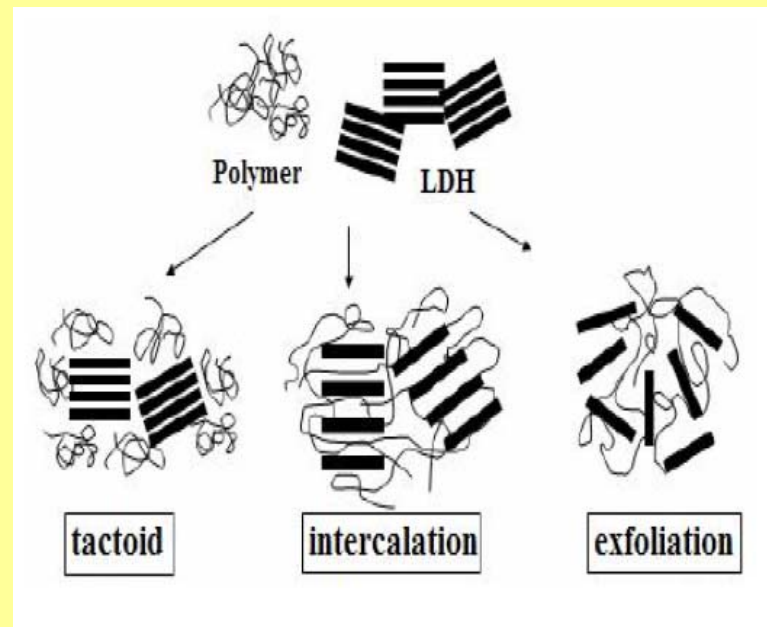
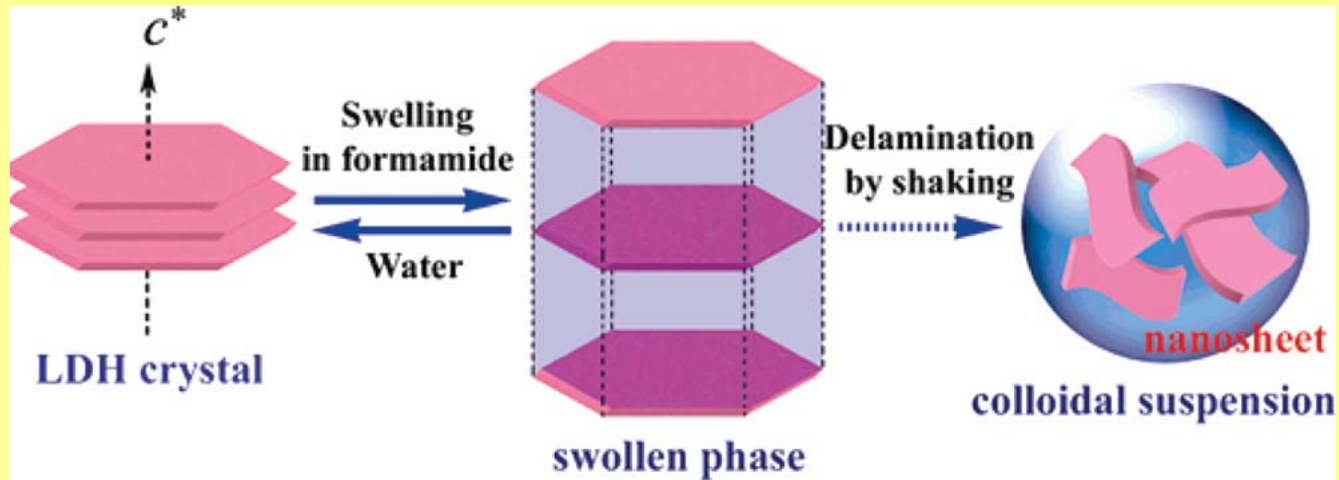
Intercalate anions $[\text{Cr}(\text{C}_2\text{O}_4)_3]^{3-}$



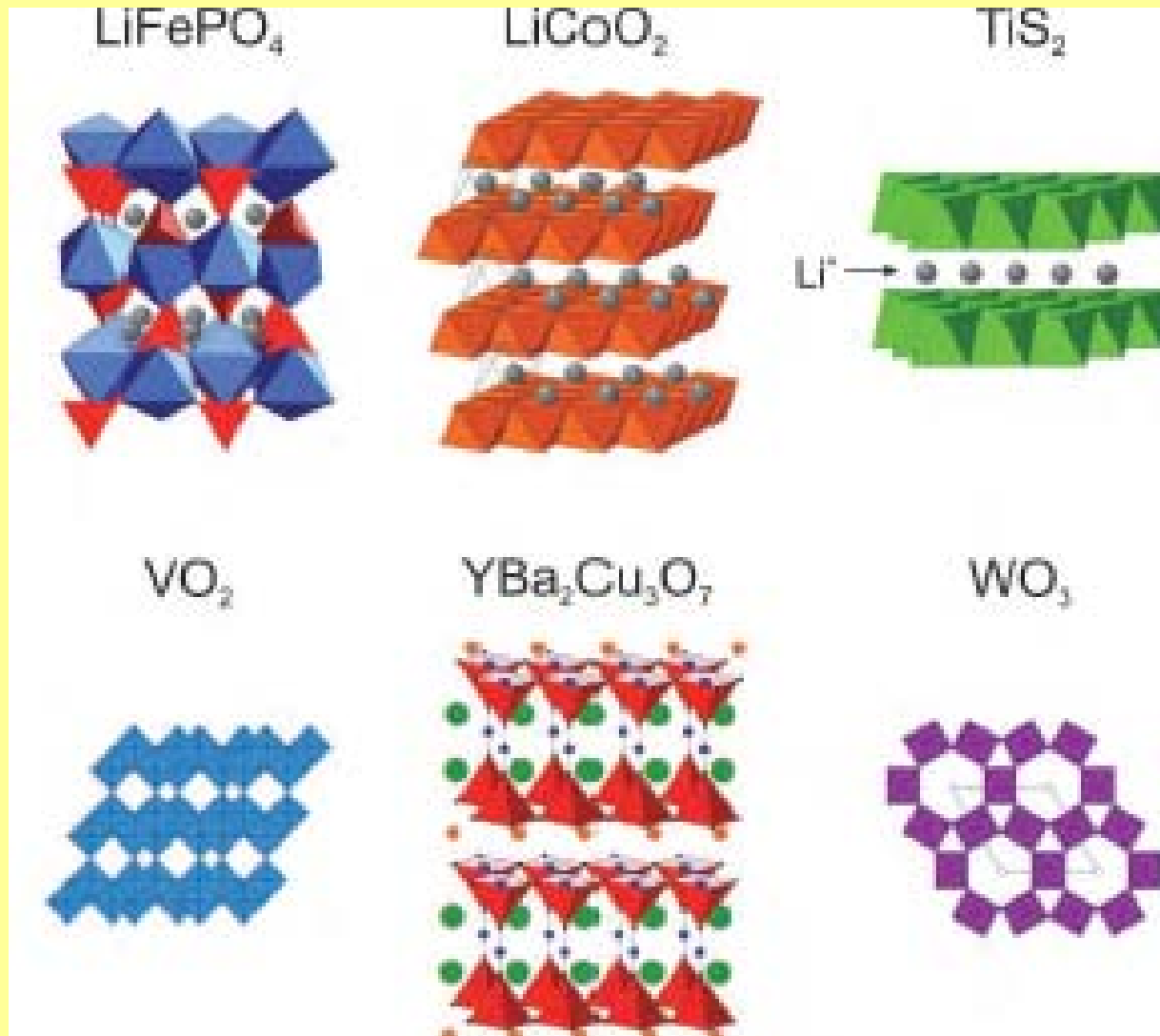
The Anionic Exchange Capacity (AEC)



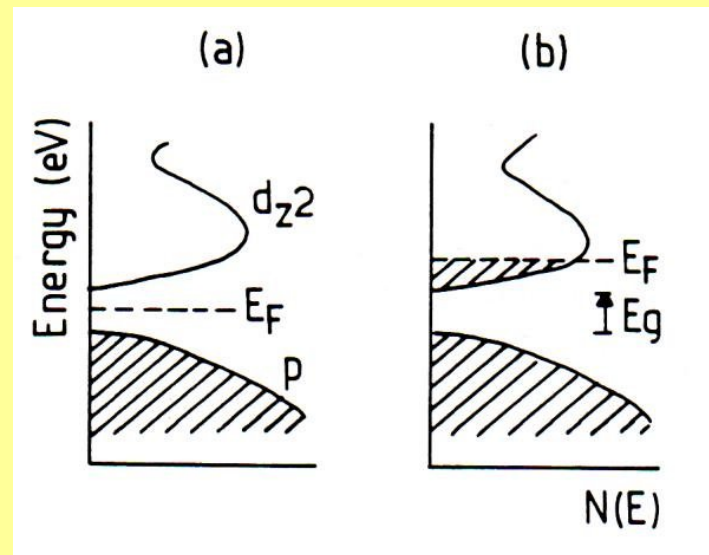
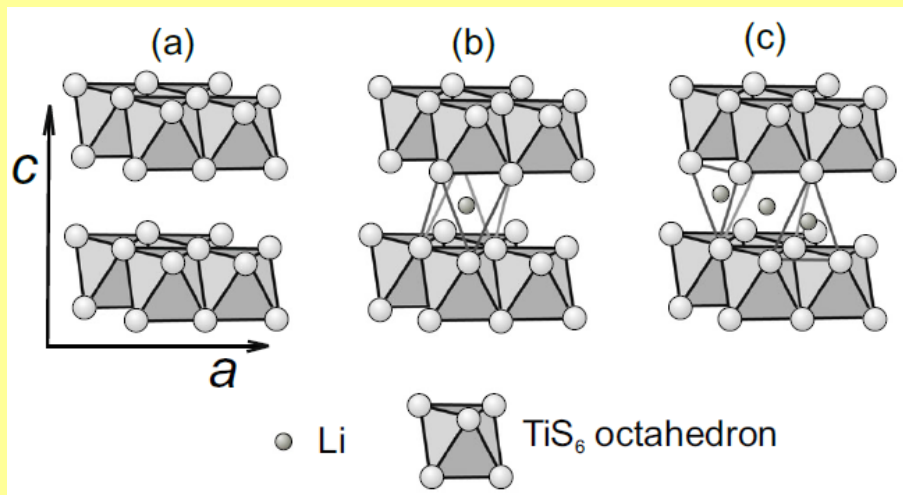
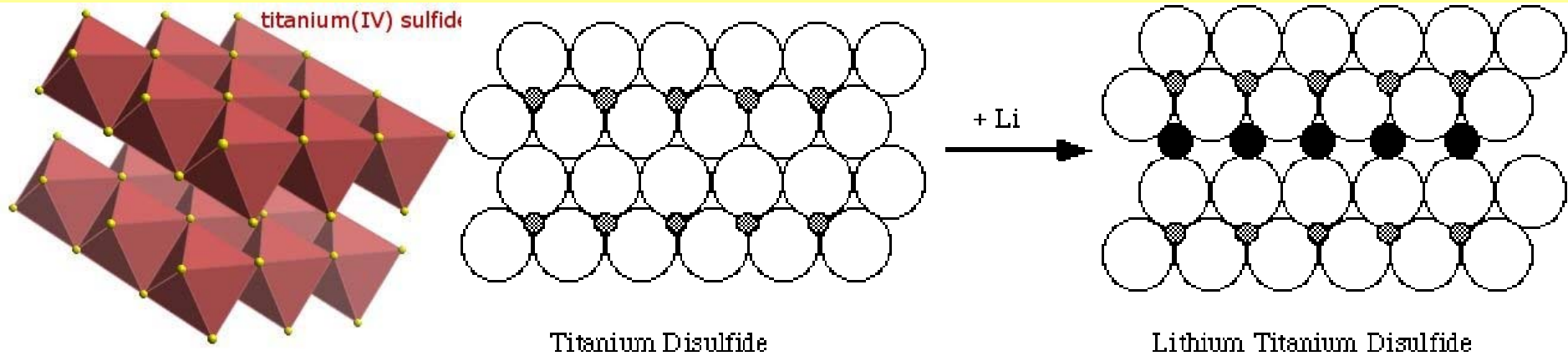
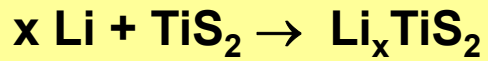
LDH Composite Structures



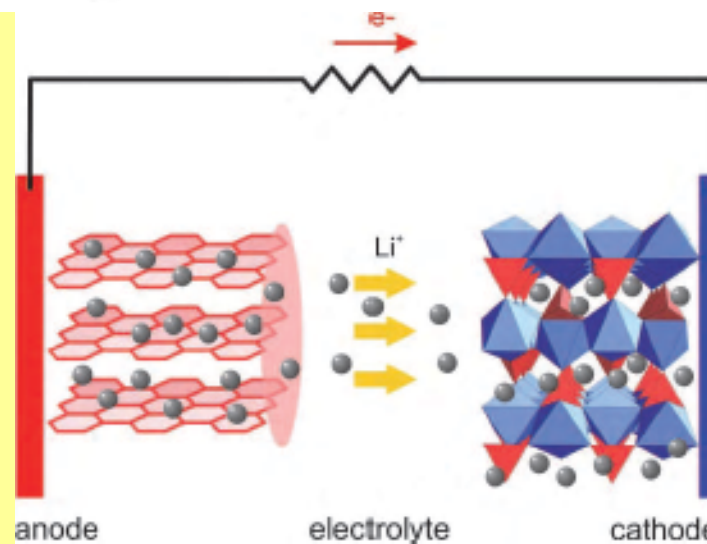
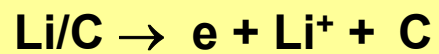
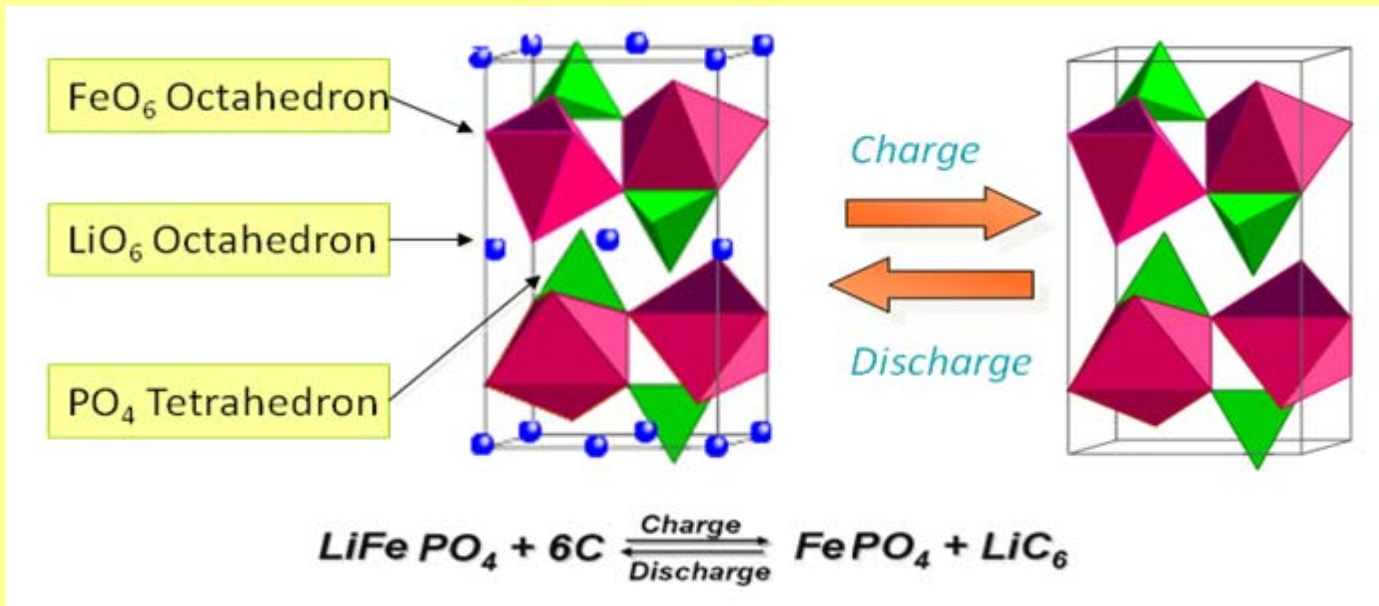
Li Intercalation Compounds



Li Intercalation



Li Intercalation

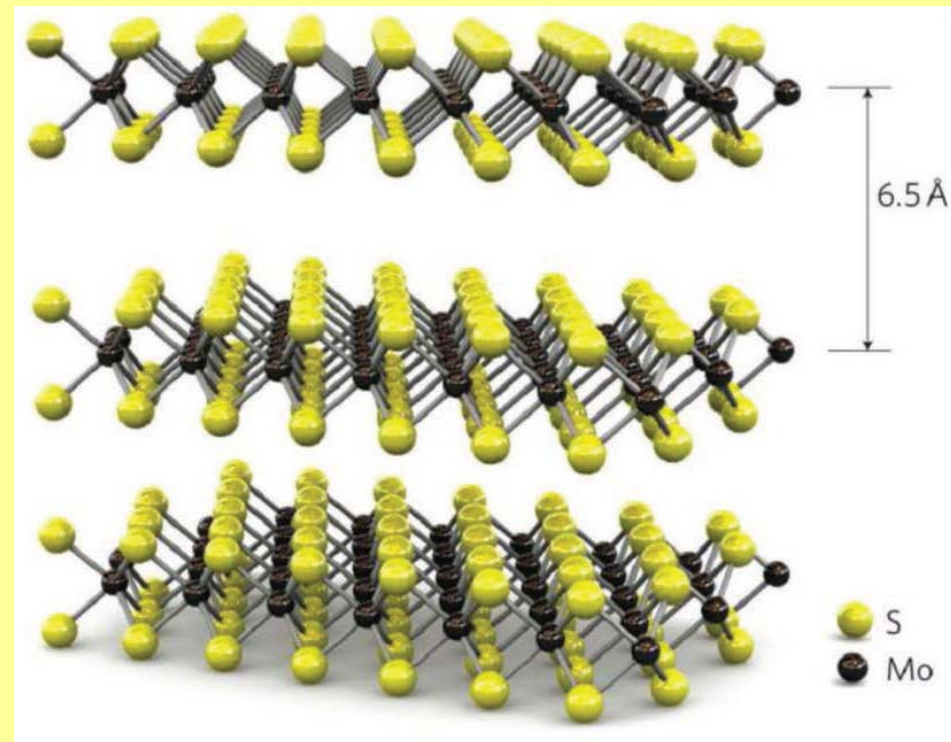


Molybdenum Disulfide (MoS_2)

Mineral molybdenite

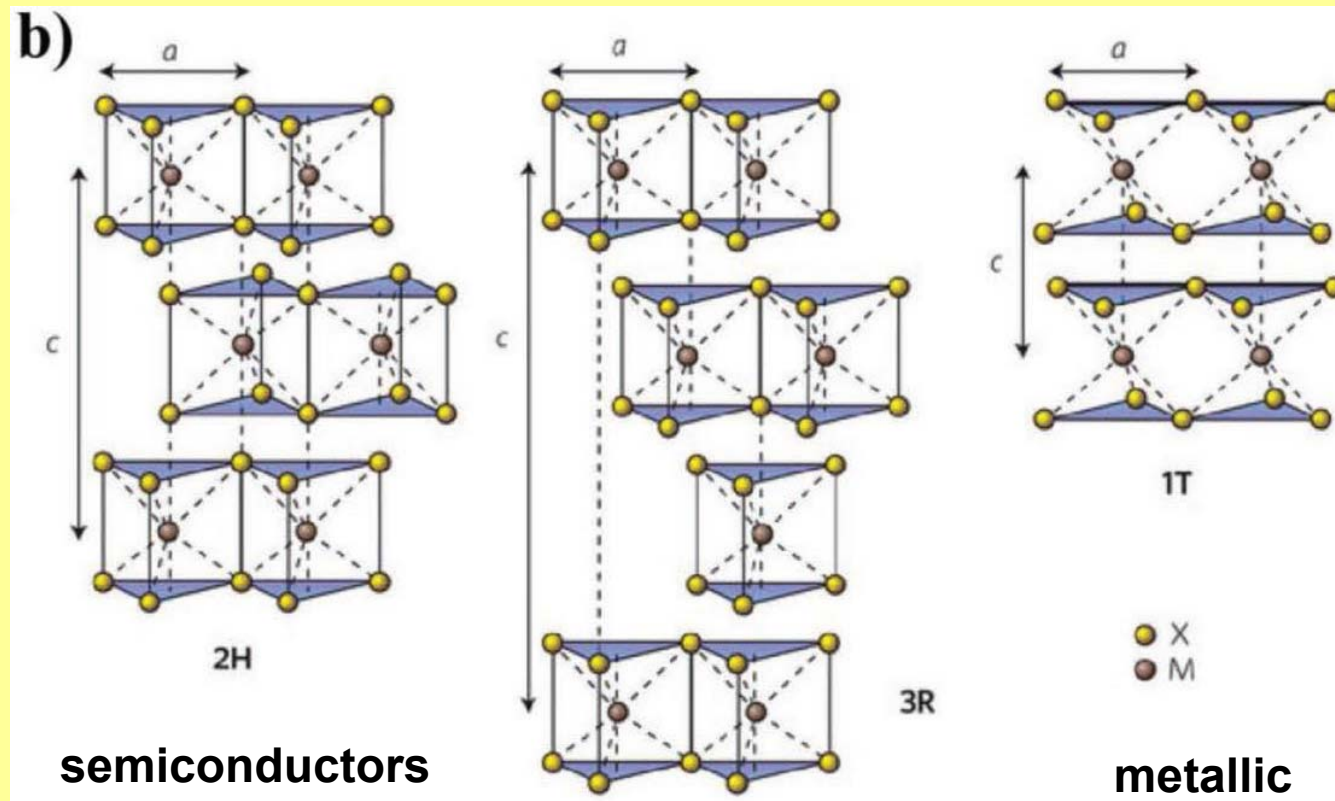
Hydrodesulfurization catalyst
at edges

Lubricant

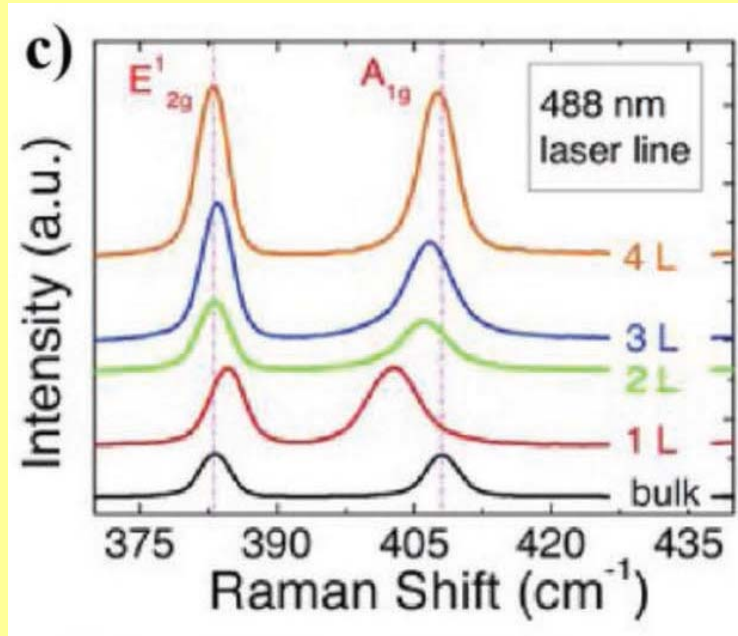


Molybdenum Disulfide (MoS_2)

Polymorphs of MoS_2

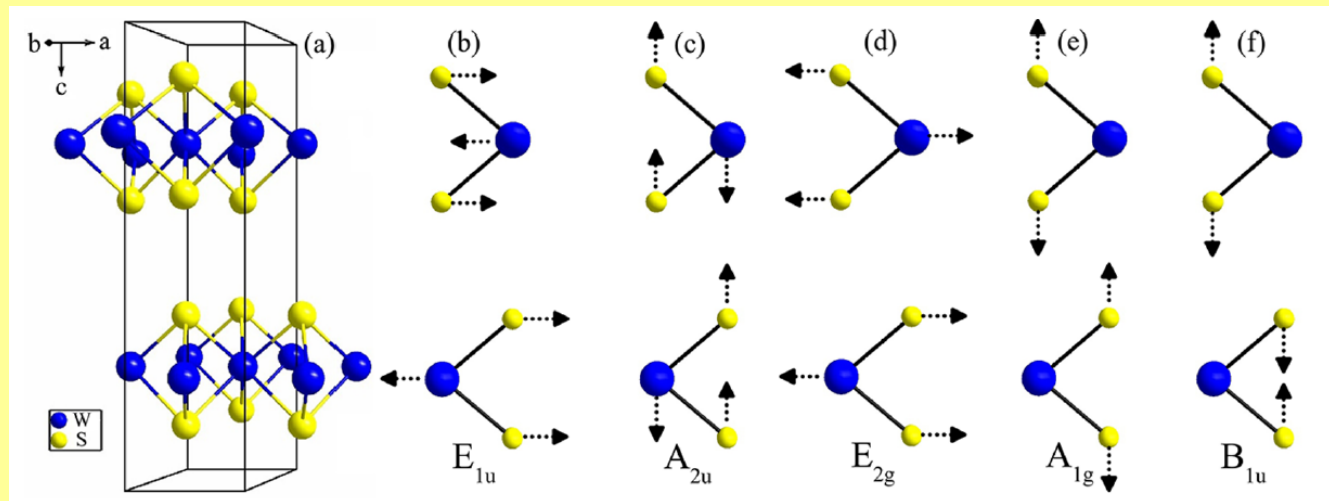


Molybdenum Disulfide (MoS₂)

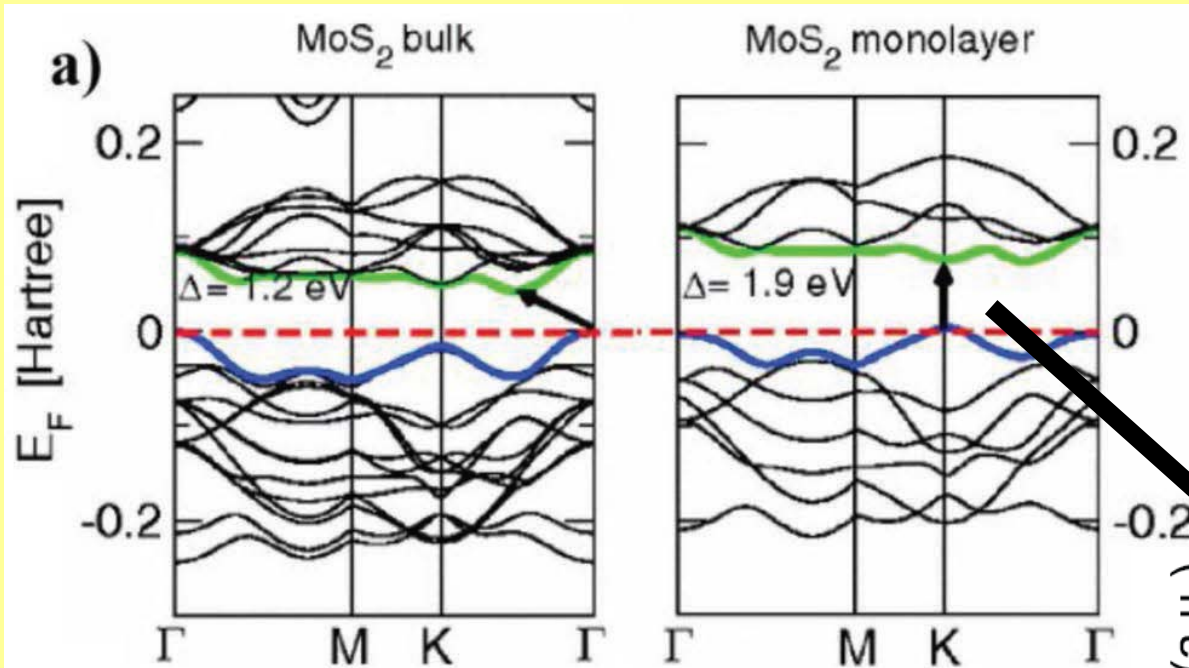


Frequency of A_{1g} band is increasing while that of E_{2g}¹ is decreasing with increase in number of layers

(b,c) infrared and (d-f) Raman-active



Molybdenum Disulfide (MoS₂)



An indirect band gap
1.2 eV

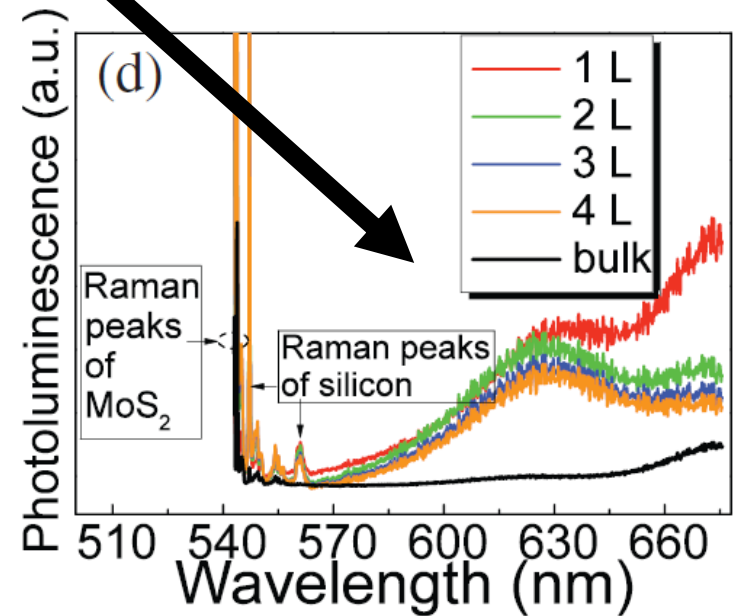
A direct band gap
1.8 eV

Conduction band

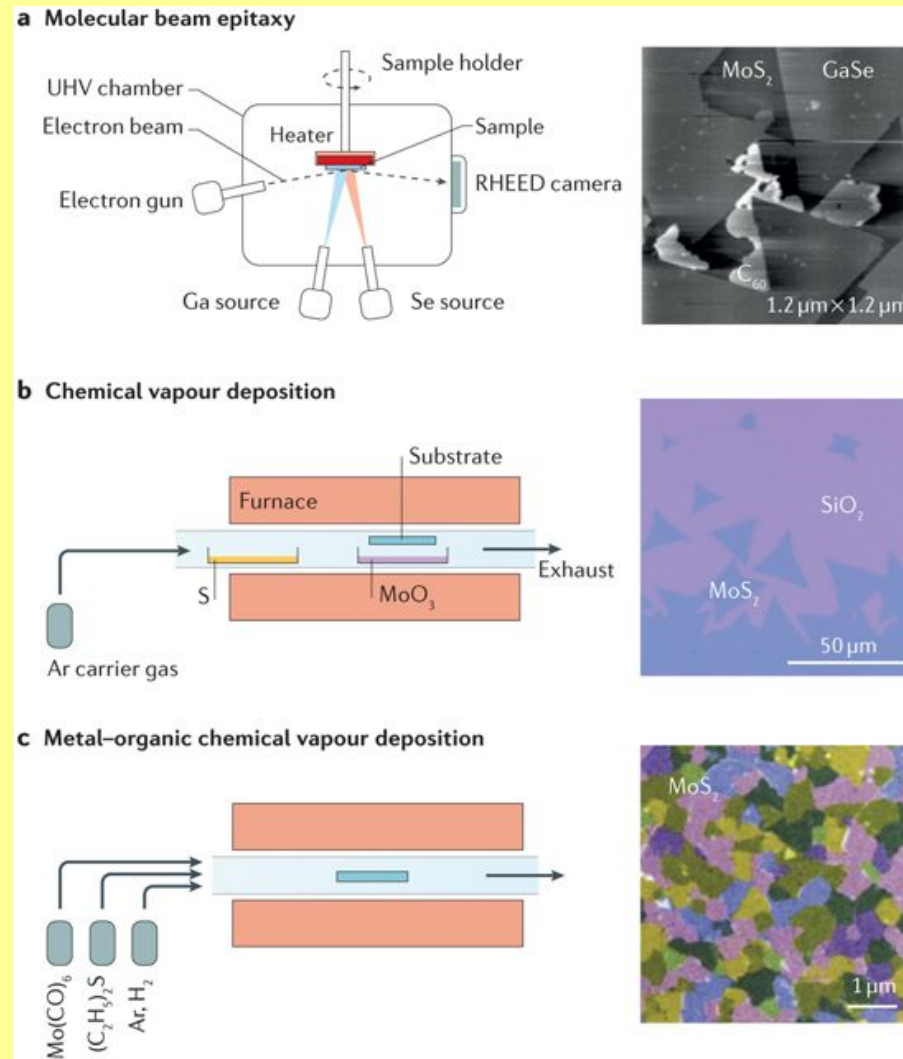
Fermi level

Valence band

photoluminescence

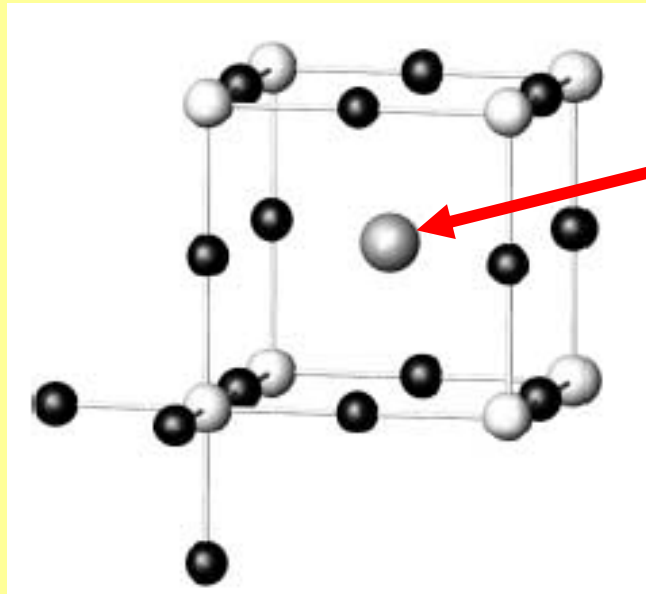


Molybdenum Disulfide (MoS_2)



3D Intercalation Compounds

Cu_3N and Mn_3N crystallize in the (anti-) ReO_3 -type structure



the large cuboctahedral void in the structure can be filled

By Pd to yield (anti-) perovskite-type PdCu_3N

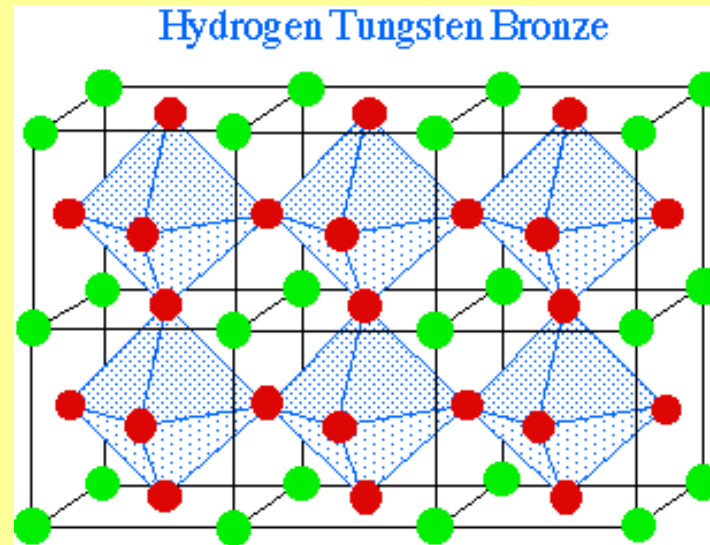
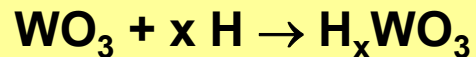
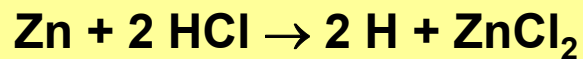
By $M = \text{Ga}, \text{Ag}, \text{Cu}$ leading to MMn_3N

3D Intercalation Compounds

Tungsten trioxide structure

= WO_6 octahedra joined at their corners

= the perovskite structure of CaTiO_3 with all the calcium sites vacant



The color and conductivity changes are due to the intercalation of protons into the cavities in the WO_3 structure, and the donation of their electrons to the conduction band of the WO_3 matrix. The material behaves like a metal, with both its conductivity and color being derived from free electron behavior.

The coloration reaction used in electrochromic displays for sun glasses, rear view mirrors in cars

0D Intercalation Compounds

$C_{60} = \text{FCC}$

$K_3 C_{60}$

